

Distribution Agreement

In presenting this thesis or dissertation as a partial fulfillment of the requirements for an advanced degree from Emory University, I hereby grant to Emory University and its agents the non-exclusive license to archive, make accessible, and display my thesis or dissertation in whole or in part in all forms of media, now or hereafter known, including display on the world wide web. I understand that I may select some access restrictions as part of the online submission of this thesis or dissertation. I retain all ownership rights to the copyright of the thesis or dissertation. I also retain the right to use in future works (such as articles or books) all or part of this thesis or dissertation.

Signature:

Russell W. Goetze

Date

A dip IN the shallow end:
SAMHD1 dNTPase specificity and how draining the dNTP pool limits HIV-1 gap repair.

By

Russell W. Goetze
Doctor of Philosophy

Graduate Division of Biological and Biomedical Science
Molecular and Systems Pharmacology

Baek Kim, Ph.D.
Advisor

Christopher Doering, Ph.D.
Committee Member

Haian Fu, Ph.D.
Committee Member

Raymond F. Schinazi, Ph.D., D.Sc.
Committee Member

Accepted:

Lisa A. Tedesco, Ph.D.
Dean of the James T. Laney School of Graduate Studies

Date

A dip IN the shallow end:
SAMHD1 dNTPase specificity and how draining the dNTP pool limits HIV-1 gap repair.

By

Russell W. Goetze
B.S., The University of Georgia, 2012

Advisor: Baek Kim, Ph.D.

An abstract of
a dissertation submitted to the Faculty of the
James T. Laney School of Graduate Studies of Emory University
in partial fulfillment of the requirements for the degree of
Doctor of Philosophy
in the Graduate Division of Biological and Biomedical Sciences,
Molecular and Systems Pharmacology
2017

Abstract

A dip IN the shallow end:
SAMHD1 dNTPase specificity and how draining the dNTP pool limits HIV-1 gap repair.

By Russell W. Goetze

Lentiviruses, including HIV-1, infect both dividing and nondividing target cells and have adapted strategies to overcome barriers to replication in these types of cells. One such barrier to in nondividing cells is tight regulation of 2'-deoxyribonucleotide (dNTP) synthesis and degradation by ribonucleotide reductase (RNR) and sterile alpha motif and histidine and aspartic acid domain containing protein 1 (SAMHD1), respectively.

SAMHD1 maintains low dNTP concentrations in nondividing cells though its triphosphohydrolase activity and is allosterically regulated by NTPs and dNTPs. Besides canonical dNTPs, SAMHD1 degrades nucleoside analogue drugs that are used to treat cancer and viral disease. However, whether these molecules are able to induce or disrupt activation by binding to either of the SAMHD1 allosteric sites or the catalytic site is unknown. We tested a number of nucleoside analogues to define key characteristics that would enable us to predict whether these molecules would fit into the active site of SAMHD1. We report that while modifications to the base moiety and some modifications to the 2' position of the sugar moiety are tolerated, modifications to the 3' and some modifications to the 2' position of the sugar moiety prevent degradation by SAMHD1. This information is valuable for designing future nucleoside analogue drugs for SAMHD1-expressing cell types.

Lentiviruses require cellular DNA repair pathways to complete integration of the viral genome into a host chromosome. Among the proteins involved, DNA Polymerase β (Pol β) has been proposed as a potential key player in this process. We generated a novel Pol β KO THP-1 cell line to examine HIV DNA repair in dividing and nondividing cells in the absence of Pol β expression. We report that dNTP concentrations, which are suppressed by SAMHD1 in nondividing cells, but not Pol β , control the rate of gap repair. Furthermore, we show that Pol β is dispensable for HIV-1 transduction in both dividing and nondividing THP-1 cells, indicating that other cellular DNA polymerases and/or RT are capable of completing the essential DNA repair step required for integration. Together, the data presented here provide insight into two ways that cellular regulation of dNTPs interfaces with lentivirus replication.

A dip IN the shallow end:
SAMHD1 dNTPase specificity and how draining the dNTP pool limits HIV-1 gap repair.

By

Russell W. Goetze
B.S., The University of Georgia, 2012

Advisor: Baek Kim, Ph.D.

A dissertation submitted to the Faculty of the
James T. Laney School of Graduate Studies of Emory University
in partial fulfillment of the requirements for the degree of
Doctor of Philosophy
in the Graduate Division of Biological and Biomedical Sciences,
Molecular and Systems Pharmacology
2017

Acknowledgements

Navigating the stress and challenges that come with graduate training was an enormous trial and I am so thankful for the support I've received from my family, particularly my wife, Elissa. You have been with me through some of the most difficult tests that I've faced and I am eternally grateful for your love and support. Thank you for pushing me when I struggled to focus, for listening to my complaints, helping me to put everything in perspective, and for your eagerness to come along wherever this journey will take us. I love you, Elissa.

My adviser, Baek Kim, has been absolutely instrumental to my success. He challenged me to be independent, to be ready to learn and adapt with the growth of a project, and to build knowledge by being inquisitive. He taught me to be rigorous, to own my research, and to put everything in context. Thank you for everything that you've done to help me become the scientist I am today, Baek.

My graduate training would not have been possible without the training, both technical and mental, that I received from many individuals. I want to thank all of the Kim Lab and LoBP members that I have had the pleasure of working with and learning from over the past few years. Particularly, Michele Daly, Joe Hollenbaugh, Louise McCormick, T Maehigashi, and Susan Schader for their invaluable training and for challenging me to think deeply about my research and to ask the right questions.

I believe that the MSP program is the best biomedical research program at Emory because of the faculty and students that we have. I am amazed by the growth that I have seen during my years at Emory. Seeing the success of our program leadership together with our new GDBBS director and his team to improve training across all of the division's programs is so exciting. I know that the program will continue to thrive because of their work and I look forward to following the program's success in the future. I will always look back with fond memories of our shared experience together and the lasting friendships that I have made here.

Table of Contents

Abstract

Acknowledgements

Chapter 1: Introduction.....1

A. HIV Biology.....2

1. AIDS and the Discovery of HIV-1.....2

2. The HIV Genome and its Products.....3

3. The HIV Replication Cycle.....10

4. Treatment of HIV Infection with Direct-acting Antivirals.....15

5. Factors Controlling HIV Target Cell Specificity.....16

B. Cellular Control of Nucleotides.....17

C. Cellular DNA Damage Sensing and Repair Mechanisms.....22

D. Genome Editing Techniques.....26

E. References.....31

Chapter 2: Substrates and Inhibitors of SAMHD1..53

A. Abstract.....54

B. Background.....54

C. Results.....56

D. Discussion.....82

E. Materials and Methods.....85

F. References.....92

Chapter 3: A CRISPR/Cas9 approach reveals that the polymerase activity of DNA

Polymerase β is dispensable for HIV-1 infection in dividing and nondividing cells.....100

A. Abstract.....	101
B. Background.....	101
C. Results.....	104
D. Discussion.....	122
E. Materials and Methods.....	127
F. References.....	142
Chapter 4: General Discussion.....	141
A. Collective Results.....	142
B. References.....	147

List of Figures

Chapter 1

Figure 1: HIV-1 genome organization and molecular structure.....	8
Figure 2: The HIV-1 replication cycle.....	13
Figure 3: Detailed mechanism of lentivirus integration.....	14
Figure 4: Allosteric regulation of RNR and SAMHD1 leads to balanced dNTP pools...21	
Figure 5: DNA damage and repair mechanisms.....	25
Figure 6: Genome editing techniques.....	30

Chapter 2

Figure 1: Cartoon for SAMHD1 homotetramerization.....	58
Figure 2: Examining the role of L150 for nucleotide specificity.....	61
Figure 3: Role of 3'-OH sugar moiety for SAMHD1's substrate specificity.....	63
Figure S1: Evaluating additional nucleotides as substrates for SAMHD1.....	64
Figure 4: Role of Y374 and C2' sugar moiety substitution in acting as substrates of SAMHD1.....	68
Figure S2: Site-directed mutagenesis for L150 and Y374.....	70
Figure S3: Evaluating additional non-canonical nucleotides as substrates for SAMHD1.....	71
Figure 5: Ara-CTP does not fit into the A2 site of SAMHD1.....	73
Figure 6: Biochemical assessment of SMDU-TP.....	75
Figure 7: Monitoring ara-CTP and gem-TP concentrations in MDMs.....	79
Figure 8: Determining nucleotide analog specificity for SAMHD1.....	81

Chapter 3

Figure 1: Generation of <i>POLB</i> KO THP-1 cell lines by CRISPR/Cas9.....	106
Figure 2: <i>POLB</i> KO THP-1 cells are sensitive to MMS-induced DNA damage.....	109
Figure S1: PMA-treated THP-1 cells have minimal levels of DNA synthesis.....	110
Figure 3: Effect of <i>POLB</i> KO on biochemical ssDNA gap repair activity with HIV-1 gap DNA substrate.....	113
Figure 4: Effect of <i>POLB</i> KO on HIV-1 transduction in dividing and nondividing THP-1 cells.....	116
Figure 5: Effect of dNTP concentration on <i>in vitro</i> HIV-1 ssDNA gap repair activity...	119
Figure S2: Effect of dNTP concentration on <i>in vitro</i> HIV-1 ssDNA gap repair activity in <i>POLB</i> KO THP-1 cells.....	121

List of Abbreviations

3TC	Lamivudine
ABC	Abacavir
AIDS	Acquired Immunodeficiency Syndrome
APOBEC3G	Apolipoprotein B mRNA editing enzyme, catalytic polypeptide-like 3G
Ara-C(TP)	Cytarabine (triphosphate)
AZT	Zidovudine
BER	Base excision repair
CA	Capsid protein
CD4	Cluster of differentiation 4
CDC	Centers for Disease Control and Prevention
CCR5	C-C chemokine receptor type 5
CRISPR	Clustered Regularly Interspaced Short Palindromic Repeat
CXCR4	C-X-C chemokine receptor type 4
d4T	Stavudine
ddC	Dideoxycytidine
ddI	Dideoxyinosine
dN	2'-deoxyribonucleoside
dNTP	2'-deoxyribonucleoside-5'-triphosphates
dRP	5'-2-deoxyribose-5-phosphate
ds	Double-stranded
DSB	Double-strand break
GeCKO	Genome-scale CRISPR knockout database
gRNA	Guide RNA
HIV-1	Human immunodeficiency virus Type 1
II	Integrase inhibitor
IN	Integrase
KD	Knockdown
KO	Knockout
LTR	Long terminal repeat
MA	Matrix protein
MDM	Monocyte-derived macrophage
MP	Monophosphate
MMS	Methyl methanesulfonate
NC	Nucleocapsid
Nef	Negative regulatory factor
NNRTI	Non-nucleoside reverse transcriptase inhibitor
NRTI	Nucleoside reverse transcriptase inhibitor
PI	Protease inhibitor
PIC	Pre-integration complex
PMA	Phorbol 12-myristate 13-acetate
Pol	DNA polymerase
PPP	Inorganic triphosphate
PR	Protease
Rev	Regulator of expression of virion proteins

RNR	Ribonucleotide reductase
rNTP	Ribonucleoside triphosphate
RT	Reverse transcriptase
SAMHD1	Sterile alpha motif and histidine/aspartic acid domain containing protein 1
sgRNA	Single-guide RNA
SIV	Simian Immunodeficiency Virus
SIV _{smm}	SIV sooty mangabey
SMDU	(2'S)-2'-methyl deoxyuridine
ss	Single-stranded
SSB	Single-strand break
TALEN	Transcription activator-like effector nucleases
Tat	Trans-activator of transcription
TP	Triphosphate
Vif	Viral infectivity factor
VLP	Virus-like particle
Vpr	Viral protein r
Vpu	Viral protein u
Vpx	Viral protein x
VSV	Vesicular Stomatitis Virus
WT	Wild-type
ZFN	Zinc-finger nuclease

Chapter 1

Introduction

A. HIV Biology

1. AIDS and the Discovery of HIV-1

Acquired immunodeficiency syndrome (AIDS) was first recognized in 1981 after Dr. Michael Gottlieb and colleagues reported five separate patients, all gay men, with *Pneumocystis carinii*, active cytomegalovirus infection, and candida infection – all opportunistic infections. All patients were young and previously in good health, which suggested a sexually transmitted disease causing severe immune dysfunction (1). By the end of 1981, more than 250 cases had been reported by the U.S. Centers for Disease Control (CDC) causing more than 100 deaths (2). The term AIDS was first used by CDC in 1982 and the definition was narrowed to describe individuals with an etiologically undefined reduction in cell-mediated immunity (3). The disease continued to spread, particularly within the gay community, intravenous drug users, and individuals requiring frequent blood transfusions (4). It was not until 1983 that the causative agent of AIDS, human immunodeficiency virus Type 1 (HIV-1), was discovered independently by the laboratories of Drs. Luc Montagnier of the Pasteur Institute in France and Robert Gallo of the National Cancer Institute in the United States (5,6). Prior to the discovery of HTLV-1 by Gallo's laboratory in 1980 (7), retroviruses were not known to cause human disease – a discovery that led Gallo to propose in 1982 that AIDS may, in fact, be the consequence of a retroviral infection in humans. While we now know that Gallo's hypothesis was correct, the idea was quite controversial at the time. Previous work by Gallo's laboratory led to the discovery of interleukin-2, which enabled the development of an *in vitro* immune cell culture system. This permitted researchers to grow HIV and other T-cell viruses in culture contributing enormously to our understanding of HIV and other retroviruses today (8).

2. The HIV Genome and its Products

Structurally, HIV is a spherical, enveloped virus that carries two copies of the (+)-sense single-stranded (ss) RNA genome. The genome is approximately 10 kb long with highly similar sequences, termed long terminal repeats (LTRs), at each end. The 5' and 3' LTRs contain unique sequences, referred to as U5 and U3, respectively, which are copied during reverse transcription so that both are included at each end of the viral dsDNA. The U3 region includes both transcriptional promoter and enhancer sequences, which drive expression of viral genes once the provirus integrated into a host cell chromosome. Downstream of the LTR, the viral genome contains a packaging signal, termed the Psi sequence, which is required for directing the viral genomic RNA into newly formed viral particles through interactions with certain viral proteins. The viral RNA messages contain nine distinct genes of which three, *gag*, *pol*, and *env*, encode structural proteins required for viral replication. The additional six genes encode accessory and regulatory proteins. Each of the structural genes is expressed as an unprocessed polyprotein that undergoes cleavage by the viral protease (PR) or cellular proteases during the maturation process or within the cellular secretory pathway, respectively. In total, the HIV-1 genome encodes 15 separate proteins that function in viral replication and combatting host-cell defenses (9,10) (Fig. 1).

The *gag* gene encodes a 54 kD polyprotein consisting of four substituents: matrix (MA), capsid (CA), nucleocapsid (NC), and p6. The *gag* polyprotein is processed by the HIV protease (PR) during viral particle maturation to produce these four products. The MA portion of the *gag* polyprotein is co-translationally myristoylated, which targets the polyprotein to the plasma membrane where it is recruited into new viral particles (11). The mature MA protein is part of

the pre-integration complex (PIC) and is thought to facilitate nuclear import of the PIC (12). Mature CA is a 24 kD protein that makes up the core protein structure that encases the viral ssRNA within viral particles (13). The assembled CA core is visible by electron microscopy and forms a conical structure in mature virions, which can be used to distinguish these from immature virions (14). The NC protein is a 7 kD RNA binding protein that interacts with the HIV-1 RNA genome through its zinc finger motif. NC is important for controlling the secondary structure of the viral RNA and acts as a chaperone for RT during viral DNA synthesis to prevent incorrect priming from occurring (15). p6 is responsible for recruiting the viral accessory protein Vpr to the cell plasma membrane to be incorporated into new virions (16).

The *pol* gene itself contains no start codon, but is translated when the ribosome “slips” and continues past the *gag* stop codon, which produces a gag-pol fusion polyprotein (17). The gag-pol polyprotein occurs as at frequency of 1/10 to 1/20 that of gag and is affected by mutations at the slippage site, suggesting that this ratio is evolutionarily optimized for maintaining an ideal level of the enzymes encoded by *pol* (18). *Pol* encodes four enzymes required for viral replication: PR, reverse transcriptase (RT), ribonuclease (RNase) H, and integrase. The viral PR is responsible for post-translational cleavage at several sites within the viral polyproteins, including cleavage of its own linker sequence, which joins the C-terminal of PR to the N-terminal of RT (19). PR is an aspartyl protease that becomes activated by low pH that occurs in viral particles (20). The viral RT is a heterodimer comprised of 51 and 66 kD subunits termed p51 and p66, respectively. The p51 subunit is composed solely of the RT, while the p66 subunit is made up of the p51 subunit and the 15 kD RNase H domain. Initially, a p66 homodimer is formed, but is processed by PR to yield the heterodimer (19). RT, the viral polymerase, converts the genomic ssRNA into dsDNA through RNA-dependent and DNA-

dependent DNA polymerase activities (21). A more detailed mechanism of reverse transcription is discussed later. The RNase H domain of the RT heterodimer is a hybridase that hydrolyzes the RNA component of the RNA/DNA hybrid (22). Certain regions of high purine density, termed the poly-purine tracts (PPTs), resist this activity of RNase H and are important for RT priming during reverse transcription (23). IN forms the C-terminal region of the *pol* polyprotein. IN possesses both RNA and DNA binding activity, which is necessary for both correct packaging of the genomic RNA into virions and for the integration of the viral dsDNA into the host cell genome (24,25). The integration process involves several distinct steps, which will be discussed in greater detail later.

The *env* gene encodes the viral envelope glycoprotein, which is translated as a 160 kD polyprotein. This precursor polyprotein is proteolytically processed by the host protease, furin, into two products: gp41 and gp120, which together heterodimerize to form the envelope glycoprotein of the virus, gp160 (26). Expression and processing of the gp140 protein is required for entry into the host target cell and is mediated by interactions with both the gp41 and gp120 subunits and the surface of the host cell. As the only surface-exposed viral protein on the viral envelope, the host adaptive immune response is directed primarily to gp160 (28). However, few infected individuals develop broadly neutralizing antibodies that lead to long-term viral suppression. This is primarily due to the presence of the hypervariable region within the gp120 subunit, which evolves over the course of infection (29-31).

The HIV-1 genome expresses two regulatory proteins, Tat and Rev, which function in viral transcription and post-transcriptional regulation, respectively. Tat, or transactivator of transcription, interacts with the trans-activating response element, a highly structured element of the viral RNA, and enables efficient transcription through positive modulation of the cellular

transcriptional elongation complex (32). Rev functions by altering the number of unspliced HIV-1 transcripts that are exported into the cytoplasm. During early HIV-1 transcription, splicing produces primarily mRNAs that encode the regulatory proteins, which are essential for driving the increase in viral transcripts during early cellular infection. During mid-late infection, high levels of Rev allow the number of unspliced transcripts that encode the structural proteins of the viral to increase. This occurs through interactions between Rev and the Rev response element, a sequence located within the viral mRNA and is required for efficient production of new viral particles from infected cells (33).

There are four accessory proteins expressed by HIV-1: Vpr, Vpu, Nef, and Vif. In general, the accessory proteins perform functions that counteract host antiviral mechanisms and prevent cell death in order to increase the amount of virus produced from each infected cell.

Viral protein R (Vpr) is thought to perform two main functions. First, it is part of the PIC and its nuclear localization signal interacts with the nuclear pore, which allows entry of the complex into the nucleus (34). Because of this, it is required for infection of nondividing target cells. Secondly, Vpr induces G2 cell cycle arrest in dividing target cells, a function believed to prevent p34cdc2 activation and thereby delay or prevent the infected cell from undergoing apoptosis (35). Vpr is co-packaged into virions through interactions with p6 (16).

Viral protein U (Vpu) counteracts the host protein, tetherin, by inducing its degradation by the proteasome. Tetherin is a host integral membrane protein that traps viral particles at the cell surface through interactions with gp160, thereby preventing the release of new virions (36,37).

Negative factor (Nef) has two functions in preventing innate immune activation in infected cells. First, it downregulates the expression of CD4, which is required viral entry (38).

This reduces the potential for other virions to infect the cell and also limits the scope of T cell activation that can occur, which allows the cell to produce a greater number of new viral particles while allowing a heightened response later in infection that enhances recruitment and subsequent infection of additional CD4+ T cells (39,40). Secondly, Nef modulates the expression of MHC class I molecules and allows for immune avoidance by preventing antigen presentation to cytotoxic T lymphocytes (41).

Viral infectivity factor (Vif) also functions by counteracting a host protein: apolipoprotein B mRNA editing enzyme, catalytic polypeptide-like 3G (APOBEC3G). APOBEC3G is a member of the cytidine deaminase family, enzymes that convert cytidine residues in ssDNA to uridine, which restricts HIV-1 infection by targeting ssDNA formed during reverse transcription and causing hypermutation (42). Like other HIV-1 accessory proteins, Vif functions by targeting APOBEC3G to the host proteasome for degradation (43).

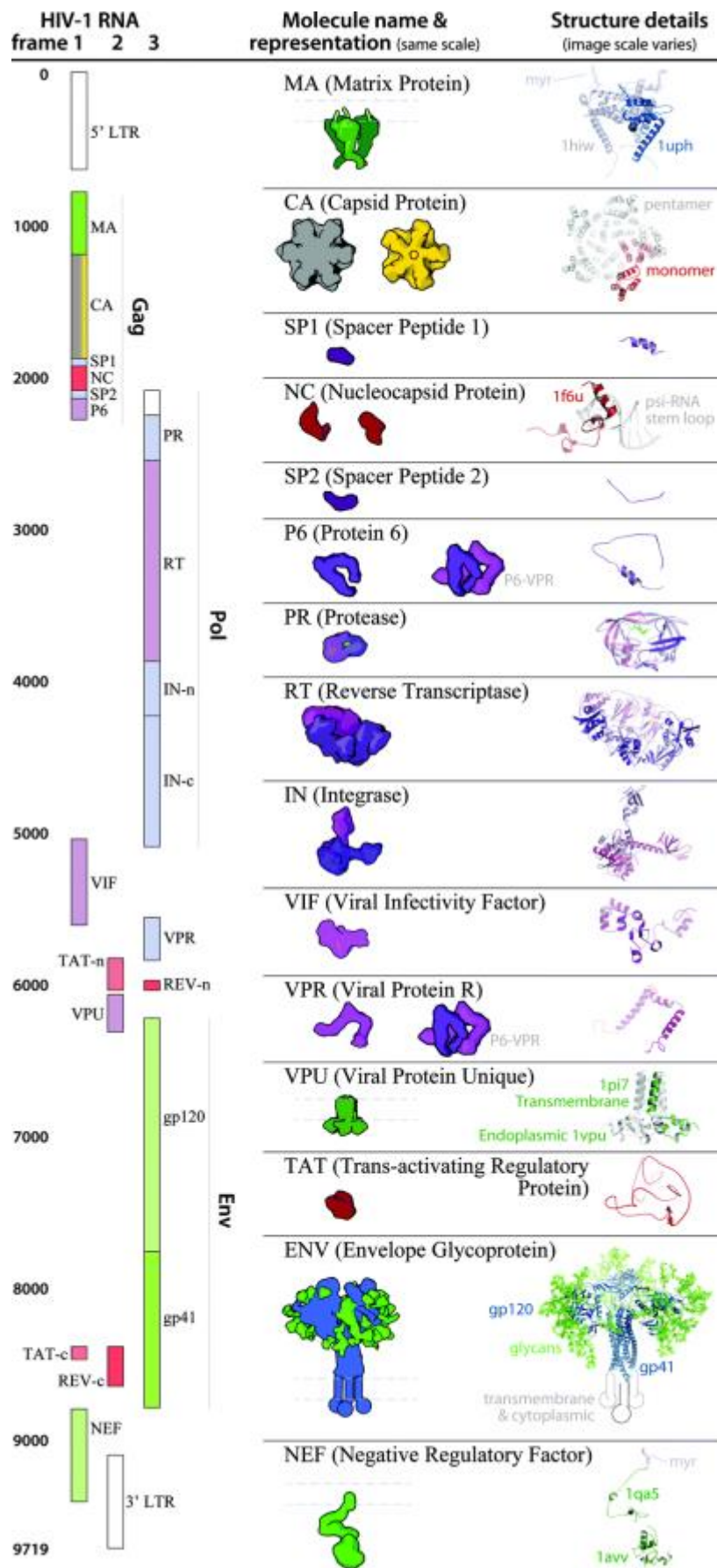


Figure 1: HIV-1 genome organization and molecular structure. A map of the HIV-1 genome (left) shows each coding region alongside a rendering of the 3-dimensional protein structure of mature viral proteins using a surface (center) and ribbon (right) view. This work by Graham T. Johnson, et. al. is reused with permission licensed under the [Creative Commons Attribution-NonCommercial 3.0 Unported License](#) from *Faraday Discussions*.

3. The HIV Replication Cycle

HIV-1, like other lentiviruses, undergoes a complex replication cycle that involves interaction with both viral and host proteins (Fig. 2). Mature HIV virions enter the cell through direct contacts with two host cell surface proteins. First, the gp120 subunit of gp160 binds tightly to CD4 on the cell surface, anchoring the virion to the cell and inducing a conformation change in gp160 (44). Secondly, the conformation change that occurs during CD4 binding allows a secondary interaction between the gp41 subunit of gp160 and a secondary co-receptor on the cell surface. Binding by gp41 to the co-receptor allows for membrane fusion, which releases the viral capsid into the cell. The most well described co-receptors are the chemokine receptors CXCR4 and CCR5 (45,46). In general, HIV-1 is adapted to recognize a specific co-receptor with higher affinity, which contributes the cellular tropism of the virus (47-50). However, viruses with affinity to multiple co-receptors (e.g. 89.6) have been studied as well (51,52).

Inside the host cell, reverse transcription of the viral ssRNA genome is completed. Reverse transcription occurs in several steps and is catalyzed by the viral RT. First, the cellular tRNA_{Lys3} is used to prime reverse transcription at the primer binding site on the ssRNA genome (53). Next, the 5' LTR, is reverse transcribed and terminates upon reaching the 5' end of the genome – termed the first strong stop (54). The viral RNase H removes the RNA portion of the DNA-RNA hybrid and liberates the nascent ssDNA, which then anneals to its corresponding reverse complement on the 3' end of the ssRNA genome (55,56). From here, RT converts the remaining length of the viral ssRNA genome to ssDNA. Two regions of high purine density (the central and 3' PPTs) are resistant to RNase H activity and act as primers to allow RT to synthesize the second strand of the viral ssDNA (23). Conversion of the ssRNA genome to

double-stranded (ds) DNA is a highly error-prone process and results in frequent mutations in the viral genome (57).

The dsDNA forms a complex with a number of viral and cellular proteins, which make up the PIC. The full composition of the PIC remains to be elucidated but includes RT, IN, MA, CA, and Vpr, in addition to a number of cellular proteins (58,59). The function of the PIC is to prepare the viral dsDNA for integration into the host genome, to facilitate the import of the viral dsDNA into the nucleus of the infected cell, and to mediate its interaction with a chromosome (60,61).

Integration is made up of three distinct biochemical steps (Fig. 3), each of which is required to successfully insert the viral dsDNA into the host genome: 1) two to three nucleotides are removed from both 3' ends of the viral dsDNA by the viral integrase (IN), 2) the 3' ends of the viral dsDNA are covalently linked to the host's chromosomal DNA by transesterification catalyzed by IN (62), and 3) a four to six nucleotide ss DNA gap between the 5' end of the viral DNA and 3' end of the host chromosomal DNA is filled and ligated after removing mismatches at the 5' ends of the viral DNA, resulting in a completely integrated provirus. The viral IN catalyzes the first two steps, while the cellular DNA repair machinery is thought to carry out the third step (61). Within the context of integration, at least three enzymatic steps are required for gap repair: strand displacement synthesis by a DNA polymerase, removal of the DNA overhang by a flap endonuclease, and ligation of the resulting nicked DNA (63).

Once integrated, the provirus is transcribed by the host transcriptional machinery, which undergoes splicing to yield the early transcripts that code for Rev and Tat. Tat interacts with the trans-activation response element within the viral RNA, which in turn stimulates the cellular transcriptional elongation complex and increases the production of viral RNA (64,65). Rev,

which contains a nuclear import signal, binds to unspliced viral RNA and allows the full-length transcript to be exported to the cytosol where it encodes the viral polyproteins (33). Packaging of viral proteins and polyproteins produced from this full-length transcript occurs at the cell surface where new viral particles are released (66).

Immature virions are released from infected cells and require pH-dependent activation of PR, which leads to processing of each of the viral proteins and ultimately the formation of a mature, infectious viral particle (67). During the maturation process, distinct morphological changes occur within the virion and are observable by electron microscopy (68). Within the virion, the viral RNA genome is encapsidated by the core capsid protein (CA), the matrix protein (MA), and the nucleocapsid protein (NC), which interacts directly with the RNA genome. Once assembled, the now mature virions are able to infect new target cells (67).

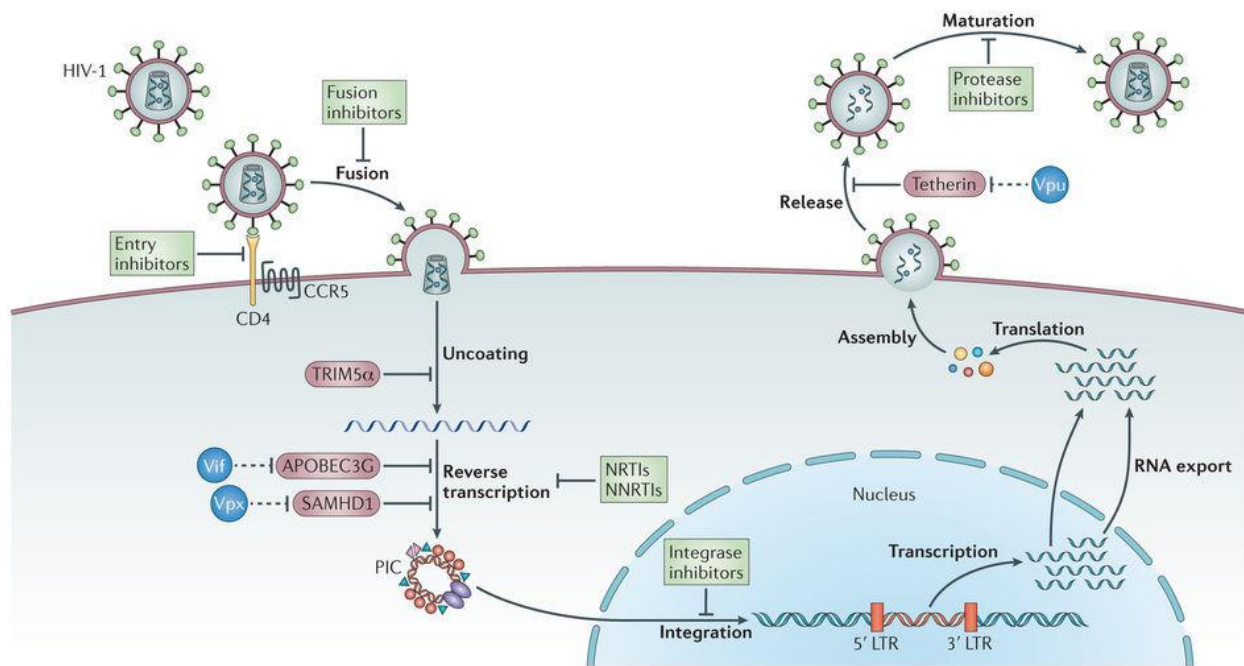


Figure 2: The HIV-1 replication cycle. Essential steps in the HIV-1 replication cycle are shown with pharmacologically targetable steps indicated (green boxes). Cellular restriction factors (red bubbles) interfere with replication as denoted and are counteracted by HIV-1 (or SIV/HIV-2 for Vpx) accessory proteins (blue circles). Adapted by permission from Macmillan Publishers Ltd: *Nature Reviews Microbiology*. Barré-Sinoussi, et. al., copyright (2013).

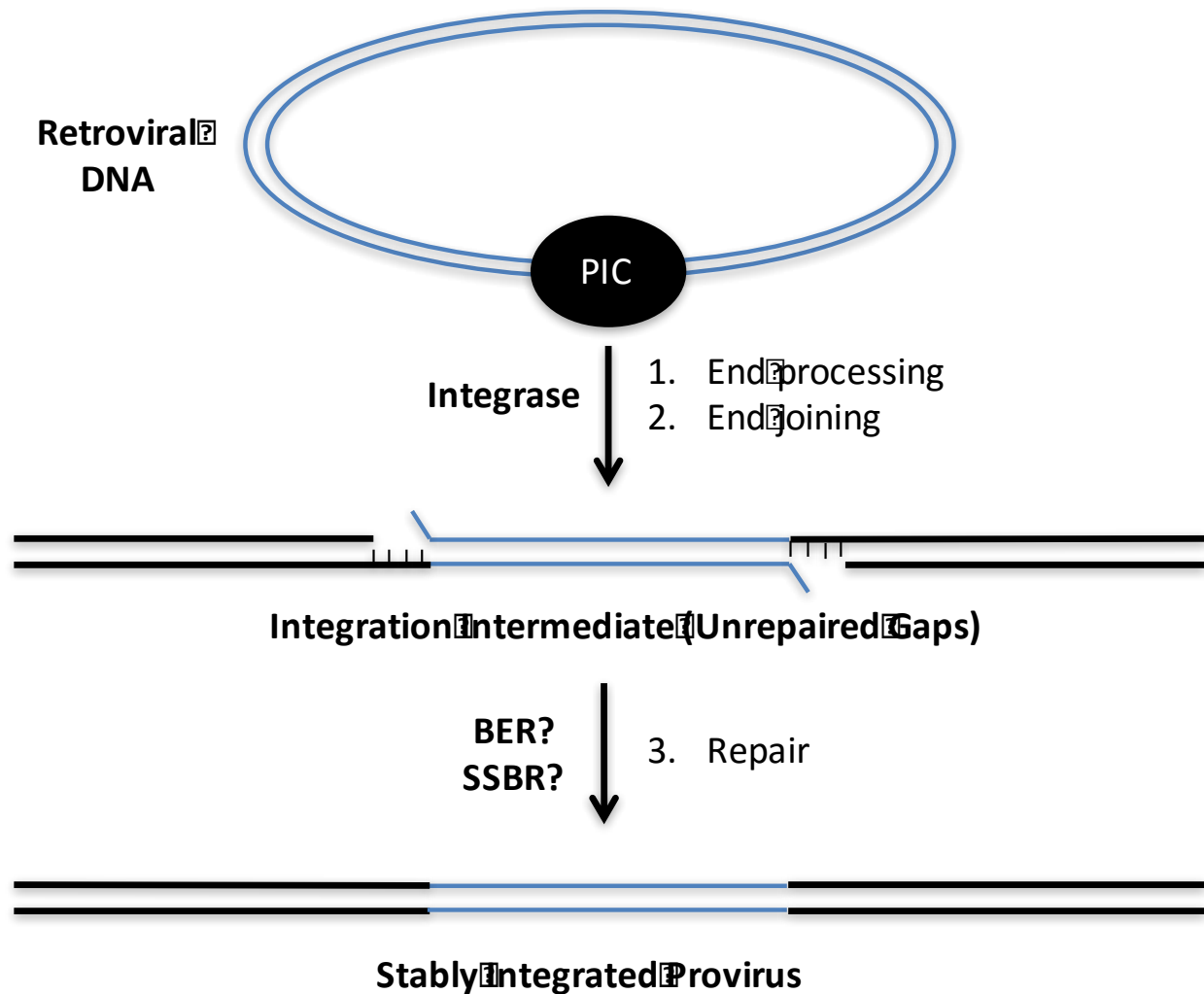


Figure 3: Detailed mechanism of lentivirus integration. HIV-1 IN, as part of the pre-integration complex (PIC; black oval) processes the 3' ends of linear viral dsDNA (blue) by removing two nucleotides, which are used as the substrate in a transesterification reaction (strand transfer or end joining) that covalently links the viral and host DNA. 5' end processing is thought to be performed by the host cell DNA damage repair machinery. There is no conclusive evidence that a single repair pathway is solely responsible for processing the 5' end of the viral genome and may vary between cell types or depend on cellular context. For example, whether this process relies on different enzymes in dividing and nondividing cells is not well characterized.

4. Treatment of HIV Infection with Direct-acting Antivirals

Combinations of direct-acting antiviral drugs that target viral replication enzymes are the primary treatment for HIV-1 infection. The first class of drug used to treat infection was the nucleoside reverse transcriptase inhibitor (NRTI). Among these drugs, zidovudine (AZT) was the first to be introduced in the clinic in 1985 (69). A number of other NTRIs followed shortly after AZT: zalcitabine (ddC), didanosine (ddI), and stavudine (d4T) (70-72). NRTIs work either by directly inhibiting reverse transcription through chain termination, which occurs due to the absence of a 3'-OH to which further nucleotides can be added (73). Alternatively, NRTIs may act by acting as mutagens. Mutagenic nucleoside analogs have non-canonical bases that produce abnormal base pairing and therefore cause hypermutation of the second DNA strand as it is reverse transcribed, which leads to the production of non-functional proteins from the mutated DNA (74). The development of lamivudine (3TC), another nucleoside analog, was a particularly important step in the treatment of HIV-1. Because it acts synergistically with AZT, the two drugs could be used in a combination therapy that allowed a significantly lower amount of the relatively toxic AZT to be used and reduce the side effects associated with AZT monotherapy (75).

Two new classes of drugs for HIV-1 treatment were introduced in the mid-1990s – the non-nucleoside reverse transcriptase inhibitors (NNRTI) and the protease inhibitors (PI). NNRTI binds to an allosteric site on RT and inhibits enzyme activity by inducing a conformation change in the enzyme. Nevirapine reached the market in 1996 as the first NNRTI to be introduced (76). Monotherapy with NNRTI leads to rapid selection for resistance mutations and therefore NNRTI are used only in combination with other antiviral drugs (77). The first protease inhibitor to gain regulatory approval was saquinavir, which entered the market in 1995 (78). The development of

additional protease inhibitors allowed for several iterations of combination therapy to be evaluated in the clinic and led to significant improvements in patient lifespan (79-81).

Entry and fusion inhibitors were the next class of drugs developed for HIV treatment. These drugs act by disrupting the interactions between the viral surface glycoprotein and their cognate cellular receptors. These drugs, however, are generally used only as a last resort when other treatment regimens fail due to their relatively poor route of administration (enfuvirtide) or poor side effect profile (maraviroc) (82,83).

Another significant advancement occurred in the mid-2000s with the development of the integrase inhibitors (II). These drugs bind to the active site of the viral IN and disrupt metal binding that is required for enzyme activity. Raltegravir was the first II introduced in 2007 (84). Combination therapies consisting of two NRTI and either an II or PI are the typical standard of care today in developed countries and have led to significant improvements in patient outcomes including in so-called salvage therapy – treatment of patients who have failed previous treatments with antiretroviral drugs (85,86).

5. Factors Controlling HIV Target Cell Specificity

The specificity for certain types of target cells by a virus is referred to as its tropism. Tropism is determined by a number of factors including expression of the appropriate receptors required for binding by the viral envelope glycoprotein, which in the case of HIV are CD4 (primary) and CXCR4 or CCR5 (secondary co-receptor) (44-52). However, while expression of the correct entry receptors is required for successful infection of a target cell, it is not necessarily sufficient. For example, as described above, there are a number of host factors that function to restrict the capacity of HIV to replicate inside infected cells (37,42). Without viral proteins that

disrupt such functions, viral replication is inefficient, if not impossible in the presence of these factors (36,37,43). Alternatively, a virus may require cell-specific processes to replicate or transmit efficiently. For example, some viruses depend on specific cellular transcription factors to produce viral mRNA (87-89). Collectively, the network of host-pathogen interactions that exist between a virus and specific cell types defines the ideal target cells of the virus. Additionally, viruses may evolve different strategies for overcoming an individual block to a step in its replication – even within closely related viruses. Notably, HIV and other lentiviruses infect both dividing and nondividing cells (90). Since the active metabolic state of these two groups varies significantly (i.e. the requirement or lack thereof for DNA replication and cell division), there are different barriers that must be overcome for successful replication to occur in both cell types. One such barrier is the availability of 2'-deoxyribonucleoside-5'-triphosphates (dNTPs) (91).

B. Cellular Control of Nucleotides

Regulation of cellular nucleotides is critical for maintaining homeostasis. Not only are nucleotides and deoxyribonucleotides the building blocks of RNA and DNA, respectively, but they are also critical signaling molecules that are required for cellular growth, replication, and function. Structurally, nucleotides are composed of three moieties: a sugar, a base, and a phosphate. The sugar moiety of nucleotides is a ribose molecule. The base moiety is synthesized through one of two pathways: *de novo* synthesis or salvage. In *de novo* synthesis, a series of enzymatic reactions creates base molecules from other cellular metabolites. Five base molecules make up the majority of nucleotides in the cell: adenosine, guanine, thymine, cytidine, and uracil; modification of these bases occur as both part of normal cellular function and from

exposure to reactive molecules such as reactive oxygen species. The salvage pathway utilizes available preformed base molecules available from the degradation of nucleotides to attach to ribose molecules and generate new nucleotides. Lastly, nucleotides contain a phosphate group attached to the 5' hydroxyl group of the sugar. This group may be a mono-, di-, or triphosphate. The addition of each phosphate group, particularly the gamma phosphate, increases the potential energy of the nucleotide. A number of cellular enzymes catalyze the phosphorylation of nucleotides and deoxyribonucleotides in a base-specific manner. Nucleotide triphosphates and deoxyribonucleotide triphosphates are required for the synthesis of RNA and DNA, respectively (92).

Deoxyribonucleotides are synthesized from nucleotides by direct reduction of the sugar, ribose, to the dehydrated deoxyribose. The heterodimeric enzyme, ribonucleotide reductase (RNR), catalyzes the reduction of nucleotide diphosphates to deoxyribonucleotide diphosphates (93). RNR activity is allosterically regulated at two distinct sites. The first allosteric binding site controls the activity of the enzyme. This site binds ATP and dATP, which control the oligomerization of the enzyme complex. Low concentrations of dATP will allow binding of ATP and activation of enzyme activity. With increasing concentrations of dATP, ATP is displaced and a conformational change in RNR induces hexamerization and inhibits enzyme activity. The second allosteric site regulates the affinity of RNR for different nucleotide bases. This site binds ATP, GTP, dATP, and dGTP. Binding by each of these molecules induces a distinct conformational change in RNR, which leads to differential affinity for its substrate. Through regulation by both allosteric sites, RNR function is balanced to yield a pool of nucleotides and deoxyribonucleotides that suits the energetic needs of the cell (94,95).

Additionally, dNTP concentrations are regulated through their controlled degradation by the sterile alpha motif and histidine and aspartic acid domain containing protein 1 (SAMHD1). SAMHD1 is a triphosphohydrolase that cleaves the triphosphate at the alpha linkage yielding a triphosphate molecule and a deoxyribonucleoside (dN) (96-98). SAMHD1 is expressed in all cells, but its stability is regulated by the cell cycle. SAMHD1 is phosphorylated by cyclin A2/CDK1 at threonine 592 in cycling cells, which leads to a decrease in its triphosphohydrolase activity (99,100). SAMHD1 expression and activity was shown to restrict retrovirus and DNA virus replication in nondividing myeloid cells, which have high levels of SAMHD1 expression (101,102). The level of restriction in these cells correlates with the dNTP concentration and SAMHD1 triphosphohydrolase activity (103). Like RNR, SAMHD1 is allosterically regulated by nucleotides and deoxyribonucleotides. SAMHD1 monomers are catalytically inactive, but assemble into an active homotetramer through interactions bridged by the binding of allosteric activators in two distinct allosteric binding pockets. Binding of GTP or dGTP in the first allosteric site allows two SAMHD1 monomers to dimerize and subsequent binding of any dNTP to the second allosteric site allows two dimers to join forming the active tetramer (104). The active state of SAMHD1 shows varying affinity towards the four canonical dNTPs (105). Together RNR and SAMHD1 control the temporal availability of dNTPs throughout the cell cycle (Fig. 4).

Lentiviruses have evolved two different strategies for bypassing the replication block presented by SAMHD1 in nondividing cells, which are well illustrated by the example of HIV-1 and the related virus, HIV-2. Unlike the highly pathogenic HIV-1, which is responsible for the worldwide AIDS crisis, HIV-2 is endemic to certain regions in West Africa and progresses to clinical disease much more slowly (106). Based on sequence identity, HIV-2 is closely related to

simian immunodeficiency virus (SIV) from sooty mangabeys (SIV_{smm}) (107). Both HIV-2 and SIV_{smm} code for a protein called viral protein X (Vpx), which arose from a gene duplication event that resulted in a second copy of *vpr* being introduced into the viral genome. The duplicated gene diverged to give rise to the modern *vpx* gene (108). Similarly to Vpr, Vpx functions by acting as an adaptor to the host cell ubiquitin ligase system and drives degradation of cellular proteins through this interaction. Specifically, Vpx targets SAMHD1 for degradation and there is a corresponding increase in dNTPs in cells infected with Vpx-expressing lentiviruses. By targeting SAMHD1, lentiviruses that express Vpx are able to bypass the block on reverse transcription by increasing the availability of intracellular dNTPs (109,110). In contrast, HIV-1 and its SIV predecessor from chimpanzees (SIV_{cpz}) evolved without Vpx and its benefit of higher dNTP availability during infection of nondividing cells. However, studies of lentivirus enzyme kinetics have revealed that due to this selective pressure viruses that do not encode Vpx have evolved to encode RT enzymes that catalyze DNA synthesis with higher efficiency at low dNTP concentrations relative to their counterparts from Vpx-coding viruses (111,112).

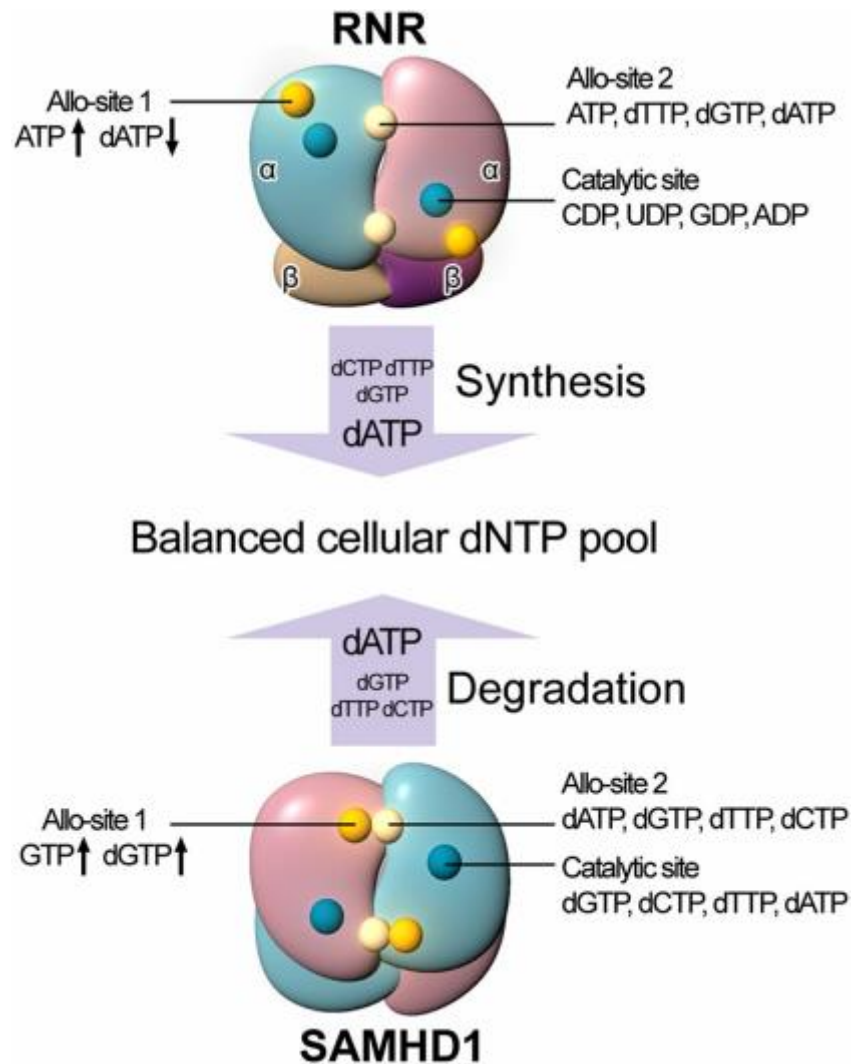


Figure 4: Allosteric regulation of RNR and SAMHD1 leads to balanced dNTP pools. Assembly of RNR and SAMHD1 oligomers is dependent upon binding of dNTPs at allosteric sites. These two enzymes perform inverse functions that both balance dNTP pools through base-driven specificity and overall dNTP levels as dictated by cell cycle and division status through cellular signaling mechanisms. Detailed analysis of whether many non-canonical dNTPs and nucleoside analogues are allosteric activators and/or substrates for SAMHD1 has yet to be determined. Figure reproduced from Ji, Xiaoyun, et al. (2014). Structural basis of cellular dNTP regulation by SAMHD1. *Proceedings of the National Academy of Sciences*, 111(41): E4305-E4314.

C. Cellular DNA Damage Sensing and Repair Mechanisms

Damage to the genome occurs through both normal cellular processes and exposure to damaging agents. DNA replication has an intrinsic rate of base pair mismatching that requires correction in order to preserve the accuracy of the genetic code (113). Additionally, metabolic processes that generate reactive oxygen and nitrogen species may react with DNA, yielding oxidative damage. Exposure to chemical entities that form adducts on DNA (e.g. alkylating agents) produces DNA changes that interfere with transcription and DNA replication and require repair before normal cellular function can resume (114). Because such damage to DNA results in the inability to faithfully reproduce the genome or carry out normal function, organisms have evolved mechanisms to detect and repair DNA damage (115) (Fig. 5).

In a broad sense, DNA repair comes in three flavors. Excision-based repair removes damaged components of DNA by cutting the damaged piece out and replacing it with a new component (116,117). Single-strand break (SSB) repair fixes damage that leaves one strand of DNA broken, but the complementary strand intact (118). Double-strand break (DSB) repair deals with damage that results in a break that leaves both strands broken and creates two free ends (119). Each type of DNA repair involves three broad classes of molecules: sensors, transducers, and effectors (120). Sensors identify damaged DNA sites within the genome and recruit signal transducers, which transmit a signal through phosphorylation cascades. Sensors include the MRN complex and DDB2/XPC complex, but it is thought that many other sensors remain undiscovered (121,122). Transducers are primarily kinases that include the phospho-inositol kinase-related proteins including ATM and ATR. These molecules signal to downstream checkpoint kinases such as Chk1 and Chk2. This signaling cascade acts to amplify the DNA damage response (123). Effectors are the targets of these kinases and include transcriptional

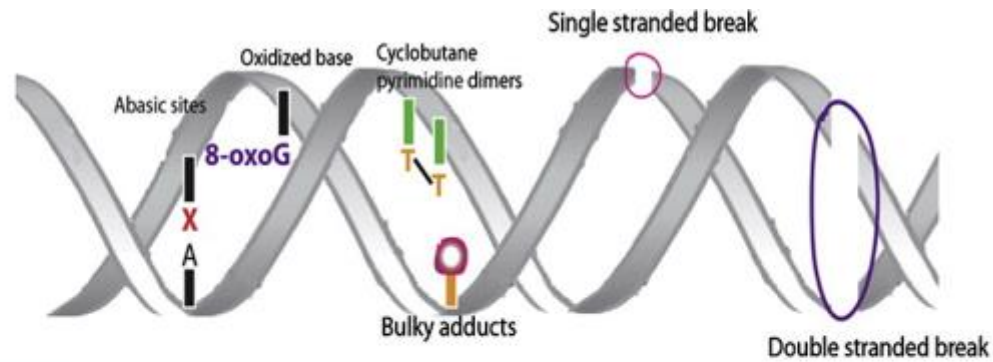
regulators, which halt cell cycle progression and initiate the expression of enzymes that directly repair the damaged DNA (120,124). Since each type of DNA damage is biochemically distinct, the makeup of sensors, transducers, and effectors that acts on a particular substrate is fairly complex and varies based on many factors (115,120).

A number of studies have examined the type of DNA damage that occurs during retroviral integration and the cellular repair mechanisms that are involved in its sensing and repair. Several enzymes involved in DSB repair including ATM, ATR, DNA-PK, and PARP-1 were shown to be beneficial to HIV replication in early experiments (125-128). However, further study showed that these enzymes perform a cytoprotective function that prevents linear viral dsDNA from accumulating in the nucleus of infected cells. Linear viral dsDNA is sensed by innate immune molecules that trigger an apoptotic cascade in the absence of these DNA repair enzymes, which circularize the dsDNA into episomal structures referred to as 1- and 2-LTR circles (129). While this mechanism is protective, it is not essential for integration (130).

Other studies have developed *in vitro* substrate models that mimic the structure of the integration intermediate. These models have been used to biochemically demonstrate which enzymes are required to repair a defined oligonucleotide substrate derived from an HIV LTR sequence. From these experiments, we know that repair of a single-strand gapped intermediate requires, at minimum, a DNA polymerase to fill in the gap, an endonuclease to remove the flap displaced by the DNA polymerase, and a ligase to seal the nicked DNA strand. This study revealed that any of a number of different DNA polymerases (Pols) including Pols β , δ (together with PCNA), and RT could perform the gap filling reaction (63). Although these studies are very informative in terms of defining the biochemistry of gap repair, it remained unclear whether such redundancy was relevant in cellular systems. Further studies demonstrated the effect of

knockdown (KD) and knockout (KO) of DNA repair enzymes on retrovirus replication. Of note, it was proposed that KD or KO of Pol β limited HIV replication and that Pol β may represent a pharmacological target for blocking HIV gap repair (131,132).

Pol β is a member of the family X DNA polymerases, which includes Pols β , λ , and μ (133). Pol β is a 39 kD monomeric protein encoded by the *POLB* gene. It consists of two domains: an N-terminal 5'-2-deoxyribose-5-phosphate (dRP) lyase domain and a C-terminal polymerase domain (134). Both the dRP lyase and polymerase domains perform critical functions in DNA repair. Pol β was shown to be involved in DNA polymerization steps required for the base excision repair (BER) pathway (135). Furthermore, it was shown that Pol β is involved in both short- and long-patch repair mechanisms of the BER pathway (136). Additionally, the lyase activity was required to maintain BER activity in cellular models tested with the alkylating agent methyl methanesulfonate (MMS) (137). In the absence of Pol β , Pol λ has been shown to perform its role in BER, though with lower efficiency (63). Pol λ also possesses both dRP lyase and DNA polymerase activity (133). To date, it has not been definitively shown whether either Pols β or λ are required for efficient HIV integration.



Type of lesions		Single base damage (oxidation, alkylation, deamination, abasic sites)	Modification that distort DNA double helix (Bulky adducts/ crosslinks)	Single stranded breaks (SSBs)	Double stranded breaks (DSBs)	
Major sources of lesion		Reactive oxygen/nitrogen species and other metabolic products	UV Chemical agents Reactive oxygen species	Ionizing radiation Chemotherapy reagents Reactive oxygen species Aborted TOP1 activity	Ionizing radiation Chemotherapy reagents Aborted TOPII activity Neuronal activity	
Repair pathway		BER	GG-NER TC-NER	SSBR	DSBR-HR	DSBR-NHEJ
Key molecules involved	Detection		XPC-HR23B CSA,CSB	PARP1	ATM, MRE11-RAD50-NBS1	KU70/80, DNAPK
	Damage removal/end processing	DNA Glycosylases	XPB, XPD, XPA, TFIIH, RPA	PNKP, APE1, APTX, TDP1	BRCA1, CtIP, EXO1, RPA	WRN, TDP2, Artemis,
	Gap filling/DNA synthesis	APE1	ERCC1-XPF, XPG	Pol β PCNA, Pol δ/ε/κ	RAD51, BRCA1/2, XRCC2/3	Pol
	Ligation	Pol β PCNA, Pol δ/ε/κ	PCNA, RFC, Pol δ/ε/κ	XRCC1-LIG3 FEN1, LIG1	Pol LIG1	XRCC4, LIG4, XLF
Associated neurological diseases			Xeroderma Pigmentosum, Cockayne Syndrome, Trichothiodystrophy	AOA1, SCAN1	A-T, ATLD, NBS, ATR-Seckel Syndrome, LIG4 Syndrome, XLF Syndrome	

Figure 5: DNA damage and repair mechanisms. DNA damage occurs due to many sources and depends on multiple pathways to sense, transmit signals to, and activate effector molecules that repair the damage. Outlines are provided for BER, NER, SSB repair, and DSB repair. Note, Pol β participates in both BER and SSB repair. Whether Pol β is essential for repair in the context of HIV gap repair or in DNA repair, in general, in nondividing cells is unknown. Reprinted from *Journal of Molecular Biology*, 426(20), Ling Pan, et. al., Chromatin Regulation of DNA Damage Repair and Genome Integrity in the Central Nervous System, 3376-3388, Copyright (2014), with permission from Elsevier.

D. Genome Editing Techniques

Genome editing techniques have come into the spotlight of medical technology because of their promise to treat a vast array of human diseases from viral infections to congenital metabolic disorders. In addition to their utility as therapeutic agents, such editing techniques also have tremendous capability to shape our understanding of cellular and molecular biology with the ability to introduce genetic changes at will into established or novel cell lines. With the ability to make on-demand changes to the genome, researchers are now equipped to ask questions about gene function in both a high throughput and streamlined fashion.

The current technology includes four different nuclease-based strategies that introduce changes at the genome level by relying on cellular DNA repair machinery. Meganucleases, zinc finger nucleases (ZFNs), transcription activator-like effector nucleases (TALENs), and clustered regularly interspaced short palindromic repeats (CRISPR) coupled with Cas nuclease have all been demonstrated as effective technology for genome editing in a number of cellular and living systems.

The discovery of homologous recombination, a type of homology-directed repair used to repair DSBs, was an essential prerequisite for the development of gene editing technology (138). The first attempts at nuclease-directed HDR editing in mammalian genome used the yeast meganuclease, *I-SceI*. *I-SceI* recognized a rare 18 base pair sequence within the genome and cut the DNA at this sequence, resulting in a DSB (139,140). By providing a complementary donor DNA in tandem, the cell could repair the break and introduce any additional sequence included between the complementary sequences on each end of the donor DNA. Meganucleases engineered to recognize a specific sequence were first used to modify human cells in 2009 (141).

Around this time, the first ZFNs were being developed. Like all current gene editing technologies, ZFNs consist of a nuclease domain and a DNA binding domain and rely on cellular repair systems to perform HR or NHEJ. In this case, the endonuclease domain is derived from the restriction enzyme, *FokI*. The DNA binding domain is comprised of an array of zinc-fingers, which confer specificity designed to recognize the desired genomic sequence. Each zinc-finger recognizes a three-nucleotide sequence and can be combined with other custom fingers that can create unique binding domains that recognize up to about 18 nucleotides (142). ZFNs have been used to develop new gene therapy strategies, create novel animal models for both large and small species, and for creating novel cell lines (143-146). However, the method used to engineer custom ZFNs is largely proprietary and has therefore limited the use of this strategy for gene editing due to its relatively high cost compared to TALENs and CRISPR (147). Additionally, the affinity of ZFNs for their target sequences has relatively poor affinity compared to these other technologies (148). Because of these limitations, ZFNs have failed to find the level of mainstream success of other gene editing methods.

TALENs were developed shortly after ZFNs and in 2011 the first KO rats were created using this technology (149). The DNA binding domain of TALENs is derived from the plant pathogen, *Xanthomonas*, which expresses the transcription activator-like effector (TALE) proteins. These TALE proteins allow the bacteria to activate certain genes that enhance their ability to colonize their hosts. Researchers have used TALE proteins alone to activate or suppress genes of interest by engineering their specificity (150). Additionally, through coupling with the *FokI* endonuclease, TALENs are able to induce DSBs in target genes using the same engineering process (151). However, compared to other systems, engineering unique TALE proteins requires lengthy molecular cloning steps that make the system relatively more complex

to set up. Furthermore, it remains difficult to predict whether engineered TALE proteins will have a highly specific binding interaction with their desired target sequence and require more extensive validation processes relatively to other gene editing technology (152).

Most recently, CRISPR technology has become the tool of choice for laboratories performing genetic engineering and gene editing studies. CRISPR is a type of bacterial adaptive defense system that stores piece of genetic material from viruses, which is then used to protect against subsequent infection. The genetic material is stored within the bacterial genome as a spacer sequence between clusters of repeating palindromic sequences. Transcription of these spacers produces RNA complementary to the viral DNA sequence initially encountered. When this RNA is coupled with a Cas protein, which is an effector nuclease, the spacer RNA (called a guideRNA or gRNA) hybridizes with the corresponding DNA sequence and allows the Cas protein to cleave the target DNA (153). By combining a customized gRNA sequence with a Cas effector protein in a vector delivery system, many desirable genomic DNA sequences can be targeted with ease (154). The simplicity of this system has made it easily accessible to laboratories with modest molecular biology capabilities. Combined with its relatively low cost, CRISPR-based gene editing systems have significant advantages over other systems. To date, CRISPR-based systems have been used to develop novel gene therapy strategies, create KO animal models, generate desired mutations in livestock and crops, and even to correct inborn genetic errors in embryos (though these embryos were not implanted due to concerns about potential off-target effects) (155-157). Although the specificity conferred by the direct Watson-Crick base-pair interactions between the gRNA and the target genomic DNA is greater than the protein-DNA interactions of other systems, it is not without the potential for error. Off-target

binding and cleavage is the most significant concern with the CRISPR-Cas system and represents an area of ongoing development (158-160).

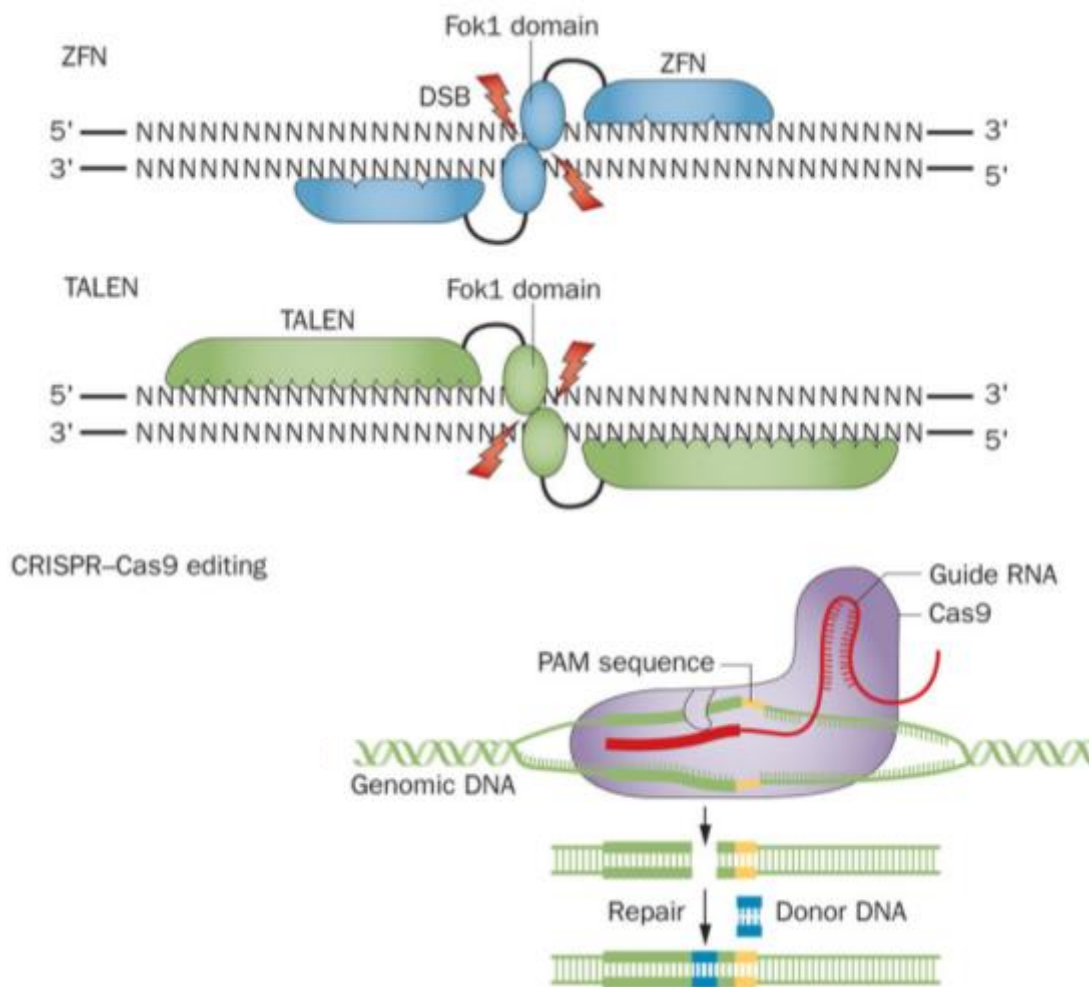


Figure 6: Genome editing techniques. ZFN, TALEN, and CRISPR work through the same molecular mechanism. Each system relies on a nuclease domain – Fok1 in the case of ZFN and TALEN, while CRISPR most frequently uses Cas9 nuclease. Nuclease dimers cut both DNA strands, resulting in a DSB (lightning bolt). Repair by NHEJ frequently results in inserts or deletions. If a homologous donor DNA is provided, HDR can result in genomic repair that includes the desired sequence. ZFNs and TALENs use engineered proteins (blue and green, respectively) to specifically recognize a desired DNA sequence, while CRISPR uses Watson-Crick base pairing between a gRNA (red) and the DNA target. Adapted by permission from Macmillan Publishers Ltd: *Nature Reviews Neurology*. Khurana, et. al., copyright (2015).

E. References

1. Centers for Disease Control and Prevention (CDC). 1981, June 5. *Pneumocystis* Pneumonia --- Los Angeles. *MMWR. Morbidity and Mortality Weekly Reports*. Retrieved from https://www.cdc.gov/mmwr/preview/mmwrhtml/june_5.htm
2. Haverkos, H. W., & Curran, J. W. (1982). The current outbreak of Kaposi's sarcoma and opportunistic infections. *CA: a cancer journal for clinicians*, 32(6), 330-339.
3. Centers for Disease Control and Prevention (CDC). 1982, September 24. Current Trends Update on Acquired Immune Deficiency Syndrome (AIDS) –United States. *MMWR. Morbidity and Mortality Weekly Reports*. Retrieved from <https://www.cdc.gov/mmwr/preview/mmwrhtml/00001163.htm>
4. Centers for Disease Control and Prevention (CDC). 1983, March 4. Current Trends Prevention of Acquired Immune Deficiency Syndrome (AIDS): Report of Inter-Agency Recommendations. *MMWR. Morbidity and Mortality Weekly Reports*. Retrieved from <https://www.cdc.gov/mmwr/preview/mmwrhtml/00001257.htm>
5. Barré-Sinoussi, F., Chermann, J. C., Rey, F., Nugeyre, M. T., Chamaret, S., Gruest, J., Dauguet, C., Axler-Blin, C., Vézinet-Brun, F., Rouzioux, C., Rozenbaum, W., and Montagnier, L. (1983) Isolation of a T-lymphotropic retrovirus from a patient at risk for acquired immune deficiency syndrome (AIDS). *Science* 220, 868-871
6. Gallo, R. C., Sarin, P. S., Gelmann, E. P., Robert-Guroff, M., Richardson, E., Kalyanaraman, V. S., ... & Leibowitch, J. (1983). Isolation of human T-cell leukemia virus in acquired immune deficiency syndrome (AIDS). *Science*, 220(4599), 865-867.
7. Poiesz, B. J., Ruscetti, F. W., Gazdar, A. F., Bunn, P. A., Minna, J. D., & Gallo, R. C. (1980). Detection and isolation of type C retrovirus particles from fresh and cultured

- lymphocytes of a patient with cutaneous T-cell lymphoma. *Proceedings of the National Academy of Sciences*, 77(12), 7415-7419.
8. Morgan, D. A., Ruscetti, F. W., & Gallo, R. (1976). Selective in vitro growth of T lymphocytes from normal human bone marrows. *Science*, 193(4257), 1007-1008.
 9. Coffin, J. M., Hughes, S. H., and Varmus, H. E. (1997) *Retroviruses*, Cold Spring Harbor Laboratory Press, Cold Spring Harbor, NY
 10. Frankel, A. D., & Young, J. A. (1998). HIV-1: fifteen proteins and an RNA.
 11. Saad, J. S., Miller, J., Tai, J., Kim, A., Ghanam, R. H., & Summers, M. F. (2006). Structural basis for targeting HIV-1 Gag proteins to the plasma membrane for virus assembly. *Proceedings of the National Academy of Sciences*, 103(30), 11364-11369.
 12. Gallay, P., Swingler, S., Song, J., Bushman, F., & Trono, D. (1995). HIV nuclear import is governed by the phosphotyrosine-mediated binding of matrix to the core domain of integrase. *Cell*, 83(4), 569-576.
 13. Von Schwedler, U. K., Stemmler, T. L., Klishko, V. Y., Li, S., Albertine, K. H., Davis, D. R., & Sundquist, W. I. (1998). Proteolytic refolding of the HIV-1 capsid protein amino-terminus facilitates viral core assembly. *The EMBO journal*, 17(6), 1555-1568.
 14. Zhao, G., Perilla, J. R., Yufenyuy, E. L., Meng, X., Chen, B., Ning, J., ... & Zhang, P. (2013). Mature HIV-1 capsid structure by cryo-electron microscopy and all-atom molecular dynamics. *Nature*, 497(7451), 643.
 15. Post, K., Kankia, B., Gopalakrishnan, S., Yang, V., Cramer, E., Saladores, P., ... & Levin, J. G. (2009). Fidelity of plus-strand priming requires the nucleic acid chaperone activity of HIV-1 nucleocapsid protein. *Nucleic acids research*, 37(6), 1755-1766.

16. Selig, L., Pages, J. C., Tanchou, V., Preveral, S., Berlioz-Torrent, C., Liu, L. X., ... & Benichou, S. (1999). Interaction with the p6 domain of the gag precursor mediates incorporation into virions of Vpr and Vpx proteins from primate lentiviruses. *Journal of virology*, 73(1), 592-600.
17. Dinman, J. D., Icho, T., & Wickner, R. B. (1991). A-1 ribosomal frameshift in a double-stranded RNA virus of yeast forms a gag-pol fusion protein. *Proceedings of the National Academy of Sciences*, 88(1), 174-178.
18. Kontos, H., Naphthine, S., & Brierley, I. (2001). Ribosomal pausing at a frameshifter RNA pseudoknot is sensitive to reading phase but shows little correlation with frameshift efficiency. *Molecular and cellular biology*, 21(24), 8657-8670.
19. Kohl, N. E., Emini, E. A., Schleif, W. A., Davis, L. J., Heimbach, J. C., Dixon, R. A., ... & Sigal, I. S. (1988). Active human immunodeficiency virus protease is required for viral infectivity. *Proceedings of the National Academy of Sciences*, 85(13), 4686-4690.
20. Davies, D.R. (1990) The structure and function of the aspartic proteinases. *Annual Review of Biophysics and Biophysical Chemistry* **19**: 189-215.
21. Hizi, A., Tal, R., Shaharabany, M., & Loya, S. (1991). Catalytic properties of the reverse transcriptases of human immunodeficiency viruses type 1 and type 2. *Journal of Biological Chemistry*, 266(10), 6230-6239.
22. Hansen, J., Schulze, T., Mellert, W., & Moelling, K. (1988). Identification and characterization of HIV-specific RNase H by monoclonal antibody. *The EMBO journal*, 7(1), 239.
23. Woehrl, B. M., & Moelling, K. (1990). Interaction of HIV-1 ribonuclease H with polypurine tract containing RNA-DNA hybrids. *Biochemistry*, 29(44), 10141-10147.

24. Cherepanov, P., Sun, Z. Y. J., Rahman, S., Maertens, G., Wagner, G., & Engelman, A. (2005). Solution structure of the HIV-1 integrase-binding domain in LEDGF/p75. *Nature structural & molecular biology*, 12(6).
25. Kessl, J. J., Kutluay, S. B., Townsend, D., Rebensburg, S., Slaughter, A., Larue, R. C., ... & Kvaratskhelia, M. (2016). HIV-1 integrase binds the viral RNA genome and is essential during virion morphogenesis. *Cell*, 166(5), 1257-1268.
26. Decroly E, Benjannet S, Savaria D and Seidah NG (1997) Comparative functional role of PC7 and furin in the processing of the HIV envelope glycoprotein gp160. *Febs Letters* 405(1): 68-72.
27. Bahraoui E, Benjouad A, Guetard D, Kolbe H, Gluckman JC and Montagnier L (1992) Study of the interaction of HIV-1 and HIV-2 envelope glycoproteins with the CD4 receptor and role of N-glycans. *AIDS Research and Human Retroviruses* 8(5): 565-573.
28. Javaherian, K., Langlois, A., LaRosa, G. J., Profy, A. T., Bolognesi, D. P., Herlihy, W. C., ... & Matthews, T. J. (1990). Broadly neutralizing antibodies elicited by the hypervariable neutralizing determinant of HIV-1. *Science*, 250(4987), 1590-1594.
29. Masuda, T., Matsushita, S., Kuroda, M. J., Kannagi, M., Takatsuki, K., & Harada, S. (1990). Generation of neutralization-resistant HIV-1 in vitro due to amino acid interchanges of third hypervariable env region. *The Journal of Immunology*, 145(10), 3240-3246.
30. Martins, L. P., Chenciner, N., & Wain-hobson, S. (1992). Complex intrapatient sequence variation in the V1 and V2 hypervariable regions of the HIV-1 gp120 envelope sequence. *Virology*, 191(2), 837-845.

31. Ji, J., & Loeb, L. A. (1994). Fidelity of HIV-1 reverse transcriptase copying a hypervariable region of the HIV-1 env gene. *Virology*, *199*(2), 323-330.
32. Ott, M., Geyer, M., & Zhou, Q. (2011). The control of HIV transcription: keeping RNA polymerase II on track. *Cell host & microbe*, *10*(5), 426-435.
33. Fischer, U., Huber, J., Boelens, W. C., Mattajt, L. W., & Lührmann, R. (1995). The HIV-1 Rev activation domain is a nuclear export signal that accesses an export pathway used by specific cellular RNAs. *Cell*, *82*(3), 475-483.
34. Connor, R. I., Chen, B. K., Choe, S., & Landau, N. R. (1995). Vpr is required for efficient replication of human immunodeficiency virus type-1 in mononuclear phagocytes. *Virology*, *206*(2), 935-944.
35. He, J., Choe, S., Walker, R., Di Marzio, P., Morgan, D. O., & Landau, N. R. (1995). Human immunodeficiency virus type 1 viral protein R (Vpr) arrests cells in the G2 phase of the cell cycle by inhibiting p34cdc2 activity. *Journal of virology*, *69*(11), 6705-6711.
36. Strebel, K., Klimkait, T., & Martin, M. A. (1988). A novel gene of HIV-1, vpu, and its 16-kilodalton product. *Science*, *241*(4870), 1221.
37. Neil, S. J., Zang, T., & Bieniasz, P. D. (2008). Tetherin inhibits retrovirus release and is antagonized by HIV-1 Vpu. *Nature*, *451*(7177), 425-430.
38. Garcia, J. V., & Miller, A. D. (1991). Serine phosphorylation-independent downregulation of cell-surface CD4 by nef. *Nature*, *350*(6318), 508-511.
39. Abraham, L., & Fackler, O. T. (2012). HIV-1 Nef: a multifaceted modulator of T cell receptor signaling. *Cell Communication and Signaling*, *10*(1), 39.

40. Laguette, N., Brégnard, C., Benichou, S., & Basmaciogullari, S. (2010). Human immunodeficiency virus (HIV) type-1, HIV-2 and simian immunodeficiency virus Nef proteins. *Molecular aspects of medicine*, 31(5), 418-433.
41. Lubben, N. B., Sahlender, D. A., Motley, A. M., Lehner, P. J., Benaroch, P., & Robinson, M. S. (2007). HIV-1 Nef-induced down-regulation of MHC class I requires AP-1 and clathrin but not PACS-1 and is impeded by AP-2. *Molecular biology of the cell*, 18(9), 3351-3365.
42. Harris, R. S., Bishop, K. N., Sheehy, A. M., Craig, H. M., Petersen-Mahrt, S. K., Watt, I. N., ... & Malim, M. H. (2003). DNA deamination mediates innate immunity to retroviral infection. *Cell*, 113(6), 803-809.
43. Sheehy, A. M., Gaddis, N. C., & Malim, M. H. (2003). The antiretroviral enzyme APOBEC3G is degraded by the proteasome in response to HIV-1 Vif. *Nature medicine*, 9(11), 1404-1408.
44. Stein, B. S., Gowda, S. D., Lifson, J. D., Penhallow, R. C., Bensch, K. G., & Engleman, E. G. (1987). pH-independent HIV entry into CD4-positive T cells via virus envelope fusion to the plasma membrane. *Cell*, 49(5), 659-668.
45. Choe, H., Farzan, M., Sun, Y., Sullivan, N., Rollins, B., Ponath, P. D., ... & Gerard, N. (1996). The β -chemokine receptors CCR3 and CCR5 facilitate infection by primary HIV-1 isolates. *Cell*, 85(7), 1135-1148.
46. Deng, H., Liu, R., Ellmeier, W., Choe, S., Unutmaz, D., Burkhart, M., ... & Davis, C. B. (1996). Identification of a major co-receptor for primary isolates of HIV-1. *Nature*, 381(6584), 661-666.

47. Åsjö, B., Albert, J., Karlsson, A., Morfeldt-Månson, L., Biberfeld, G., Lidman, K., & Fenyö, E. (1986). Replicative capacity of human immunodeficiency virus from patients with varying severity of HIV infection. *The Lancet*, 328(8508), 660-662.
48. Lu, Z. H., Berson, J. F., Chen, Y. H., Turner, J. D., Zhang, T. Y., Sharron, M., ... & Hoxie, J. A. (1997). Evolution of HIV-1 coreceptor usage through interactions with distinct CCR5 and CXCR4 domains. *Proceedings of the National Academy of Sciences*, 94(12), 6426-6431.
49. Björndal, A., Deng, H., Jansson, M., Fiore, J. R., Colognesi, C., Karlsson, A., ... & Fenyö, E. M. (1997). Coreceptor usage of primary human immunodeficiency virus type 1 isolates varies according to biological phenotype. *Journal of virology*, 71(10), 7478-7487.
50. Bleul, C. C., Wu, L., Hoxie, J. A., Springer, T. A., & Mackay, C. R. (1997). The HIV coreceptors CXCR4 and CCR5 are differentially expressed and regulated on human T lymphocytes. *Proceedings of the National Academy of Sciences*, 94(5), 1925-1930.
51. Collman, R., Balliet, J. W., Gregory, S. A., Friedman, H., Kolson, D. L., Nathanson, N., & Srinivasan, A. (1992). An infectious molecular clone of an unusual macrophage-tropic and highly cytopathic strain of human immunodeficiency virus type 1. *Journal of virology*, 66(12), 7517-7521.
52. Doranz, B. J., Rucker, J., Yi, Y., Smyth, R. J., Samson, M., Peiper, S. C., ... & Doms, R. W. (1996). A dual-tropic primary HIV-1 isolate that uses fusin and the β -chemokine receptors CKR-5, CKR-3, and CKR-2b as fusion cofactors. *Cell*, 85(7), 1149-1158.
53. Barat, C., Lullien, V., Schatz, O., Keith, G., Nugeyre, M. T., Grüninger-Leitch, F., ... & Darlix, J. L. (1989). HIV-1 reverse transcriptase specifically interacts with the anticodon domain of its cognate primer tRNA. *The EMBO journal*, 8(11), 3279.

54. Isel, C., Ehresmann, C., Keith, G., Ehresmann, B., & Marquet, R. (1995). Initiation of Reverse Transcription of HIV-1: Secondary Structure of the HIV-1 RNA/tRNA|rlmbopopnbop| Lys| clobop| 3 (Template/Primer) Complex. *Journal of Molecular Biology*, 247(2), 236-250.
55. Peliska, J. A., & Benkovic, S. J. (1992). Mechanism of DNA strand transfer reactions catalyzed by HIV-1 reverse transcriptase. *Science*, 258, 1112-1112.
56. Gopalakrishnan, V., Peliska, J. A., & Benkovic, S. J. (1992). Human immunodeficiency virus type 1 reverse transcriptase: spatial and temporal relationship between the polymerase and RNase H activities. *Proceedings of the National Academy of Sciences*, 89(22), 10763-10767.
57. Preston, B. D., Poiesz, B. J., & Loeb, L. A. (1988). Fidelity of HIV-1 reverse transcriptase. *Science*, 242(4882), 1168-1171.
58. Farnet, C. M., & Haseltine, W. A. (1991). Determination of viral proteins present in the human immunodeficiency virus type 1 preintegration complex. *Journal of virology*, 65(4), 1910-1915.
59. Popov, S., Rexach, M., Zybarth, G., Reiling, N., Lee, M. A., Ratner, L., ... & Bukrinsky, M. (1998). Viral protein R regulates nuclear import of the HIV-1 pre-integration complex. *The EMBO journal*, 17(4), 909-917.
60. Shun, M. C., Raghavendra, N. K., Vandegraaff, N., Daigle, J. E., Hughes, S., Kellam, P., ... & Engelman, A. (2007). LEDGF/p75 functions downstream from preintegration complex formation to effect gene-specific HIV-1 integration. *Genes & development*, 21(14), 1767-1778.

61. Craigie, R. (2001). HIV integrase, a brief overview from chemistry to therapeutics. *Journal of Biological Chemistry*, 276(26), 23213-23216.
62. Engelman, A., Mizuuchi, K., & Craigie, R. (1991). HIV-1 DNA integration: mechanism of viral DNA cleavage and DNA strand transfer. *Cell*, 67(6), 1211-1221.
63. Yoder, K. E., & Bushman, F. D. (2000). Repair of gaps in retroviral DNA integration intermediates. *Journal of Virology*, 74(23), 11191-11200.
64. Parada, C. A., & Roeder, R. G. (1996). Enhanced processivity of RNA polymerase II triggered by Tat-induced phosphorylation of its carboxy-terminal domain. *Nature*, 384(6607), 375-378.
65. Parada, C. A., & Roeder, R. G. (1999). A novel RNA polymerase II-containing complex potentiates Tat-enhanced HIV-1 transcription. *The EMBO journal*, 18(13), 3688-3701.
66. Ono, A., & Freed, E. O. (2001). Plasma membrane rafts play a critical role in HIV-1 assembly and release. *Proceedings of the National Academy of Sciences*, 98(24), 13925-13930.
67. Swanstrom, R., & Wills, J. W. (1997). *Synthesis, assembly, and processing of viral proteins*. Cold Spring Harbor Laboratory Press, Cold Spring Harbor (NY).
68. Tang, C., Louis, J. M., Aniana, A., Suh, J. Y., & Clore, G. M. (2008). Visualizing transient events in amino-terminal autoprocessing of HIV-1 protease. *Nature*, 455(7213), 693.
69. Yarchoan, R., Weinhold, K., Lyerly, H. K., Gelmann, E., Blum, R., Shearer, G., ... & Markham, P. (1986). Administration of 3'-azido-3'-deoxythymidine, an inhibitor of HTLV-III/LAV replication, to patients with AIDS or AIDS-related complex. *The Lancet*, 327(8481), 575-580.

70. Lambert, J. S., Seidlin, M., Reichman, R. C., Plank, C. S., Lavery, M., Morse, G. D., ... & Dolin, R. (1990). 2', 3'-Dideoxyinosine (ddI) in patients with the acquired immunodeficiency syndrome or AIDS-related complex: a phase I trial. *New England Journal of Medicine*, 322(19), 1333-1340.
71. Fischl, M. A., Olson, R. M., Follansbee, S. E., Lalezari, J. P., Henry, D. H., Frame, P. T., ... & Lieberman, J. (1993). Zalcitabine compared with zidovudine in patients with advanced HIV-1 infection who received previous zidovudine therapy. *Annals of internal medicine*, 118(10), 762-769.
72. Dudley, M. N., Graham, K. K., Kaul, S., Geletko, S., Dunkle, L., & Mayer, K. (1992). Pharmacokinetics of stavudine in patients with AIDS or AIDS-related complex. *Journal of Infectious Diseases*, 166(3), 480-485.
73. Arts, E. J., & Wainberg, M. A. (1996). Mechanisms of nucleoside analog antiviral activity and resistance during human immunodeficiency virus reverse transcription. *Antimicrobial agents and chemotherapy*, 40(3), 527.
74. Loeb, L. A., Essigmann, J. M., Kazazi, F., Zhang, J., Rose, K. D., & Mullins, J. I. (1999). Lethal mutagenesis of HIV with mutagenic nucleoside analogs. *Proceedings of the National Academy of Sciences*, 96(4), 1492-1497.
75. Eron, J. J., Benoit, S. L., Jemsek, J., MacArthur, R. D., Santana, J., Quinn, J. B., ... & Rubin, M. (1995). Treatment with lamivudine, zidovudine, or both in HIV-positive patients with 200 to 500 CD4+ cells per cubic millimeter. *New England Journal of Medicine*, 333(25), 1662-1669.

76. Cheeseman, S. H., Hattox, S. E., McLaughlin, M. M., Koup, R. A., Andrews, C., Bova, C. A., ... & Keirns, J. J. (1993). Pharmacokinetics of nevirapine: initial single-rising-dose study in humans. *Antimicrobial agents and chemotherapy*, *37*(2), 178-182.
77. Richman, D. D., Havlir, D., Corbeil, J., Looney, D., Ignacio, C., Spector, S. A., ... & Pauletti, D. (1994). Nevirapine resistance mutations of human immunodeficiency virus type 1 selected during therapy. *Journal of virology*, *68*(3), 1660-1666.
78. Collier, A. C., Coombs, R. W., Schoenfeld, D. A., Bassett, R. L., Timpone, J., Baruch, A., ... & Friedman, H. M. (1996). Treatment of human immunodeficiency virus infection with saquinavir, zidovudine, and zalcitabine. *New England Journal of Medicine*, *334*(16), 1011-1018.
79. Hammer, S. M., Squires, K. E., Hughes, M. D., Grimes, J. M., Demeter, L. M., Currier, J. S., ... & Chodakewitz, J. A. (1997). A controlled trial of two nucleoside analogues plus indinavir in persons with human immunodeficiency virus infection and CD4 cell counts of 200 per cubic millimeter or less. *New England Journal of Medicine*, *337*(11), 725-733.
80. Cameron, D. W., Heath-Chiozzi, M., Danner, S., Cohen, C., Kravcik, S., Maurath, C., ... & Leonard, J. (1998). Randomised placebo-controlled trial of ritonavir in advanced HIV-1 disease. *The Lancet*, *351*(9102), 543-549.
81. Ortiz, R., DeJesus, E., Khanlou, H., Voronin, E., van Lunzen, J., Andrade-Villanueva, J., ... & Vangeneugden, T. (2008). Efficacy and safety of once-daily darunavir/ritonavir versus lopinavir/ritonavir in treatment-naive HIV-1-infected patients at week 48. *Aids*, *22*(12), 1389-1397.

82. Lalezari, J. P., Henry, K., O'hearn, M., Montaner, J. S., Piliero, P. J., Trottier, B., ... & Chung, J. (2003). Enfuvirtide, an HIV-1 fusion inhibitor, for drug-resistant HIV infection in North and South America. *New England Journal of Medicine*, *348*(22), 2175-2185.
83. Dorr, P., Westby, M., Dobbs, S., Griffin, P., Irvine, B., Macartney, M., ... & Webster, R. (2005). Maraviroc (UK-427,857), a potent, orally bioavailable, and selective small-molecule inhibitor of chemokine receptor CCR5 with broad-spectrum anti-human immunodeficiency virus type 1 activity. *Antimicrobial agents and chemotherapy*, *49*(11), 4721-4732.
84. Grinsztejn, B., Nguyen, B. Y., Katlama, C., Gatell, J. M., Lazzarin, A., Vittecoq, D., ... & Isaacs, R. D. (2007). Safety and efficacy of the HIV-1 integrase inhibitor raltegravir (MK-0518) in treatment-experienced patients with multidrug-resistant virus: a phase II randomised controlled trial. *The Lancet*, *369*(9569), 1261-1269.
85. Markowitz, M., Evering, T. H., Garmon, D., Caskey, M., La Mar, M., Rodriguez, K., ... & Mohri, H. (2014). A randomized open-label study of three-versus five-drug combination antiretroviral therapy in newly HIV-1 infected individuals. *Journal of acquired immune deficiency syndromes (1999)*, *66*(2), 140.
86. Capetti, A., Meraviglia, P., Landonio, S., Sterrantino, G., Di Biagio, A., Caputo, S. L., ... & Soria, A. (2014). Four years data of raltegravir-based salvage therapy in HIV-1-infected, treatment-experienced patients: the SALIR-E Study. *International journal of antimicrobial agents*, *43*(2), 189-194.
87. Ren, J. H., Tao, Y., Zhang, Z. Z., Chen, W. X., Cai, X. F., Chen, K., ... & Huang, A. L. (2014). Sirtuin 1 regulates hepatitis B virus transcription and replication by targeting transcription factor AP-1. *Journal of virology*, *88*(5), 2442-2451.

88. Ramasubramanyan, S., Osborn, K., Al-Mohammad, R., Naranjo Perez-Fernandez, I. B., Zuo, J., Balan, N., ... & Jenner, R. G. (2015). Epstein–Barr virus transcription factor Zta acts through distal regulatory elements to directly control cellular gene expression. *Nucleic acids research*, *43*(7), 3563-3577.
89. Bose, S. K., Kim, H., Meyer, K., Wolins, N., Davidson, N. O., & Ray, R. (2014). Forkhead box transcription factor regulation and lipid accumulation by hepatitis C virus. *Journal of virology*, *88*(8), 4195-4203.
90. Lewis, P. F., & Emerman, M. (1994). Passage through mitosis is required for oncoretroviruses but not for the human immunodeficiency virus. *Journal of virology*, *68*(1), 510-516.
91. Diamond, T. L., Roshal, M., Jamburuthugoda, V. K., Reynolds, H. M., Merriam, A. R., Lee, K. Y., ... & Kim, B. (2004). Macrophage tropism of HIV-1 depends on efficient cellular dNTP utilization by reverse transcriptase. *Journal of Biological Chemistry*, *279*(49), 51545-51553.
92. Berg J.M., Tymoczko J.L., Stryer L. Biochemistry. 5th edition. New York: W H Freeman; 2002. Chapter 25, Nucleotide Biosynthesis. Available from: <https://www.ncbi.nlm.nih.gov/books/NBK21216/>
93. Reichard, P., & Ehrenberg, A. (1983). Ribonucleotide reductase--a radical enzyme. *Science*, *221*(4610), 514-519.
94. Elledge, S. J., Zhou, Z., & Allen, J. B. (1992). Ribonucleotide reductase: regulation, regulation, regulation. *Trends in biochemical sciences*, *17*(3), 119-123.
95. Kashlan, O. B., Scott, C. P., Lear, J. D., & Cooperman, B. S. (2002). A comprehensive model for the allosteric regulation of mammalian ribonucleotide reductase. Functional

- consequences of ATP-and dATP-induced oligomerization of the large subunit. *Biochemistry*, 41(2), 462-474.
96. Goldstone, D. C., Ennis-Adeniran, V., Hedden, J. J., Groom, H. C., Rice, G. I., Christodoulou, E., ... & de Carvalho, L. P. S. (2011). HIV-1 restriction factor SAMHD1 is a deoxynucleoside triphosphate triphosphohydrolase. *Nature*, 480(7377), 379-382.
97. Powell, R. D., Holland, P. J., Hollis, T., & Perrino, F. W. (2011). Aicardi-Goutieres syndrome gene and HIV-1 restriction factor SAMHD1 is a dGTP-regulated deoxynucleotide triphosphohydrolase. *Journal of Biological Chemistry*, 286(51), 43596-43600.
98. Lahouassa, H., Daddacha, W., Hofmann, H., Ayinde, D., Logue, E. C., Dragin, L., ... & Pancino, G. (2012). SAMHD1 restricts the replication of human immunodeficiency virus type 1 by depleting the intracellular pool of deoxynucleoside triphosphates. *Nature immunology*, 13(3), 223-228.
99. Cribier, A., Descours, B., Valadão, A. L. C., Laguette, N., & Benkirane, M. (2013). Phosphorylation of SAMHD1 by cyclin A2/CDK1 regulates its restriction activity toward HIV-1. *Cell reports*, 3(4), 1036-1043.
100. White, T. E., Brandariz-Nuñez, A., Valle-Casuso, J. C., Amie, S., Nguyen, L. A., Kim, B., ... & Diaz-Griffero, F. (2013). The retroviral restriction ability of SAMHD1, but not its deoxynucleotide triphosphohydrolase activity, is regulated by phosphorylation. *Cell host & microbe*, 13(4), 441-451.
101. Hollenbaugh, J. A., Gee, P., Baker, J., Daly, M. B., Amie, S. M., Tate, J., ... & Koyanagi, Y. (2013). Host factor SAMHD1 restricts DNA viruses in non-dividing myeloid cells. *PLoS pathogens*, 9(6), e1003481.

102. Kim, E. T., White, T. E., Brandariz-Núñez, A., Diaz-Griffero, F., & Weitzman, M. D. (2013). SAMHD1 restricts herpes simplex virus 1 in macrophages by limiting DNA replication. *Journal of virology*, *87*(23), 12949-12956.
103. Kim, B., Nguyen, L. A., Daddacha, W., & Hollenbaugh, J. A. (2012). Tight interplay among SAMHD1 protein level, cellular dNTP levels, and HIV-1 proviral DNA synthesis kinetics in human primary monocyte-derived macrophages. *Journal of Biological Chemistry*, *287*(26), 21570-21574.
104. Ji, X., Wu, Y., Yan, J., Mehrens, J., Yang, H., DeLucia, M., ... & Xiong, Y. (2013). Mechanism of allosteric activation of SAMHD1 by dGTP. *Nature structural & molecular biology*, *20*(11), 1304-1309.
105. Ji, X., Tang, C., Zhao, Q., Wang, W., & Xiong, Y. (2014). Structural basis of cellular dNTP regulation by SAMHD1. *Proceedings of the National Academy of Sciences*, *111*(41), E4305-E4314.
106. Popper, S. J., Sarr, A. D., Travers, K. U., Guèye-Ndiaye, A., Mboup, S., Essex, M. E., & Kanki, P. J. (1999). Lower human immunodeficiency virus (HIV) type 2 viral load reflects the difference in pathogenicity of HIV-1 and HIV-2. *The Journal of infectious diseases*, *180*(4), 1116-1121.
107. Hirsch, V. M., Olmsted, R. A., Murphey-Corb, M., Purcell, R. H., & Johnson, P. R. (1989). An African primate lentivirus (SIVsm) closely related to HIV-2. *Nature*, *339*(6223), 389-392.
108. Tristem, M., Marshall, C., Karpas, A., Petrik, J., & Hill, F. (1990). Origin of vpx in lentiviruses. *Nature*, *347*, 341-342.

109. Yu, X. F., Yu, Q. C., Essex, M., & Lee, T. H. (1991). The vpx gene of simian immunodeficiency virus facilitates efficient viral replication in fresh lymphocytes and macrophage. *Journal of virology*, *65*(9), 5088-5091.
110. Laguette, N., Sobhian, B., Casartelli, N., Ringeard, M., Chable-Bessia, C., Ségéral, E., ... & Benkirane, M. (2011). SAMHD1 is the dendritic–and myeloid–cell–specific HIV–1 restriction factor counteracted by Vpx. *Nature*, *474*(7353), 654.
111. Lenzi, G. M., Domaoal, R. A., Kim, D. H., Schinazi, R. F., & Kim, B. (2014). Kinetic variations between reverse transcriptases of viral protein X coding and noncoding lentiviruses. *Retrovirology*, *11*(1), 111.
112. Lenzi, G. M., Domaoal, R. A., Kim, D. H., Schinazi, R. F., & Kim, B. (2015). Mechanistic and kinetic differences between reverse transcriptases of Vpx coding and non-coding lentiviruses. *Journal of Biological Chemistry*, *290*(50), 30078-30086.
113. Loeb, L. A., & Kunkel, T. A. (1982). Fidelity of DNA synthesis. *Annual review of biochemistry*, *51*(1), 429-457.
114. Hoeijmakers, J. H. (2009). DNA damage, aging, and cancer. *New England Journal of Medicine*, *361*(15), 1475-1485.
115. Ciccia, A., & Elledge, S. J. (2010). The DNA damage response: making it safe to play with knives. *Molecular cell*, *40*(2), 179-204.
116. Seeberg, E., Eide, L., & Bjørås, M. (1995). The base excision repair pathway. *Trends in biochemical sciences*, *20*(10), 391-397.
117. Aboussekhra, A., Biggerstaff, M., Shivji, M. K., Vilpo, J. A., Moncollin, V., Podust, V. N., ... & Wood, R. D. (1995). Mammalian DNA nucleotide excision repair reconstituted with purified protein components. *Cell*, *80*(6), 859-868.

118. Caldecott, K. W. (2008). Single-strand break repair and genetic disease. *Nature Reviews Genetics*, 9(8), 619-632.
119. Szostak, J. W., Orr-Weaver, T. L., Rothstein, R. J., & Stahl, F. W. (1983). The double-strand-break repair model for recombination. *Cell*, 33(1), 25-35.
120. Zhou, B. B. S., & Elledge, S. J. (2000). The DNA damage response: putting checkpoints in perspective. *Nature*, 408(6811), 433-439.
121. Uziel, T., Lerenthal, Y., Moyal, L., Andegeko, Y., Mittelman, L., & Shiloh, Y. (2003). Requirement of the MRN complex for ATM activation by DNA damage. *The EMBO journal*, 22(20), 5612-5621.
122. Dip, R., Camenisch, U., & Naegeli, H. (2004). Mechanisms of DNA damage recognition and strand discrimination in human nucleotide excision repair. *DNA repair*, 3(11), 1409-1423.
123. Bao, S., Tibbetts, R. S., Brumbaugh, K. M., Fang, Y., Richardson, D. A., Ali, A., ... & Wang, X. F. (2001). ATR/ATM-mediated phosphorylation of human Rad17 is required for genotoxic stress responses. *Nature*, 411(6840), 969-975.
124. Chaturvedi, P., Eng, W. K., Zhu, Y., Mattern, M. R., Mishra, R., Hurle, M. R., ... & Scott, G. F. (1999). Mammalian Chk2 is a downstream effector of the ATM-dependent DNA damage checkpoint pathway. *Oncogene*, 18(28).
125. Roshal, M., Kim, B., Zhu, Y., Nghiem, P., & Planelles, V. (2003). Activation of the ATR-mediated DNA damage response by the HIV-1 viral protein R. *Journal of Biological Chemistry*, 278(28), 25879-25886.

126. Lau, A., Swinbank, K. M., Ahmed, P. S., Taylor, D. L., Jackson, S. P., Smith, G., & O'Connor, M. J. (2005). Suppression of HIV-1 infection by a small molecule inhibitor of the ATM kinase. *Nature cell biology*, 7(5).
127. Nunnari, G., Argyris, E., Fang, J., Mehlman, K. E., Pomerantz, R. J., & Daniel, R. (2005). Inhibition of HIV-1 replication by caffeine and caffeine-related methylxanthines. *Virology*, 335(2), 177-184.
128. Sakurai, Y., Komatsu, K., Agematsu, K., & Matsuoka, M. (2009). DNA double strand break repair enzymes function at multiple steps in retroviral infection. *Retrovirology*, 6(1), 114.
129. Li, L., Olvera, J. M., Yoder, K. E., Mitchell, R. S., Butler, S. L., Lieber, M., ... & Bushman, F. D. (2001). Role of the non-homologous DNA end joining pathway in the early steps of retroviral infection. *The EMBO journal*, 20(12), 3272-3281.
130. Ariumi, Y., Turelli, P., Masutani, M., & Trono, D. (2005). DNA damage sensors ATM, ATR, DNA-PKcs, and PARP-1 are dispensable for human immunodeficiency virus type 1 integration. *Journal of virology*, 79(5), 2973-2978.
131. Espeseth, A. S., Fishel, R., Hazuda, D., Huang, Q., Xu, M., Yoder, K., & Zhou, H. (2011). siRNA screening of a targeted library of DNA repair factors in HIV infection reveals a role for base excision repair in HIV integration. *PLoS One*, 6(3), e17612.
132. Yoder, K. E., Espeseth, A., Wang, X. H., Fang, Q., Russo, M. T., Lloyd, R. S., ... & Fishel, R. (2011). The base excision repair pathway is required for efficient lentivirus integration. *PLoS One*, 6(3), e17862.

133. Yamtich, J., & Sweasy, J. B. (2010). DNA polymerase family X: function, structure, and cellular roles. *Biochimica et Biophysica Acta (BBA)-Proteins and Proteomics*, 1804(5), 1136-1150.
134. Pelletier, H., Sawaya, M. R., Wolffe, W., Wilson, S. H., & Kraut, J. (1996). Crystal structures of human DNA polymerase β complexed with DNA: implications for catalytic mechanism, processivity, and fidelity. *Biochemistry*, 35(39), 12742-12761.
135. Sobol, R. W., Horton, J. K., Kühn, R., Gu, H., Singhal, R. K., Prasad, R., ... & Wilson, S. H. (1996). Requirement of mammalian DNA polymerase- β in base-excision repair. *Nature*, 379(6561), 183-186.
136. Fortini, P., & Dogliotti, E. (2007). Base damage and single-strand break repair: mechanisms and functional significance of short-and long-patch repair subpathways. *DNA repair*, 6(4), 398-409.
137. Sobol, R. W., Prasad, R., Evenski, A., Baker, A., Yang, X. P., Horton, J. K., & Wilson, S. H. (2000). The lyase activity of the DNA repair protein [beta]-polymerase protects from DNA-damage-induced cytotoxicity. *Nature*, 405(6788), 807-811.
138. Smithies, O., et al. "Homologous recombination with DNA introduced into mammalian cells." *Cold Spring Harbor symposia on quantitative biology*. Vol. 49. Cold Spring Harbor Laboratory Press, 1984.
139. Jacquier, A., & Dujon, B. (1985). An intron-encoded protein is active in a gene conversion process that spreads an intron into a mitochondrial gene. *Cell*, 41(2), 383-394.
140. Choulika, A., Perrin, A., Dujon, B., & Nicolas, J. F. (1995). Induction of homologous recombination in mammalian chromosomes by using the I-SceI system of *Saccharomyces cerevisiae*. *Molecular and cellular biology*, 15(4), 1968-1973.

141. Grizot, S., Smith, J., Daboussi, F., Prieto, J., Redondo, P., Merino, N., ... & Blanco, F. J. (2009). Efficient targeting of a SCID gene by an engineered single-chain homing endonuclease. *Nucleic acids research*, 37(16), 5405-5419.
142. Urnov, F. D., Miller, J. C., Lee, Y. L., Beausejour, C. M., Rock, J. M., Augustus, S., ... & Holmes, M. C. (2005). Highly efficient endogenous human gene correction using designed zinc-finger nucleases. *Nature*, 435(7042), 646-651.
143. Rémy, S., Tesson, L., Ménoret, S., Usal, C., Scharenberg, A. M., & Anegón, I. (2010). Zinc-finger nucleases: a powerful tool for genetic engineering of animals. *Transgenic research*, 19(3), 363-371.
144. Yu, S., Luo, J., Song, Z., Ding, F., Dai, Y., & Li, N. (2011). Highly efficient modification of beta-lactoglobulin (BLG) gene via zinc-finger nucleases in cattle. *Cell research*, 21(11), 1638-1640.
145. Perez, E. E., Wang, J., Miller, J. C., Jouvenot, Y., Kim, K. A., Liu, O., ... & Guschin, D. Y. (2008). Establishment of HIV-1 resistance in CD4+ T cells by genome editing using zinc-finger nucleases. *Nature biotechnology*, 26(7), 808.
146. Lombardo, A., Genovese, P., Beausejour, C. M., Colleoni, S., Lee, Y. L., Kim, K. A., ... & Holmes, M. C. (2007). Gene editing in human stem cells using zinc finger nucleases and integrase-defective lentiviral vector delivery. *Nature biotechnology*, 25(11).
147. Swarthout, J. T., Raisinghani, M., & Cui, X. (2011). Zinc Finger Nucleases: A new era for transgenic animals. *Annals of neurosciences*, 18(1), 25.

148. Radecke, S., Radecke, F., Cathomen, T., & Schwarz, K. (2010). Zinc-finger nuclease-induced gene repair with oligodeoxynucleotides: wanted and unwanted target locus modifications. *Molecular Therapy*, 18(4), 743-753.
149. Tesson, L., Usal, C., Ménoret, S., Leung, E., Niles, B. J., Remy, S., ... & Gregory, P. D. (2011). Knockout rats generated by embryo microinjection of TALENs. *Nature biotechnology*, 29(8), 695-696
150. Moscou, M. J., & Bogdanove, A. J. (2009). A simple cipher governs DNA recognition by TAL effectors. *Science*, 326(5959), 1501-1501.
151. Miller, J. C., Tan, S., Qiao, G., Barlow, K. A., Wang, J., Xia, D. F., ... & Dulay, G. P. (2011). A TALE nuclease architecture for efficient genome editing. *Nature biotechnology*, 29(2), 143-148.
152. Seruggia, D., & Montoliu, L. (2014). The new CRISPR–Cas system: RNA-guided genome engineering to efficiently produce any desired genetic alteration in animals. *Transgenic research*, 23(5), 707-716.
153. Barrangou, R., Fremaux, C., Deveau, H., Richards, M., Boyaval, P., Moineau, S., ... & Horvath, P. (2007). CRISPR provides acquired resistance against viruses in prokaryotes. *Science*, 315(5819), 1709-1712.
154. Jinek, M., Chylinski, K., Fonfara, I., Hauer, M., Doudna, J. A., & Charpentier, E. (2012). A programmable dual-RNA–guided DNA endonuclease in adaptive bacterial immunity. *Science*, 337(6096), 816-821.
155. Hsu, P. D., Lander, E. S., & Zhang, F. (2014). Development and applications of CRISPR-Cas9 for genome engineering. *Cell*, 157(6), 1262-1278.

156. Niu, D., Wei, H. J., Lin, L., George, H., Wang, T., Lee, I. H., ... & Lesha, E. (2017). Inactivation of porcine endogenous retrovirus in pigs using CRISPR-Cas9. *Science*, 357(6357), 1303-1307.
157. Kang, X., He, W., Huang, Y., Yu, Q., Chen, Y., Gao, X., ... & Fan, Y. (2016). Introducing precise genetic modifications into human 3PN embryos by CRISPR/Cas-mediated genome editing. *Journal of assisted reproduction and genetics*, 33(5), 581-588.
158. Fu, Y., Foden, J. A., Khayter, C., Maeder, M. L., Reyon, D., Joung, J. K., & Sander, J. D. (2013). High-frequency off-target mutagenesis induced by CRISPR-Cas nucleases in human cells. *Nature biotechnology*, 31(9), 822-826.
159. Kleinstiver, B. P., Pattanayak, V., Prew, M. S., Tsai, S. Q., Nguyen, N., Zheng, Z., & Joung, J. K. (2016). High-fidelity CRISPR-Cas9 variants with undetectable genome-wide off-targets. *Nature*, 529(7587), 490.
160. Doench, J. G., Fusi, N., Sullender, M., Hegde, M., Vaimberg, E. W., Donovan, K. F., ... & Virgin, H. W. (2016). Optimized sgRNA design to maximize activity and minimize off-target effects of CRISPR-Cas9. *Nature biotechnology*, 34(2), 184.

Chapter 2

Substrates and Inhibitors of SAMHD1

This research was published in *PLoS one*.

Joseph A. Hollenbaugh, Jadd Shelton, Sijia Tao, Sheida Amiralaei, Peng Liu, Xiao Lu, Russell W. Goetze, Longhu Zhao, James H. Nettles, Raymond F. Schinazi, and Baek Kim.

Substrates and Inhibitors of SAMHD1.

PLoS one. 2017, 12(1), e0169052.

© Hollenbaugh, et. al.

Conceptualization: JAH JS.

Data curation: JAH ST.

Formal analysis: JAH ST JHN.

Funding acquisition: RFS BK.

Investigation: JAH RWG JHN BK.

Methodology: JAH JS BK ST.

Project administration: JAH RFS BK.

Resources: SA XL LZ PL RWG.

Software: JAH JHN ST.

Supervision: JAH RFS BK.

Validation: JAH ST SA XL LZ PL.

Visualization: JAH.

Writing – original draft: JAH RFS JS.

Writing – review & editing: JAH JS RWG JHN XL.

A. Abstract

SAMHD1 hydrolyzes dNTPs into dNs and inorganic triphosphate products. In this paper, we evaluated the impact of 2' sugar moiety substitution for different nucleotides on being substrates for SAMHD1 and mechanisms of actions for the results. We found that dNTPs ((2'*R*)-2'-H) are only permissive in the catalytic site of SAMHD1 due to L150 exclusion of (2'*R*)-2'-F and (2'*R*)-2'-OH nucleotides. However, arabinose ((2'*S*)-2'-OH) nucleoside-5'-triphosphates analogs are permissive to bind in the catalytic site and be hydrolyzed by SAMHD1. Moreover, when the (2'*S*)-2' sugar moiety is increased to a (2'*S*)-2'-methyl as with the SMDU-TP analog, we detect inhibition of SAMHD1's dNTPase activity. Our computational modeling suggests that (2'*S*)-2'-methyl sugar moiety clashing with the Y374 of SAMHD1. We speculate that SMDU-TP mechanism of action requires that the analog first docks in the catalytic pocket of SAMHD1 but prevents the A351-V378 helix conformational change from being completed, which is needed before hydrolysis can occur. Collectively we have identified stereoselective 2' substitutions that reveal nucleotide substrate specificity for SAMHD1, and a novel inhibitory mechanism for the dNTPase activity of SAMHD1. Importantly, our data is beneficial for understanding if FDA-approved antiviral and anticancer nucleosides are hydrolyzed by SAMHD1 *in vivo*.

B. Background

Sterile alpha motif domain and histidine/aspartic acid domain containing protein 1 (SAMHD1) hydrolyzes canonical dNTPs into dNs and inorganic triphosphates (PPP) products (1, 2). The dNTP triphosphohydrolase activity occurs in the HD domain of SAMHD1. The dNTPase activity appears to require homotetramer complex assembly, which is regulated by

sequential binding of allosteric activators (3, 4). However the SAMDH1C (120–626) truncated protein, which cannot form homotetramers, has been shown to have dNTPase activity (1, 5). Further studies are needed to determine if putative interacting protein partners, Aicardi–Goutières syndrome mutations, other point mutations or other truncation mutants of SAMHD1 may block homotetramerization while still permit dNTPase activity (1, 5–8)

It has been shown that SAMHD1 inhibits retrovirus infection, most likely by acting as a key regulator for cellular dNTPs levels, which can influence such infection (9–11). Recent reports indicate that T592 phosphorylation of SAMHD1 also influences retrovirus restriction in myeloid cells and can modulate triphosphohydrolase activity (12–15). Furthermore, SAMHD1 has been investigated in the context of how cellular dNTP concentrations influence the efficacy of NRTIs for lentiviral infection (16–19). Nucleoside derivatives–ribonucleoside, dN, or arabinose nucleoside analogs–are antimetabolites, which represent an important class of chemotherapeutic agents used to treat cancers and viral infections (20–22). These antimetabolites enter the cell through active transport mechanisms and require phosphorylation by several cellular kinases to produce their monophosphate (MP), diphosphate (DP) and triphosphate (TP) analog forms. In addition, certain dNTP analogs, arabinose nucleoside-5'-TP analogs and dUTP can compete with naturally occurring canonical dNTPs as substrates for host DNA polymerases or viral DNA polymerases (23, 24). This competition promotes mutagenesis and apoptosis of cancer cells or termination of viral replication (25, 26). Therefore, maintaining a proper cellular dNTP balance is important biologically for ensuring DNA fidelity during replication and repair (27–30).

In this study we specifically explore the effect of stereoselective 2' substitution of nucleoside analogs on SAMHD1 activity. We use computational modeling to place our results

into a structural context that may help better understand the larger mechanistic details of SAMHD1 substrate specificity. The L150 and Y374 of SAMHD1 have been proposed to contribute to the formation of a tight catalytic pocket (31). Using an HPLC-based assay, we found that the L150 of SAMHD1 acted as a steric gate to prevent (2'*R*)-2'-F-dCTP and CTP from being hydrolyzed by SAMHD1, which supports published results (31). Modeling of the catalytic site with dCTP and ara-CTP ((2'*S*)-2'-OH) did not show a clash with Y374, whereas SMDU-TP analog did show a clash. Biochemical analysis showed that dCTP and ara-CTP were substrates for SAMHD1, whereas SMDU-TP blocked dNTPase activity of SAMHD1. Y374 is part of a helix that undergoes a conformational change to move closer to the dNTP (5). We hypothesize that the (2'*S*)-2'-methyl substituted nucleotide (SMDU-TP) blocks the helix conformation change at the catalytic site, providing a novel mechanism for inhibiting the dNTPase activity of SAMHD1. Collectively, our data show that stereoselective 2' substitution for nucleotides can impact the substrate specificity and dNTPase activity of SAMHD1.

C. Results

Cartoon for SAMHD1 homotetramerization

The process of SAMHD1 tetramerization begins when SAMHD1 monomers binds GTP or dGTP at the allosteric 1 (A1) site to promote homodimer formation (Fig 1) (39, 40). The intracellular GTP concentration is maintained at around 400 μ M as compared to 1–3 μ M dGTP in activated T cells and 40 nM dGTP in macrophages (41, 42). At these physiological levels, GTP should always be docked within the A1 site and limit the amount of free SAMHD1 monomer within the cell (40). The SAMHD1 homodimers then bind canonical dNTPs at allosteric 2 (A2) sites, allowing for a homotetramer complex to form. The homotetramer of

SAMHD1 then permits binding of dNTPs into the catalytic (Cat) sites. Some of the interactions known are metal ion, coordinated by H167, H206, D207 and D311, binds to the γ -phosphate to further stabilize the dNTP in the catalytic pocket of SAMHD1. There are interactions with the different bases that contribute to K_m differences between the different dNTPs. Initiating dNTP triphosphohydrolase activity appears to occur after the dNTP has docked in the catalytic site of SAMHD1 and conformational change in the homotetramer (39). Comparison of dGTP-bound tetramer to non-substrate bound dimer (3U1N) showed that the A351-V378 helix moves closer to the dNTP allowing for better substrate binding within the binding pocket (5). Once the helix conformational change has been completed, then R366 may interact with the γ -phosphate to further stabilize the dNTP in the catalytic pocket. Hydrolysis occurs by the attack of the phosphodiester bond between the α -phosphate and sugar to liberate dN and iPPP products from the four active sites of SAMHD1 (5, 31). Several laboratories have characterized and reported substrate specificity of SAMHD1 for ribonucleoside-5'-triphosphate (rNTPs), dNTPs and HIV NRTIs (1, 16–18, 34, 39, 40, 43). It should be noted that all the canonical dNTPs are substrates for SAMHD1 as well as competitive inhibitors amongst themselves due to their slight differences in K_m values (44).

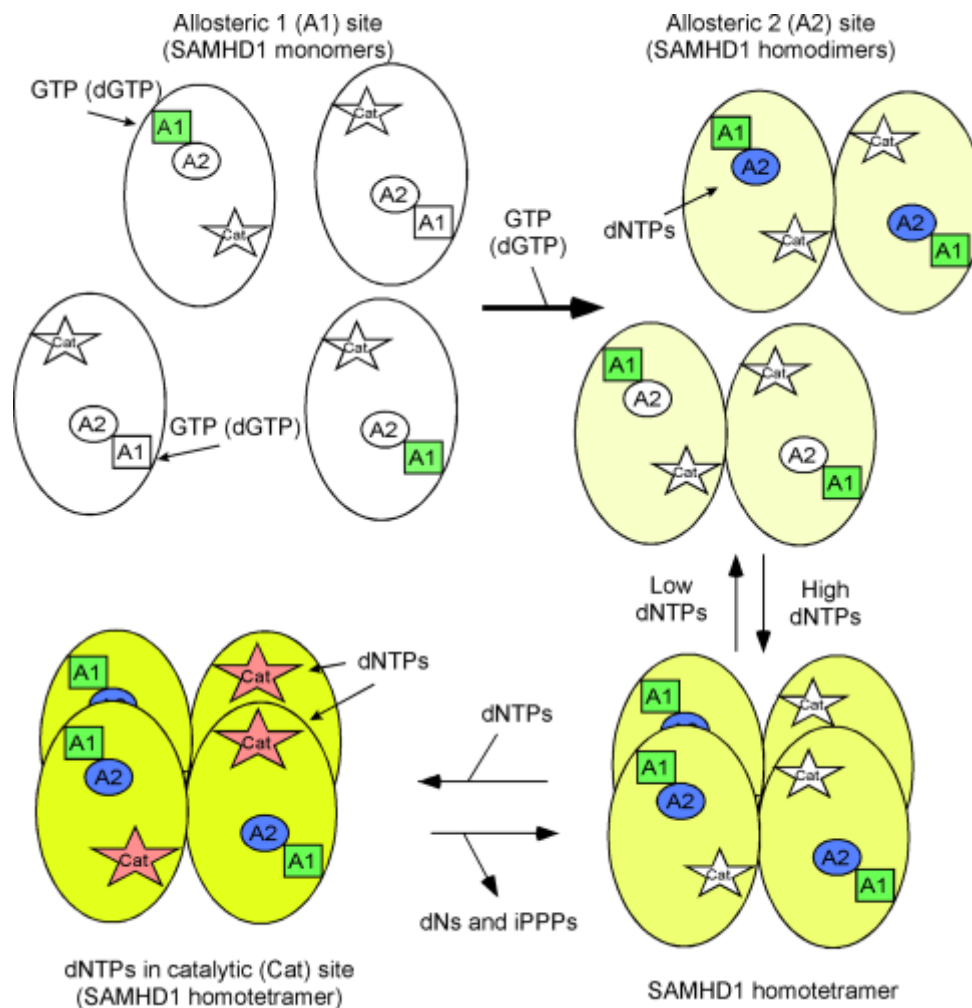


Figure 1: Cartoon for SAMHD1 homotetramerization.

SAMHD1 monomers bind GTP (or dGTP) at allosteric 1 (A1) site leading to the formation of homodimers. Next, dNTPs bind to allosteric 2 (A2) sites allowing for the formation of homotetramers. The catalytic (Cat) site then can accompany dNTPs for hydrolysis, leading to the generation of dNs and PPP.

Role of the 2'R and 3'R sugar moieties for nucleotide hydrolysis

Ji *et al.* reported the crystal structure of SAMHD1 and suggested that L150 and Y374 were involved in generating a tight catalytic binding pocket (31). These amino acids might exclude rNTPs, which has a (2'R)-2'-OH sugar moiety (ribose), from docking at the catalytic pocket due to a steric clash with L150. To begin, we modeled dCTP (Fig 2A) into the catalytic site of SAMHD1 with the point of view focused on the L150 of SAMHD1. We observed that dCTP fits within the catalytic site of SAMHD1 without touching L150, see arrow (Fig 2A). Next, we tested dCTP using a semi-quantitative HPLC-based assay (32). Essentially, nucleotide analogs were incubated with and without 1.6 μ M of SAMHD1 enzyme and dGTP, which acts as the A1 site activator and also an internal positive control to ensure the enzyme is working. HPLC data were analyzed by calculating the changes in peak area of the compound for with and without SAMHD1 protein, while using dCMP as an internal loading control. The normalized peak area for the SAMHD1 negative control (no SAMHD1) reaction was set to 100% analog remaining. Data for reactions containing SAMHD1 protein are then statically compared to the no SAMHD1 reactions ($n = 3$). As displayed in Fig 2B, both dCTP and dGTP were significantly hydrolyzed ($p < 0.001$; T test) in the presence of SAMHD1. Moreover, dATP, dTTP and decitabine-TP were also tested and are also substrates for SAMHD1 (S1 Fig). Next (2'R)-2'-F-dCTP was modeled in the catalytic site of SAMHD1 (Fig 2C); it appears to clash with L150 (see arrow). Using the biochemical assay, (2'R)-2'-F-dCTP was not hydrolyzed by SAMHD1 (Fig 2D), whereas the dGTP in the same reaction tube was significantly decreased ($p < 0.001$) by SAMHD1. In addition, (2'R)-2'-F-dATP was not degraded by SAMHD1 (S1 Fig). Finally, CTP was modeled in the catalytic site of SAMHD1 and also illustrates a clash with L150 (Fig 2E). CTP was not hydrolyzed by SAMHD1 *in vitro* (Fig 2F), while the dGTP internal control was

significantly hydrolyzed ($p < 0.001$). Consistent with the above results, ATP, GTP and UTP were not substrates for SAMHD1 (S1 Fig). Collectively, these data indicate that the sugar, not the nucleoside base, plays an important role in determining substrate specificity for SAMHD1.

Ji *et al.* proposed that the 3'-OH of the sugar is required for hydrogen bonding interactions with D319 and Q149 of SAMHD1 in the catalytic pocket (31). From Fig 2A, we illustrate D319 having a hydrogen bond interaction with the 3'-OH of dCTP. Using the biochemical assay, 2',3'-ddATP (Fig 3A), 2',3'-ddGTP (Fig 3B), 2',3'-ddCTP (Fig 3C) and 2',3'-ddITP (Fig 3D) are showed not to be significantly (n.s.) hydrolyzed by SAMHD1, nor did these analogs negatively impact dGTP hydrolysis by SAMHD1 (Fig 3A–3D). 2',3'-ddC (zalcitabine) and 2',3'-ddI (didanosine) are FDA-approved NRTI compounds to treat HIV. Our findings are consistent with previously reports (17, 40).

Collectively, these data indicate that L150 may effectively exclude any nucleotides-5'-triphosphates with a (2'*R*)-2' sugar moiety larger than a hydrogen atom from properly fitting into the catalytic site of SAMHD1. Thus L150 may act as a steric gate for SAMHD1. Secondly, the base does not restrict access to the catalytic site of SAMHD1, but it can influence the overall *K_m* of the nucleotides (44), i.e., the canonical dNTPs compete between themselves at the catalytic site. Third, 3'-OH sugar moiety and being a triphosphate are essential for permitting hydrolysis of nucleotide analogs.

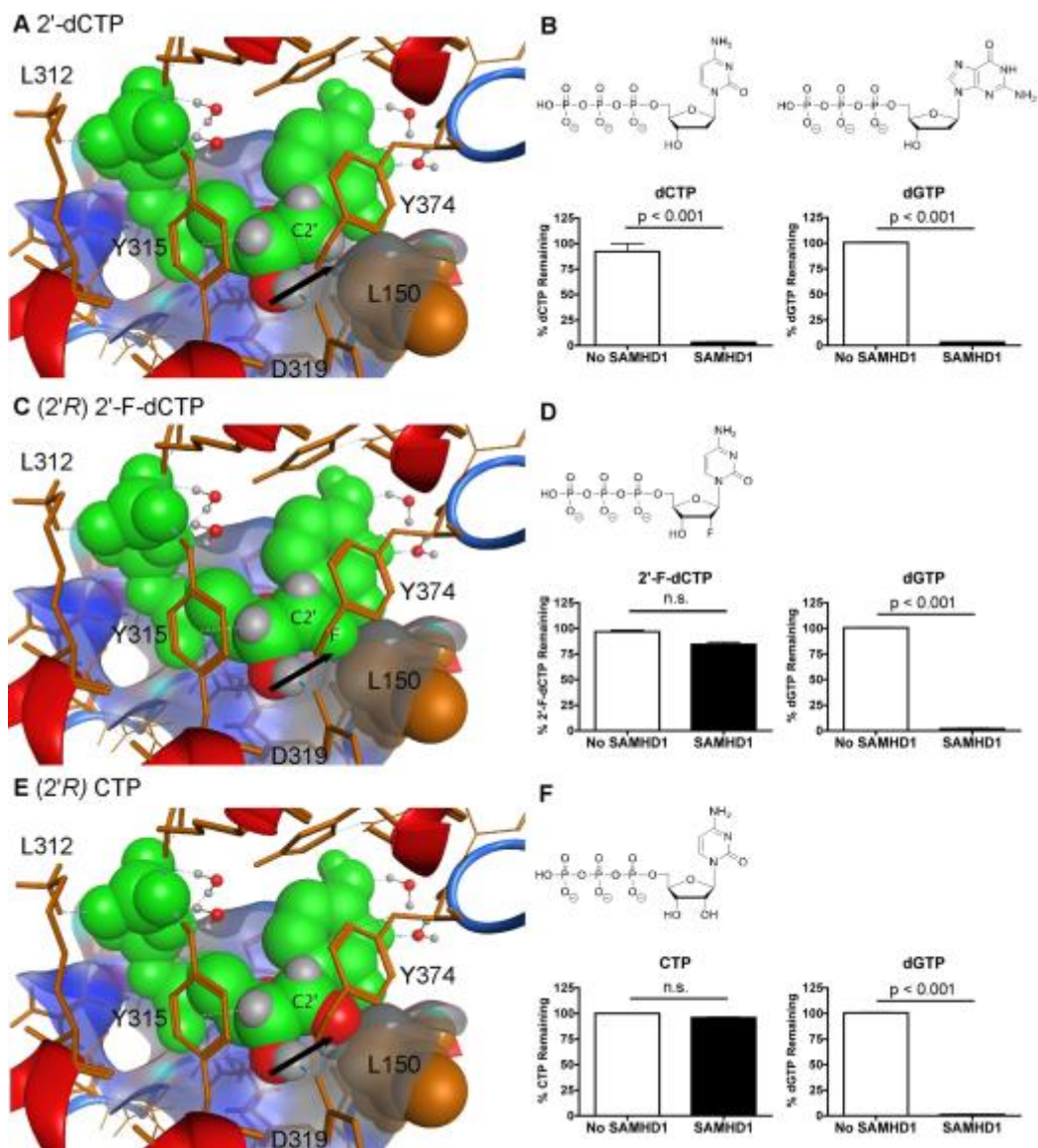


Figure 2: Examining the role of L150 for nucleotide specificity.

A) dCTP, C) (2'R) 2'-F-dCTP and E) CTP nucleotides (in green) are modeled in the catalytic site of SAMHD1. L150 clashes with (2'R) 2'-F-dCTP and CTP, but not dCTP (see arrows) within the catalytic pocket of SAMHD1. B, D and F) Determining if dCTP, (2'R) 2'-F-dCTP and CTP can be hydrolyzed for SAMHD1 in vitro. Structures of the compounds are above the HPLC graphs. Using semi-quantitative HPLC analysis method, compounds were incubated with and without 1.6 μ M of SAMHD1 enzyme plus dGTP (A1 site activator) to determine if they are substrates of

SAMHD1. Data are presented as the percent compound remaining (y-axis). dCTP and dGTP were significantly hydrolyzed ($p < 0.001$; T test). No significant (n.s.) differences were detected between samples with and without SAMHD1 protein for (2'R) 2'-F-dCTP and CTP analogs. HPLC analysis of each nucleoside was done twice in triplicate. Mean and SEM are plotted with significant or no significant (n.s.) differences determined by T test analysis.

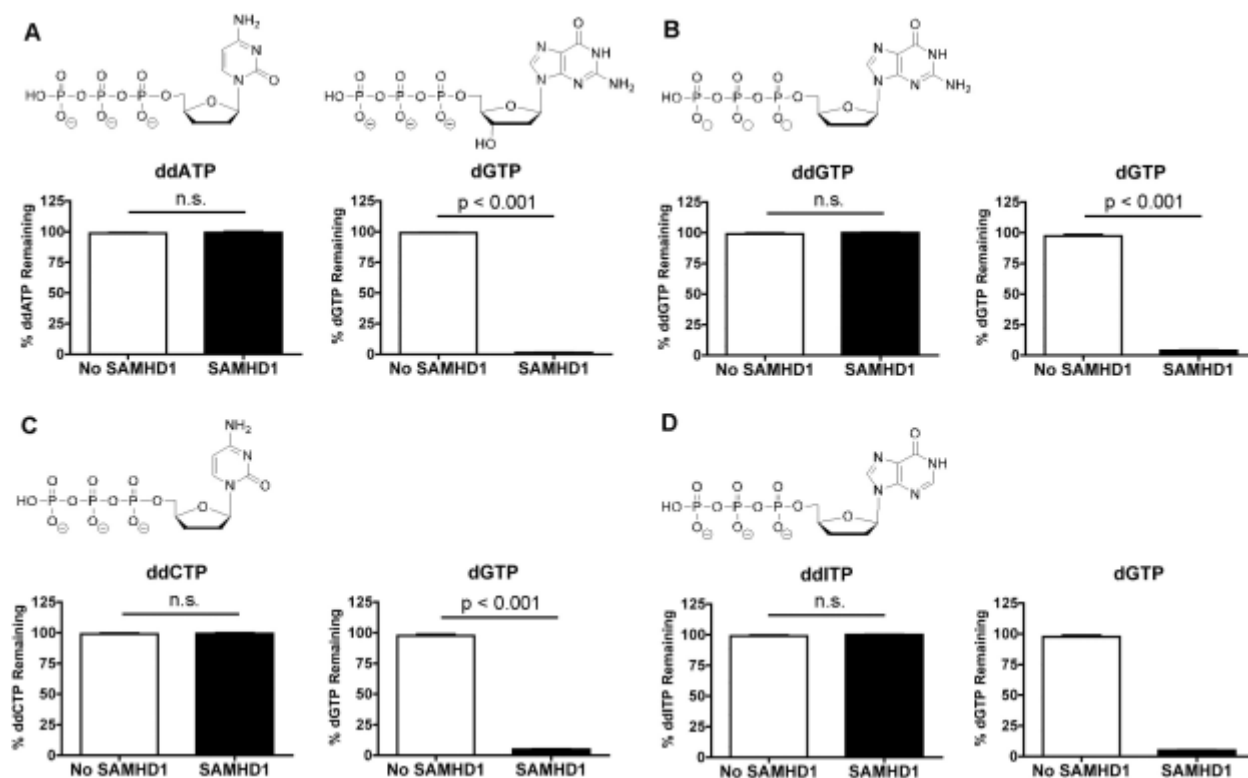


Figure 3: Role of 3'-OH sugar moiety for SAMHD1's substrate specificity.

A-D) Using semi-quantitative HPLC analysis method, 2',3'-ddATP, 2',3'-ddGTP, 2',3'-ddCTP and 2',3'-ddITP are incubated with and without 1.6 μM of SAMHD1 enzyme plus dGTP (A1 site activator) to determine if they are substrates of SAMHD1. Data are presented as the percent compound remaining (y-axis), showing that none of these nucleoside analogs were hydrolyzed by SAMHD1. dGTP is also used as an internal positive control and is significantly hydrolyzed ($p < 0.001$) by SAMHD1 in the presence of all the 2',3'-ddNTP. Mean and SEM are plotted with significant or no significant (n.s.) differences determined by T test analysis.

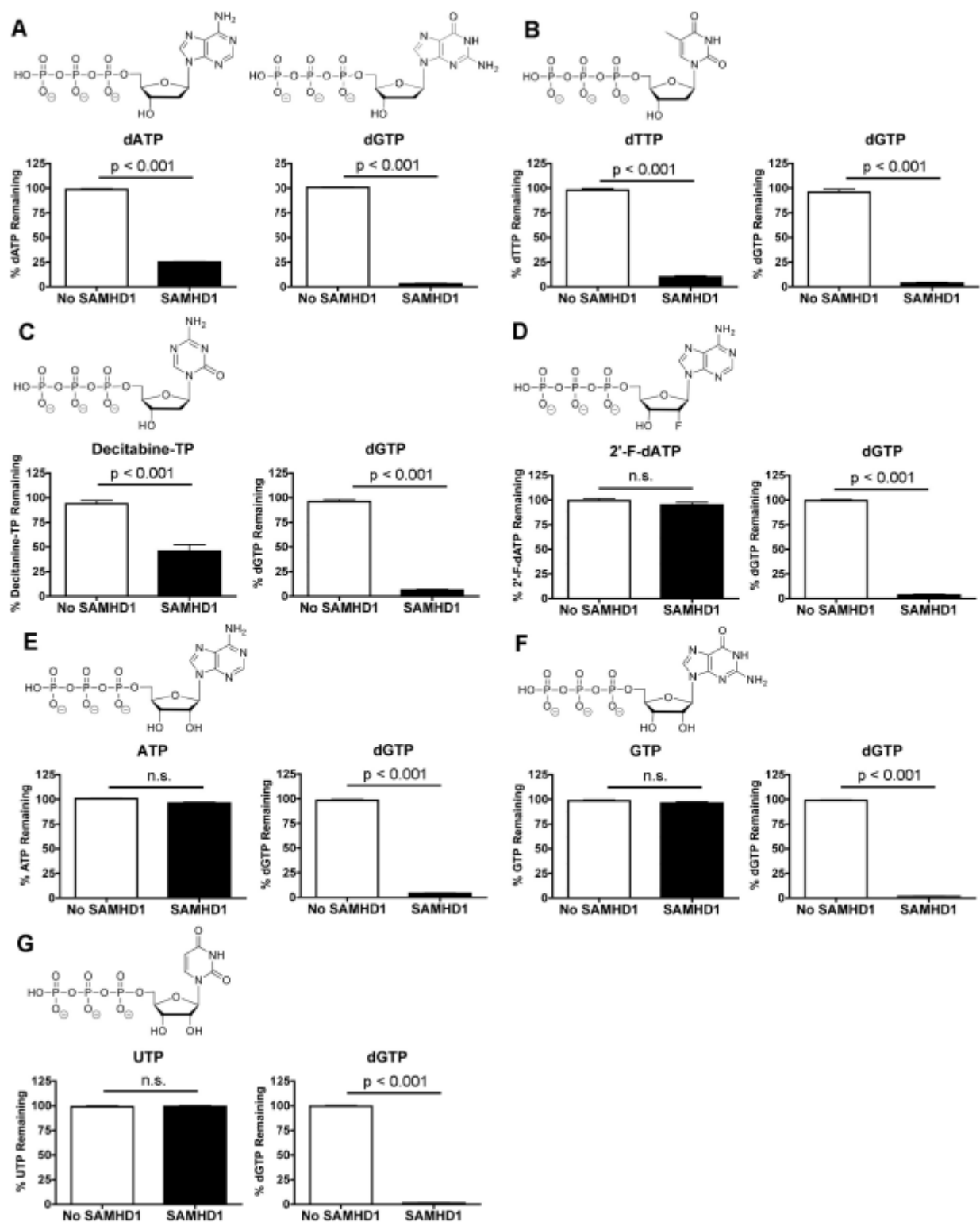


Figure S1: Evaluating additional nucleotides as substrates for SAMHD1.

A and B) canonical dATP and dTTP were analyzed. Using semi-quantitative HPLC analysis method, compounds were incubated with and without 1.6 μ M of SAMHD1 enzyme plus dGTP (A1 site activator) to determine if they are substrates of SAMHD1. dATP, dTTP and dGTP are significantly ($p < 0.001$) hydrolyzed in the presence of SAMHD1. C) Decitabine-5'-triphosphate (decitabine-TP) is a base modified nucleotide. Decitabine-TP and dGTP are significantly ($p < 0.001$) hydrolyzed in the presence of SAMHD1. D) (2'R)-2'-F-dATP was not hydrolyzed for SAMHD1 in vitro, whereas the internal dGTP control in the same reaction was significantly ($p < 0.001$) hydrolyzed in the presence of SAMHD1. E-G) Ribonucleotide-5'-triphosphates: ATP, GTP and UTP are evaluated in the biochemical assay and were not significantly hydrolyzed by SAMHD1. Mean and SEM are plotted with significant or no significant (n.s.) differences determined using T test analysis.

Examining the role of Y374 for SAMHD1 substrate specificity

We examined the contribution of Y374 within the catalytic pocket of SAMHD1 (31). Y374 might be important for excluding (2'*S*)-2' sugar moiety modification from the catalytic site. Our modeling now focuses on the Y374 and shows that a (2'*S*)-2'-H group of dCTP (Fig 4A) fits in the catalytic site. Both dCTP and dGTP were significantly hydrolyzed ($p < 0.001$) by SAMHD1 (Fig 4B). We further modeled ara-CTP, which has a (2'*S*)-2'-OH group (Fig 4C). It also fits into the pocket without a clash with Y374 (Fig 4C, see arrow). We observed that both ara-CTP and dGTP are significantly hydrolyzed ($p < 0.001$) by SAMHD1 (Fig 4D). Additionally, we tested ara-ATP and ara-UTP, and both were degraded by SAMHD1 (S3 Fig). Finally, we examined SMDU-TP, which has a (2'*S*)-2'-methyl (CH₃) group (Fig 4F). SMDU-TP appears to clash with Y374 of SAMHD1 (Fig 4E; see arrow). Using our biochemical assay, SMDU-TP was not hydrolyzed by SAMHD1 (Fig 3F). Moreover, dGTP hydrolysis was reduced in the presence of SMDU-TP, suggesting it may be a dNTPase inhibitor. To further investigate this analog, 0.1 mM SMDU-TP was tested in the presence of 1 mM dGTP (S3 Fig). Under these experimental conditions, dGTP was significantly hydrolyzed ($p < 0.001$) by SAMHD1, suggesting that SMDU-TP may act as a competitive SAMHD1 inhibitor. Additionally, PSI-6206-TP, (2'*S*)-2'-methyl, (2'*R*)-2'-F-2'-deoxyuridine-5'-triphosphate, was tested and found not to be a substrate for SAMHD1 nor did it inhibit dGTP hydrolysis (S3 Fig), which is consistent with other (2'*R*)-2'-F nucleotide analogs (Fig 2D and S1 Fig). We attempted to further evaluate if Y374 acts as a steric gate, but the Y374I, Y374F and Y374A mutants are catalytically dead (S2 Fig). Collectively, these data suggest that a (2'*S*)-2' sugar moiety as large as a methyl group is permissive for entry into the catalytic site of SAMHD1. Our model illustrations are based on crystal structures that are closed around an α -thio-dGTP, which is a poorly hydrolysable

substrate (31). Since the helix A351-V378 moves 10Å towards the dNTP in order to bind the substrate better (5), we speculated that SMDU-TP impedes the completion of the conformational helical changes within the four catalytic sites, which in turn blocks the dNTP hydrolysis activity of SAMHD1. Therefore, the Y374 may not act by a steric gate mechanism like L150 to exclude certain nucleotides from the catalytic pocket of SAMHD1.

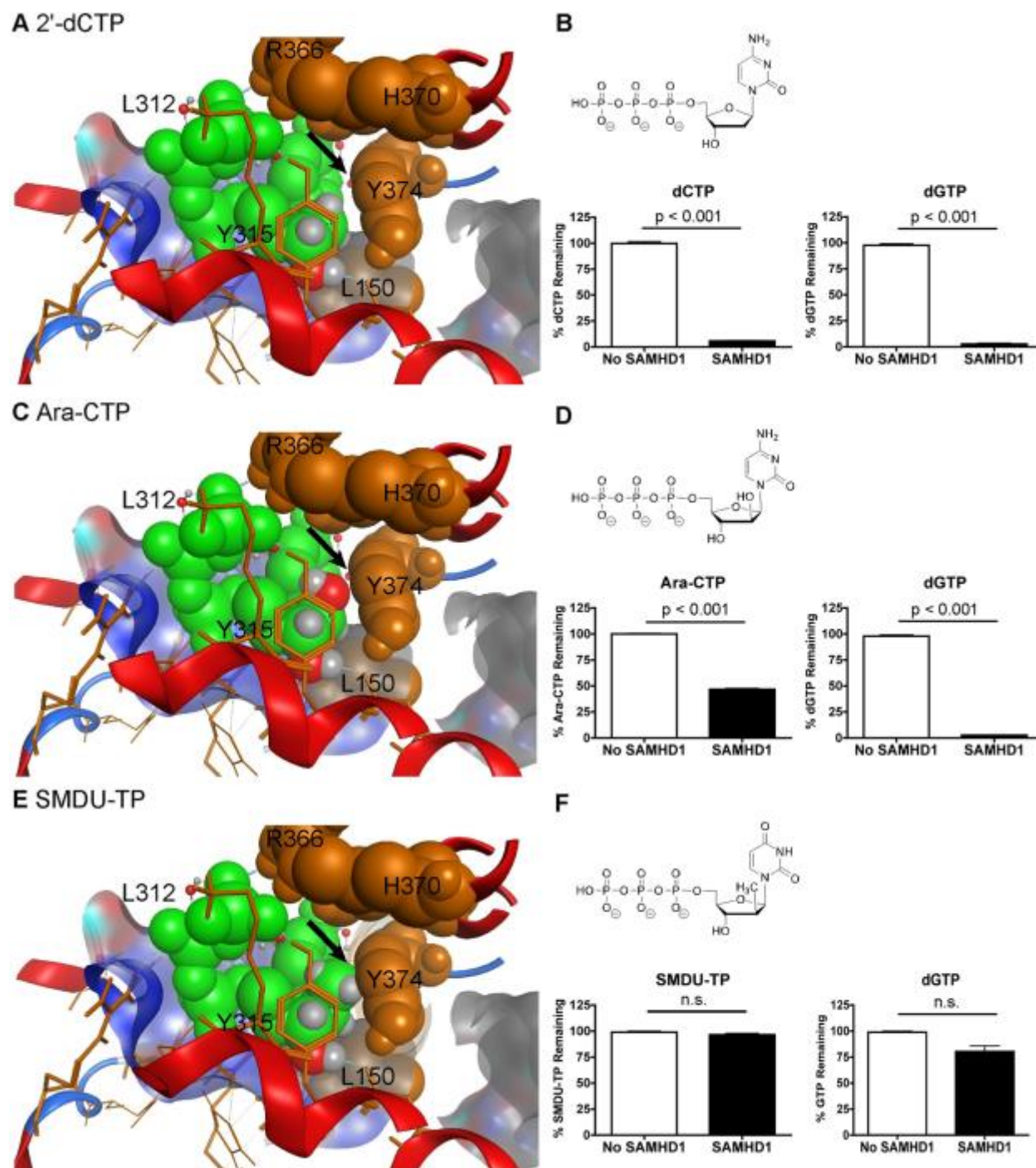


Figure 4: Role of Y374 and C2' sugar moiety substitution in acting as substrates of SAMHD1.

A) dCTP, C) ara-CTP and E) SMDU-TP nucleotides (in green) are modeled within the catalytic site of SAMHD1. Both dCTP and ara-CTP do not clash with Y374 (see arrow).

However the model shows that the (2'S)-2'-methyl group of SMDU-TP clashes with Y374 in the catalytic pocket of SAMHD1. B, D and F) Determining if dCTP, ara-CTP and SMDU-TP can be hydrolyzed for SAMHD1 *in vitro*. Structures of the compounds are above the HPLC graphs with experimental conditions described in Fig 2. Data are presented as the percent compound remaining (y-axis). dCTP and ara-CTP are significantly hydrolyzed ($p < 0.001$). SMDU-TP and dGTP, in the same reaction tube, had no significant hydrolysis in the presence of SAMHD1. HPLC analysis of each nucleoside was done twice in triplicate. Mean and SEM are plotted with significant or no significant (n.s.) differences determined using T test analysis.

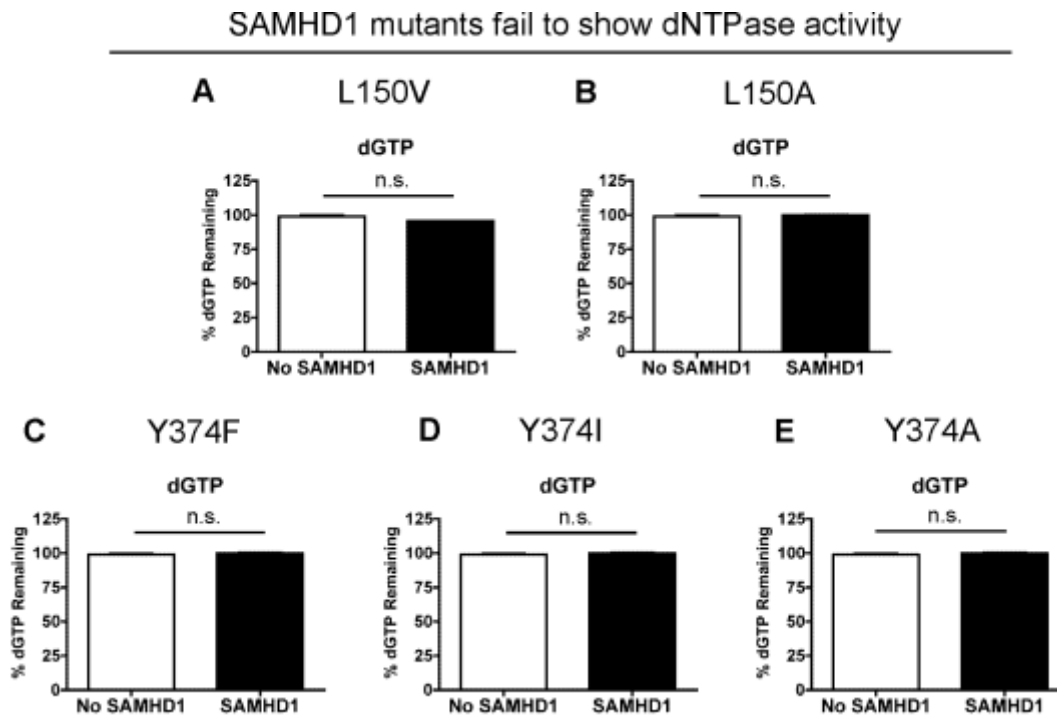


Figure S2: Site-directed mutagenesis for L150 and Y374.

A and B) Site-directed mutagenesis was used to make (A) L150V and (B) L150A mutants of SMAHD1. Biochemical analysis shows that both L150 mutants fail to significantly (n.s.) hydrolyzed dGTP. C-E) Y374 mutants: Y374F, Y374I, and Y374A were generated by site-directed mutagenesis. Biochemical analysis shows that both L150 mutants did not hydrolyze dGTP over the 2 hour incubation period. Mean and SEM are plotted with no significant (n.s.) differences determined using T test analysis.

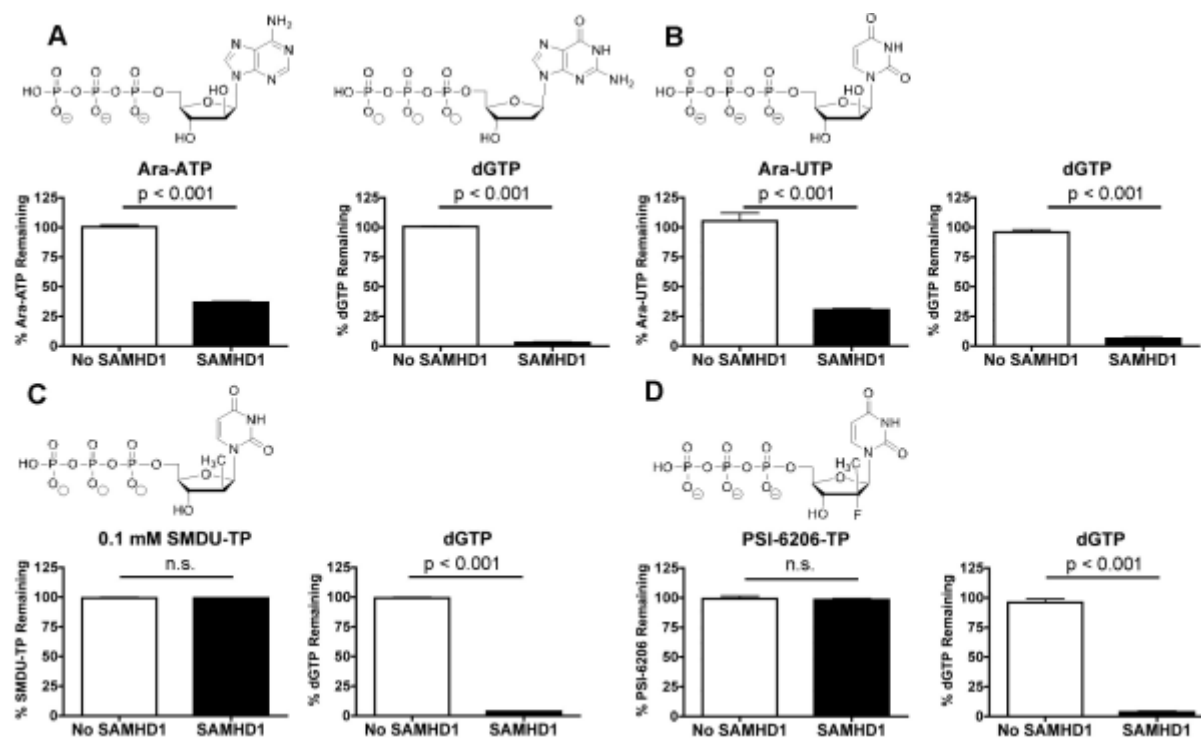


Figure S3: Evaluating additional non-canonical nucleotides as substrates for SAMHD1.

A) and B) Arabinose nucleotides: ara-ATP and ara-UTP were evaluated in the presence of dGTP using a semi-quantitative HPLC analysis method. Compounds were incubated with and without 1.6 μ M of SAMHD1 enzyme plus dGTP (A1 site activator) to determine if they are substrates of SAMHD1. Ara-ATP, Ara-UTP and dGTP are significantly ($p < 0.001$) hydrolyzed in the presence of SAMHD1. C) SMDU-TP ((2'*S*)-2'-methyl-dUTP) appears to block dGTP hydrolysis when at 1 mM for each nucleotide in the reaction tube. Therefore, 0.1 mM SMDU-TP and 1 mM dGTP are incubated for 2 h in the presence or absence of SAMHD1. No significant (n.s.) decrease in the percent SMDU-TP was detected, whereas dGTP was significantly ($p < 0.001$) hydrolyzed by SAMHD1. D) PSI-6296-TP has a (2'*R*)-2'-F, (2'*S*)-2'-methyl-dUTP. PSI-6202-TP is not hydrolyzed by SAMHD1, whereas dGTP, which is in the same reaction, is significantly ($p < 0.001$) hydrolyzed by SAMHD1.

Ara-CTP does not fit into the A2 site of SAMHD1

We then investigated if ara-CTP could permit homotetramerization of SAMHD1 by entering the A2 site. In order to accomplish this, we simply compared ara-CTP degradation in the presence of dGTP or GTP plus SAMHD1 protein. According to the SAMHD1 model (Fig 1), GTP can only occupy the A1 site, and thus requiring ara-CTP to occupy both A2 sites and catalytic sites to have hydrolysis active. However, dGTP can occupy A1, A2 and catalytic sites to promote SAMHD1 homotetramerization and hydrolysis activity. As shown in Fig 5A, when dGTP is used as the A1 activator, ara-CTP as well as dCTP (control) were significantly hydrolyzed ($p < 0.001$) when SAMHD1 was present. However, ara-CTP was not hydrolyzed when GTP and SAMHD1 was present, indicating that ara-CTP cannot occupy the A2 site of SAMHD1 in order to allow homotetramerization. For the control reaction, dCTP was significantly hydrolyzed ($p < 0.001$) in the presence of SAMHD1 and GTP (Fig 5B).

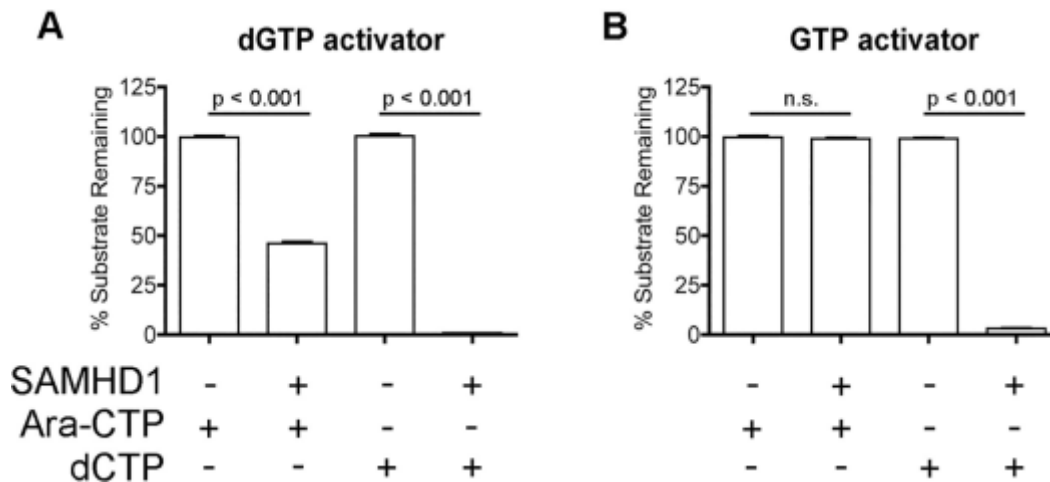


Figure 5: Ara-CTP does not fit into the A2 site of SAMHD1.

A) Evaluating ara-CTP hydrolysis in the presence of dGTP, using as A1 site activator. When dGTP was present, ara-CTP and dCTP were significantly hydrolyzed ($p < 0.001$) by SAMHD1. Data are presented as the percent compound remaining (y-axis). B) Determining if ara-CTP is hydrolysis by SAMHD1 in the presence of GTP. GTP will only fit into the A1 site of SAMHD1, thus requiring ara-CTP to occupy the A2 and catalytic sites for ara-CTP hydrolysis to occur. The percentage of ara-CTP remained constant with and without SAMHD1, indicating that ara-CTP cannot occupy the A2 site. Reactions containing dCTP was conducted and led to hydrolysis of dCTP in the presence of SAMHD1. Mean and SEM are plotted with significant or no significant (n.s.) differences determined using T test analysis.

Determining the K_i of SMDU-TP

Seamon *et al.* demonstrated that the pppCH₂dU analog, a non-hydrolysable SAMHD1 inhibitor, fits into both A2 and catalytic sites of SAMHD1, leading to two different K_i values and mechanisms of SAMHD1 inhibition. Since the (2'*S*)-2'-OH sugar moiety (ara-CTP; Fig 5) cannot fit within the A2 site of SAMHD1, we speculate that SMDU-TP analog, which has a (2'*S*)-2'-methyl moiety, will also be excluded from the A2 site. Therefore, the SMDU-TP analog may only inhibit the dNTPase activity of SAMHD1 at the catalytic site. A modified TLC assay procedure was used to determine the K_m of dTTP (substrate) and K_i of SMDU-TP analog (15). A representative TLC gel is displayed for dTTP hydrolysis by SAMHD1, showing the accumulation of the ³²-PPP product from (γ -³²P)-dTTP over 20–300 s without inhibitor (Fig 6A). Control (C), having no SAMHD1 enzyme, is used to subtract out the ³²-PPP background amount. Kinetic data are plotted and used to calculate the K_m of dTTP to be $845 \pm 229 \mu\text{M}$ (Fig 6B; dTTP only). Next SMDU-TP analog was evaluated at various concentrations: 1000–30 μM , in the presence of various concentrations of dTTP (3000–30 μM). These data were graphed in Fig 6C. The K_i for SMDU-TP analog was calculated to be $256 \pm 70 \mu\text{M}$ under our experimental conditions. We evaluated 1 mM pppCH₂dU analog or 1 mM SMDU-TP analog in the presence of 1 mM dGTP and found that both pppCH₂dU and SMDU-TP analogs could inhibit the dNTP triphosphohydrolase activity of SAMHD1 ($p < 0.01$) under our experimental HPLC assay conditions (Fig 6D). However, neither pppCH₂dU nor SMDU-TP analog could completely abolish the dNTP triphosphohydrolase activity of SAMHD1 in the presence of canonical dGTP in this assay. Overall, the SMDU-TP analog appears to be a competitive inhibitor of SAMHD1.

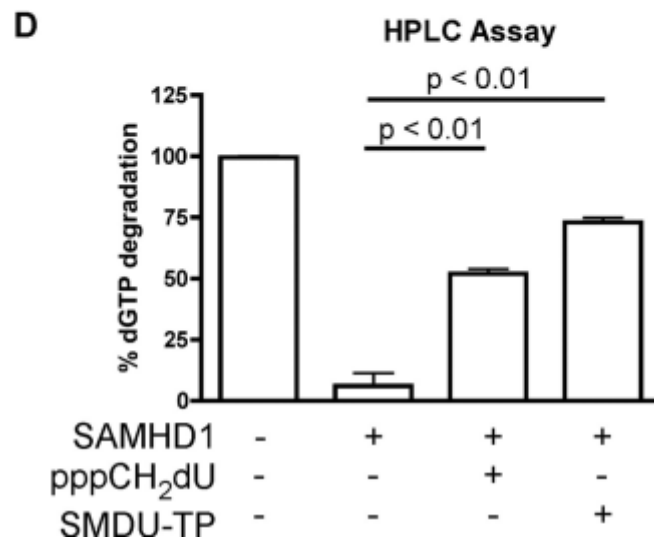
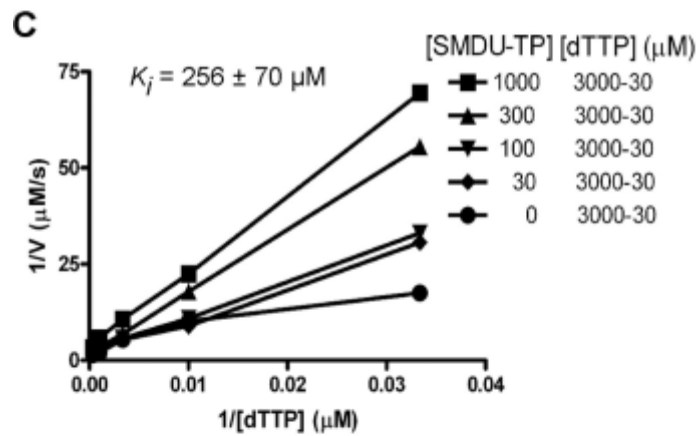
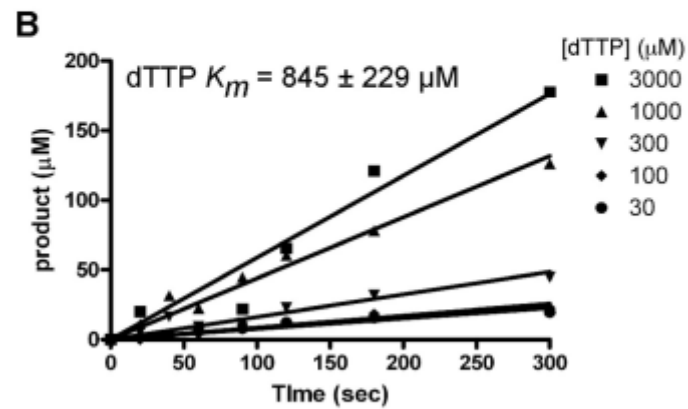
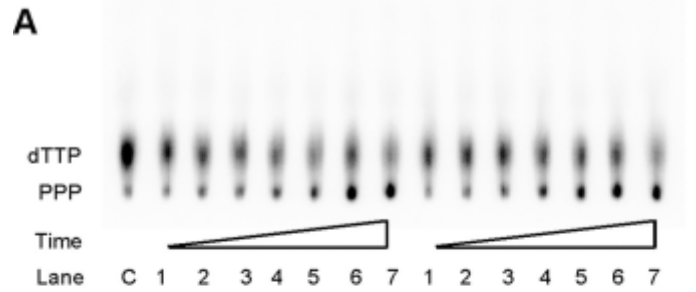


Figure 6: Biochemical assessment of SMDU-TP.

(A) Representative TLC plate showing 32 -PPP accumulations over 20–300 sec. time course when using 1.25 $\mu\text{Ci}/\mu\text{L}$ (γ - ^{32}P)-dTTP with 3000 (left side) and 1000 (right side) μM of dTTP (cold) as the substrate in the presence of 1 μM of SAMHD1 enzyme. (B) Graphing data from TLC analysis to generate slopes for the different dTTP concentrations tested. Data displayed as Product (μM) (y-axis) vs. Time (sec) (x-axis). K_m of dTTP was calculated to be $845 \pm 229 \mu\text{M}$ from the slopes generated using Prism software. (C) TLC analysis was done at various concentrations of dTTP (3000–30 μM) in the presence of various concentrations of SMDU-TP (1000–30 μM). Data are graphed as $1/V$ ($\mu\text{M}/\text{s}$) (y-axis) vs. $1/(\text{dTTP})$ (μM) (x-axis). From the slopes generated, the K_i of SMDU-TP was calculated to be $256 \pm 70 \mu\text{M}$. (D) Biochemical HPLC analysis of reactions with and without SAMHD1, and in the presence of pppCH₂dU or SMDU-TP analog is graphed. We observed that both pppCH₂dU and SMDU-TP analogs inhibit SAMHD1's activity (($p < 0.01$) by one-way ANOVA analysis with Bonferroni's multiple comparisons), leading to more dGTP substrate remaining after the 2 h incubation with enzyme. All data are representative of two independent studies with mean and SEM displayed.

Monitoring catabolism of ara-CTP by SAMHD1 in monocyte-derived macrophages

To extend our biochemical data confirming that ara-CTP (Fig 2B) is a substrate for SAMHD1, we used a well-defined tissue culture model of monocyte-derived macrophages (MDMs) treated with virus-like particles (VLP) (33, 45, 46) to evaluate changes in ara-CTP concentration in the absence of SAMHD1 *in vivo*. When MDMs are treated with VLP containing SIV_{mac239} viral protein X (Vpx), a rapid decrease in SAMHD1 protein level that last for several days after Vpx+ VLP exposure (45, 46). MDMs were exposed to VLP with and without Vpx for 24 h before the medium was replaced with fresh medium containing 10 μ M of ara-C or 10 μ M of gemcitabine. Cell lysates were collected at 24 and 48 h post VLP addition to monitor SAMHD1 protein level. Immunoblots show the depletion of SAMHD1 in MDMs treated with Vpx+ VLP, but not Vpx- VLP treated MDMs and control MDMs (no VLP treatment) (Fig 7A).

Next, cellular dNTP extracts were collected at 4, 12 and 24 h post medium change with drug. HLPC-MS/MS analysis was used to quantify the intracellular concentrations of gem-TP (2',2'-diF-dCTP) and ara-CTP. We found that the cellular gem-TP concentration at 4 h is significantly lower (**, $p < 0.01$) in Vpx+ VLP treated MDMs as compared to Vpx- VLP MDMs (Fig 7B). This could be due to changes in of cellular kinase activities that phosphorylate nucleosides. Deoxycytidine kinase, which phosphorylates dC to dCMP, is negatively regulated by dCTP, the reaction pathway end product (47). Importantly we see a comparable rate decrease in gem-TP concentration between the two treatment groups from 4 to 24 h (Fig 7B), suggesting gem-TP turnover was SAMHD1 independent. Next, we evaluated ara-C treatment in the two MDM populations (Fig 7C). The Vpx+ VLP treated MDMs had significantly (***, $p < 0.001$) higher levels of ara-CTP at 4, 12 and 24 h, as compared to Vpx- VLP treated MDMs, suggesting SAMHD1 impacts the peak intracellular ara-CTP concentration and suggest augmentation of

ara-CTP turnover rate *in vivo*. Our tissue culture findings support our biochemical studies strongly suggesting that ara-CTP may be a substrate for SAMHD1 *in vivo*. Moreover, our data reveals that an additional cellular pathway, SAMHD1 independent, is present that is involved with the turn over gem-TP in the cell, which requires additional studies to elucidate the mechanism in the future.

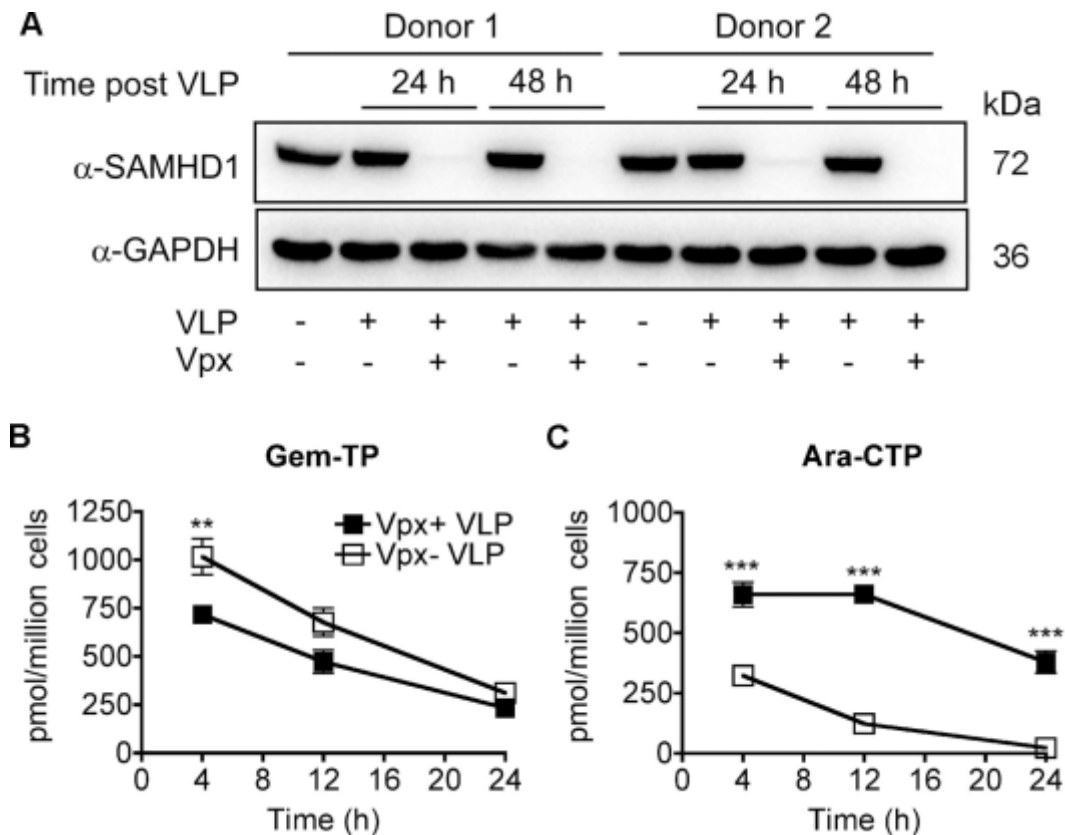


Figure 7: Monitoring ara-CTP and gem-TP concentrations in MDMs.

A) Monocyte-derived macrophages (MDMs) were pretreated with virus-like particles (VLP) one day prior to replacing the medium with fresh medium plus compounds: 10 μ M of ara-C (cytaribine- 13 C $_3$) or 10 μ M of gemcitabine. Whole cell lysates were collected at 0, 24 and 48 h post VLP addition. Lysates were analyzed by immunoblotting for SAMHD1 and GAPDH, loading control. SAMHD1 protein levels were reduced at 24 h after Vpx+ VLP exposure. Two human primary MDM donors are shown. Cellular nucleotide extracts were generated at 4, 12 and 24 h post drug addition from treated MDMs. The intracellular concentrations of B) gem-TP (2',2'-diF-dCTP) and (C) ara-CTP were quantified from the extracts using HPLC-MS/MS analysis. Data are plotted as pmol/million cells (y-axis) vs. time (h) (x-axis). Gem-TP is a significantly lower (**, $p < 0.01$; T test) in the Vpx+ VLP treated MDMs at 4 h after drug addition. However, the rate of gem-TP decay is comparable between the two groups, suggesting

that gem-TP degradation is SAMHD1 independent. Ara-CTP concentrations are significantly higher (***, $p < 0.001$) at 4, 12 and 24 h for the Vpx+ VLP treated MDMs. Moreover, the rate of decay of ara-CTP is slower in Vpx+ VLP treated group, suggesting ara-CTP turnover is SAMHD1 dependent. Data are from two independent donors tested in duplicate.

Nucleoside-5'-triphosphate substrate specificity for SAMHD1

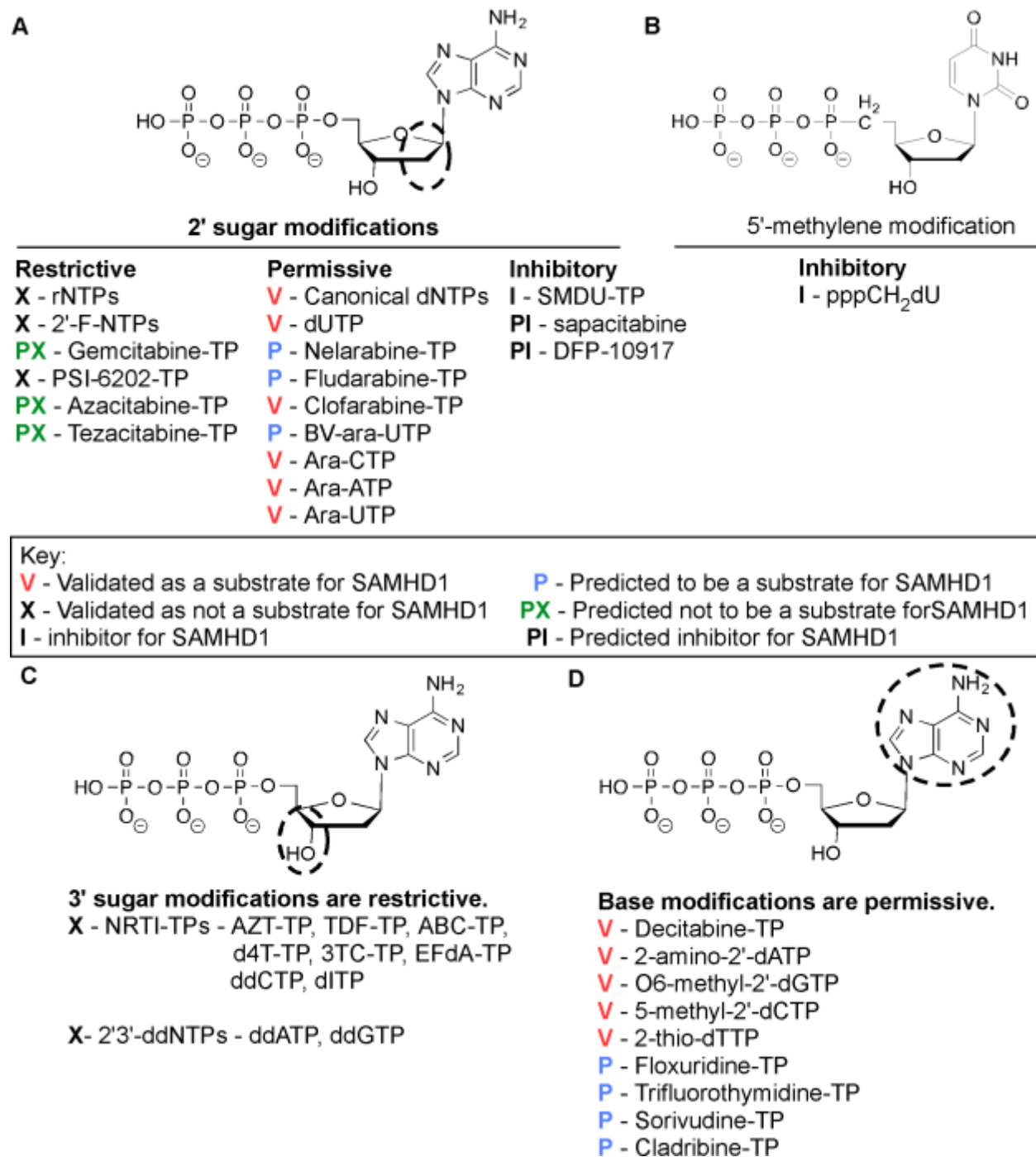


Figure 8: Determining nucleotide analog specificity for SAMHD1.

A) Modification of the 2' sugar position of a nucleotide can lead to several different outcomes.

First, (2'*R*)-2'-F and (2'*R*)-2'-OH sugar moieties have been shown not to be substrates for

SAMHD1. Additional analogs with (2'*R*)-2'-F and (2'*R*)-2'-OH sugar moieties would be predicted not to be substrates for SAMHD1. Second, canonical dNTPs and the non-canonical dUTP are substrates for SAMHD1. Our data shows that ((2'*S*)-2'-OH) arabinose nucleoside-5'-triphosphates are also substrates for SAMHD1. Therefore, we also predict several other arabinose nucleoside analogs would be substrates for SAMHD1. Moreover, clofarabine-TP ((2'*S*)-2'-F) was reported hydrolyzed by SAMHD1 (43). Finally, we found the SMDU-TP, (2'*R*)-2'-methyl sugar moiety, inhibited the triphosphohydrolase activity of SAMHD1. We postulate that the (2'*R*)-2'-methyl moiety may prevent the conformational change in the catalytic site of SAMHD1 due to the size of the methyl group clashing with Y374. Therefore, we predicted that nucleotides with a (2'*S*)-2'-cyano moiety may also inhibit dNTPase activity of SAMHD1. B) A SAMHD1 inhibitor has been reported (34). The pppCH₂-dU analog has a 5'-methylene modification, making the analog non-hydrolysable in the catalytic site, but also was shown to block homotetramerization when present in the A2 site (34). C) Modification of the 3'-OH sugar moiety is not permissive. NRTIs and ddNTPs lack a 3'-OH moiety, making them chain terminators for DNA polymerases, are not substrates for SAMHD1. D) Base modifications for different nucleoside analogs are permissive substrates for SAMHD1.

D. Discussion

In this study we explore the effect of stereoselective 2' sugar moiety substitution analogs on the dNTPase activity of SAMHD1. In Fig 8, we compile our results for what we know will influence nucleotides to be substrates for SAMHD1. Ji *et al.* proposed that L150 and Y374 of SAMHD1 form a tight catalytic pocket to exclude rNTPs. The L150 would essentially act as a steric gate to exclude rNTPs from the catalytic pocket (Fig 8A). Our computational modeling

indicates that only a dNTP can fit in the catalytic site (Fig 2A), but larger (2'R)-2'-F or (2'R)-2'-OH moieties are excluded (Fig 2C and 2E). A HPLC-bases assay confirmed that (2'R)-2'-F and (2'R)-2'-OH are not substrates for SAMHD1 (Fig 2D, 2F and S1 Fig). Therefore, the L150 acts by a steric gate mechanism, i.e. clashing of the L150 with the (2'R)-2'-F/OH moiety to exclude these nucleotides from docking in the catalytic pocket of SAMHD1. Our computational modeling indicates that (2'S)-2'-H and (2'S)-2'-OH sugar moieties can fit within the catalytic site of SAMHD1, while (2'S)-2'-methyl moiety clash with Y374 (Fig 4). Biochemical analysis showed that both dCTP ((2'S)-2'-H) and ara-CTP ((2'S)-2'-OH) are hydrolyzed in the presence of SAMHD1 (Fig 4B and 4D). We therefore postulate that ara-CTP, ara-ATP, ara-GTP, fludarabine-TP, cladribine-TP, and clofarabine-TP would be sensitive to hydrolysis by SAMHD1 *in vivo* (Fig 8A). Interestingly, the SMDU-TP analog ((2'S)-2'-methyl) blocked the triphosphohydrolase activity of SAMHD1 in the biochemical assay, making it a nucleotide inhibitor of SAMHD1. To address why SMDU-TP inhibits the dNTPase activity of SAMHD1, we postulate that SMDU-TP prevents the full A351-V378 helix 10Å movement towards a dNTP substrate in the catalytic pocket (5). This mechanism is very different from the SAMHD1 inhibitor, pppCH₂dU (Fig 8B), which acts by preventing tetramer formation and is a non-cleavable substrate for SAMHD1 (34). This means that (2'S)-2' substituted nucleotides has access to and bind within the catalytic pocket of SAMHD1. For our mechanism to work, the final changes with the A351-V378 helix movement is completed after the dNTP is docket within the catalytic site. Once the helix conformational change is completed then hydrolysis of the nucleotide analog occurs. For SMDU-TP, the (2'S)-2'-methyl clashes with Y374 preventing the helix from completing the conformational change and thus blocks hydrolysis. If our model is correct, then we would predict that sapacitabine (CYC682) and DFP-10917, which have a (2'S)-

2'-cyano (CN) moiety, would also dock within the catalytic pocket of SAMHD1 and then inhibit the dNTPase activity of SAMHD1 (Fig 8A). Sapacitabine and DFP-10917 are currently under clinical investigation as anticancer nucleoside compounds.

Additional aspects of nucleoside analogs are also examined. The 3' position of the sugar is of high importance in determining which dNTP analogs have the potential to be substrates for SAMHD1 (Fig 8C). Ji *et al.* proposed that the 3'-OH sugar moiety has hydrogen bond interactions with D319 and Q149 of SAMHD1 to promote correct alignment of the dNTP in the catalytic pocket (31). The FDA-approved antiviral NRTIs, such as AZT, d4T, 3TC, ddC; Fig 3C, ddI; Fig 3D, and abacavir (ABC) were shown not to be substrates for SAMHD1 *in vitro* (this study and (17, 18)). Additionally, we show that ddATP and ddGTP are not substrates for SAMHD1 (Fig 3A and 3B). Collectively these data validate Ji *et al.* biochemical structure model, indicating that 3'-OH sugar moiety is an essential function group of the nucleoside for SAMHD1 substrate specificity (31). As indicated in Fig 8D, the type of base or being modified does not restrict a nucleotide analog from being a substrate for SAMHD1. Presently, all canonical bases and modified bases analogs: decitabine-TP (S1 Fig), dUTP, 2-amino-2'-dATP, O6-methyl-2'-dGTP, 5-methyl-2'-dCTP and 2-thio-dTTP are hydrolyzed by SAMHD1 (34, 40). Therefore, we postulate the following non-canonical FDA-approved nucleosides: cladribine, floxuridine, trifluorothymidine, and sorivudine, when phosphorylated in the cell, are strong candidates for being SAMHD1 substrates *in vivo*. These are nucleosides used for anticancer and antiviral treatments.

Biologically, both ribonucleotide reductase and SAMHD1 have roles in maintaining proper intracellular dNTP concentrations (48–50). SAMHD1-deficient mice have a dNTP imbalance, with higher intracellular dATP and dGTP concentrations than dTTP and dCTP

concentrations (51), and a cellular dNTP imbalance can promote higher rates of mutagenesis in cancer cells, and influence the ability of DNA viruses to infect cells (33, 52–55). One can imagine that a SAMHD1 nucleoside analog inhibitor might be useful in an anticancer regimen by promoting a dNTP imbalance in rapidly dividing cancer cells or in combination therapy with FDA-approved nucleoside analogs that are sensitive to hydrolysis by SAMHD1. Alternatively, increasing SAMHD1 levels in cancer cells may slow cell growth by decreasing dNTP concentrations (56). Overall our data provides insights as to how stereoselective 2' sugar moiety substitutions impact the triphosphohydrolase activity of SAMHD1.

E. Materials and Methods

Compounds

Gemcitabine (2',2'-diF-dC), arabinose-C (ara-C; aka cytarabine), dCMP were purchased from Sigma. Gemcitabine-5'-triphosphate (gem-TP), ara-cytidine-5'-triphosphate (ara-CTP) and 5-aza-2'-deoxycytidine-5'-triphosphate (decitabine-TP) were purchased from Jena Bioscience. dGTP, dATP and dCTP was purchased from Affymetrix. ATP, CTP and GTP were purchased from Thermo Scientific. 2',3'-dideoxyinosine-5'-triphosphate (ddITP), 2',3'-dideoxadenosine-5'-triphosphate (ddATP), 2',3'-dideoxycytosine-5'-triphosphate (ddCTP) and 2',3'-dideoxguanosine-5'-triphosphate (ddGTP) were purchased from Roche. Cytarabine-¹³C₃ was purchased from Toronto Research Chemicals. (2'*R*)-2'-F-2'-deoxyadenosine-5'-triphosphate (2'-F-dATP) and (2'*R*)-2'-F-2'-deoxycytidine-5'-triphosphate (2'-F-dCTP) were purchased from TriLink BioTechnologies.

Recombinant SAMHD1-GST purification

Human SAMHD1 was cloned into pGEX-6P-1 with an N-terminal GST tag (GE Healthcare, provided by Dr. Yoshio Koyanagi) and transformed into BL21 (DE3) pLysS competent cells (Invitrogen). Cells were grown at 37°C to an A600 of 0.5, stored on ice for 2 h, and induced overnight with 0.25 mM isopropyl- α -D-1-thiogalactopyranoside at 25°C. Cells were harvested and lysed in lysis buffer (50 mM Tris-HCl [pH 7.5], 500 mM NaCl, 2 mM EDTA, 1 mg/ml chicken egg white lysozyme, and one tablet of Roche Applied Science Complete protease inhibitor mixture) for 4 h on ice. Cell debris was removed by centrifugation at $49,000 \times g$ for 15 min, and lysate was incubated overnight at 4°C with 1.5 mL of Glutathione Sepharose[®] 4B bead slurry (GE Healthcare). Beads were pelleted and washed three times with wash buffer (50 mM Tris-HCl [pH 7.5], 500 mM NaCl, 1 mM dithiothreitol, 0.5% Triton X-100), equilibrated in buffer (50 mM Tris-HCl [pH 7.5], 150 mM NaCl, 20% glycerol, 0.5% Triton X-100) and packed into a column. The column was washed three times with 30 mL of equilibration buffer, and SAMHD1 was eluted with 50 mM Tris-HCl [pH 8], 1 mM EDTA, 10% glycerol, 300 mM NaCl, 200 mM reduced glutathione. A Millipore Centricon protein concentrator (45 MWCO) was used to concentrate the protein and for buffer exchanges. Protein samples were snap frozen using liquid nitrogen and stored at -80°C until use.

HPLC-based SAMHD1 Phosphohydrolase Assay

To measure dNTP triphosphohydrolase activity of SAMHD1, 1.6 μ M recombinant SAMHD1-GST (SAMHD1) was incubated with different 500 μ M nucleoside-5'-triphosphate substrates in the presence of 500 μ M dCMP, 500 μ M GTP and reaction buffer (50 mM Tris-HCl [pH 8], 100 mM KCl, 5 mM MgCl₂, and 0.1% Triton X-100). Reactions were incubated for 2 h at 37°C and terminated by incubation for 10 min at 75°C. Reactions were separated and

quantified by anion exchange HPLC method [32]. Separation was done using two DNAPac PA100 columns equilibrated with running buffer (25 mM Tris-HCl [pH 8] and 0.5% acetonitrile) for 10 min, 30 μ L sample was injected and eluted with a linear gradient of 240 mM NH_4Cl for 12 min, run at an isocratic gradient with 240 mM NH_4Cl for 5 min, and column was again equilibrated with running buffer (Beckman Coulter System Gold 126 Solvent Module). Absorbance was measured with a Beckman Coulter System Gold 166 Detector at 254 nm. The amounts of deoxycytidine-5'-monophosphate (dCMP), dGTP and (deoxy)nucleoside-5'-TP analogs were determined by integrating the peak area using 32 Karat 8.0 Software. Data was normalized to dCMP peak area for each sample, used as a sample loading control. Determining changes for different (deoxy)nucleoside-5'-triphosphates of interest was calculated by setting sample without SAMHD1 peak area to 100%.

Cells and cell culture

Monocytes were isolated from whole blood (New York Blood Service, Long Island New York) by using MACS[®] CD14⁺ beads as described previously [33] and cultured in the presence of 5 ng/mL human GM-CSF (Miltenyi Biotec). MDMs were utilized at day 7 of maturation for experiments.

Virus-like particles generation (VLP)

T225 flasks containing 293FT cells (Invitrogen) were transfected with 40 μ g of pSIV 3+ with or without Vpx (Vpx+ VLP and Vpx- VLP, respectively; kindly provided by Dr. Nathaniel Landau) and 20 μ g of pVSV-G at a ratio of 1 μ g of DNA to 3 μ L of polyethylenimine linear MW 25,000 (Polysciences Inc.). The following day, medium was replaced with fresh DMEM medium

containing 5% FBS and antibiotics. On days 2–3 after transfection, the medium was collected and replaced with fresh medium. On the day of collection, medium was centrifuged at 400 x g for 5 min to remove cells. Supernatant was overlaid on top of 5 ml of a 25% sucrose cushion (25% (w/v) sucrose, 10 mM Tris-HCl [pH 7.5], 0.1 M NaCl and 1 mM EDTA). VLP were concentrated at 82520 x g in an SW32 Ti rotor for 90 min by ultracentrifugation. Supernatant was aspirated, and pellets were suspended in 600 µL of serum-free DMEM. Supernatant was centrifuged for 1 min at 20800 x g to remove debris using a tabletop centrifuge. Aliquots (50 µL) were stored at -80°C. The p27 antigen level was determined using an ELISA kit (Advanced BioScience Laboratories, Inc.). A minimum of 145 ng of p27/million cells was used.

HLPC-MS/MS quantification of dNTPs and NTPs

The HPLC system was a Dionex Packing Ultimate 3000 modular LC system comprising of a ternary pump, vacuum degasser, thermostated autosampler, and thermostated column compartment (Dionex, CA). A TSQ Quantum Ultra triple quadrupole mass spectrometer (Thermo Scientific, Waltham, MA, USA.) was used for detection. Thermo Xcalibur software version 2.0 was used to operate HPLC, the mass spectrometer and to perform data analyses. Gradient separation was performed on a Hypersil GOLD column (100 x 1 mm, 3 µm particle size; Thermo Scientific, Waltham, MA, USA). Mobile phase A consisted of 2 mM ammonium phosphate and 3 mM hexylamine. Acetonitrile was increased from 8 to 40% in 10 min, and kept at 40% for 2 min. Equilibration at 8% acetonitrile lasted 15 min. The total run time was 27 min. The flow rate was maintained at 50 µL/min and a 25 µL injection was used. The autosampler and the column compartment were maintained at 4.5 and 30°C, respectively. Calibration curves were generated using gem-TP, and ara-CTP to determine concentrations.

Compound synthesis

The protocol published by Seamon *et al.* was used for the synthesis of 5'-methylene-2'-deoxyuridine-5'-triphosphate (pppCH₂dU) [34]. An anomeric mixture (10:1 β:α) of (2'S)-2'-C-Me-2'-deoxyuridine (SMDU) [35] was synthesized using the procedure by Li and Piccirilli [36]. Chromatographic separation of the pure beta anomer was subsequently performed using a SorbTech Sorbet Technologies column on a Combiflash Teledyne Isco chromatography machine. PSI-6206 was synthesized as reported in [37]. Finally, the triphosphate forms of SMDU and PSI-6206 were prepared with >95% purity following a nucleoside derivative triphosphate synthesis procedure reported by Zhou *et al.* [38], generating SMDU-TP and PSI-6206-TP compounds.

TLC-based SAMHD1 Phosphohydrolase Assay

SAMHD1 (1 μM) was incubated with 1.25 μCi/μL [γ -³²P]-dTTP and various concentrations: 3,000, 1,000, 300, 100 and 30 μM of unlabeled dTTP, 500 μM GTP (as the activator), and various concentrations: 1000, 300, 100, and 30 μM of either SMDU-TP or pppCH₂dU in reaction buffer (50 mM Tris-HCl [pH 8], 100 mM KCl, 5 mM MgCl₂, and 0.1% Triton X-100). Reaction volume (10 μL) was incubated for 20, 40, 60, 90, 120, 180, and 300 s at 20°C. One microliter was removed from the reaction at the indicated times and stopped in 5 μL of 500 mM EDTA that was on wet ice. Samples were then heat inactivated at 95°C for 2 min before being stored at 4°C. Cellulose 300 PEI/UV₂₅₄ TLC plates (Macherey-Nagel; Cat # 801063) were prepared by spraying with 100% methanol and then allowed to dry. Plates were marked with a pencil one inch from the top and bottom on the plate. One microliter of the

reaction was spotted one inch from the bottom on TLC plates. Solvent (0.8 M LiCl, 0.05 M EDTA and 1 M acetic acid) front was allowed to migrate to within one inch from the top of the plate before the plate was removed and dried. TLC plates were exposed to Bio-Rad phosphoimager screen. Data was captured using PharosFX Plus Imager. Data was quantitated using Quantity One software (Bio-Rad).

Western blot analysis

Samples were processed in radioimmunoprecipitation assay buffer containing 1 μ M DTT, 10 μ M PMSF, 10 μ L/mL phosphatase inhibitor (Sigma), and 10 μ L/mL protease inhibitor (Sigma). The cells were sonicated with three 5-sec pulses to ensure complete lysis. Cellular debris was removed by centrifugation at 23000 x g for 10 min. Supernatants were stored at -80°C before use. Cell lysates (25 μ g) were resolved on 8% SDS-PAGE. Proteins were transferred to a nitrocellulose membrane. The membrane was blocked with 2% nonfat milk in TBST (10 mM Tris, 150 mM NaCl, and 0.1% Tween 20) for 1 h followed by the addition of primary antibodies: SAMHD1 (Abcam), and GAPDH (Santa Cruz). Cut membrane was incubated overnight with antibodies at 4°C. The next day, the membrane was washed (3x, 20 min with TBST) and treated with anti-mouse-HRP or anti-rabbit-HRP (GE Healthcare) for 1 h at room temperature. Membrane was washed (3x, 20 min with TBST) and developed using the SuperSignal West Femto Kit (Thermo Scientific). Images were captured using a Bio-Rad ChemiDoc Imager. ImageLab Analysis software (Bio-Rad) was used to analyze the data.

Graphing and statistical analysis

Prism (GraphPad) software was used for plotting the data. Graphs are plotted as the means and standard error of means (SEM). All the data sets were compared for significant difference using Two-way ANOVA analysis and either Bonferroni post-test analysis for significance with the dNTP data or multiple comparisons. The K_m and K_i values for dTTP and SMDU-TP are determined using Prism software.

F. References

1. Goldstone, D. C., Ennis-Adeniran, V., Hedden, J. J., Groom, H. C., Rice, G. I., Christodoulou, E., ... & de Carvalho, L. P. S. (2011). HIV-1 restriction factor SAMHD1 is a deoxynucleoside triphosphate triphosphohydrolase. *Nature*, *480*(7377), 379-382.
2. Powell, R. D., Holland, P. J., Hollis, T., & Perrino, F. W. (2011). Aicardi-Goutieres syndrome gene and HIV-1 restriction factor SAMHD1 is a dGTP-regulated deoxynucleotide triphosphohydrolase. *Journal of Biological Chemistry*, *286*(51), 43596-43600.
3. Yan, J., Kaur, S., DeLucia, M., Hao, C., Mehrens, J., Wang, C., ... & Skowronski, J. (2013). Tetramerization of SAMHD1 is required for biological activity and inhibition of HIV infection. *Journal of Biological Chemistry*, *288*(15), 10406-10417.
4. Brandariz-Nuñez, A., Valle-Casuso, J. C., White, T. E., Laguette, N., Benkirane, M., Brojatsch, J., & Diaz-Griffero, F. (2012). Role of SAMHD1 nuclear localization in restriction of HIV-1 and SIVmac. *Retrovirology*, *9*(1), 49.
5. Zhu, C., Gao, W., Zhao, K., Qin, X., Zhang, Y., Peng, X., ... & Wei, W. (2013). Structural insight into dGTP-dependent activation of tetrameric SAMHD1 deoxynucleoside triphosphate triphosphohydrolase. *Nature communications*, *4*, 2722.
6. Brandariz-Nuñez, A., Valle-Casuso, J. C., White, T. E., Nguyen, L., Bhattacharya, A., Wang, Z., ... & Ivanov, D. N. (2013). Contribution of oligomerization to the anti-HIV-1 properties of SAMHD1. *Retrovirology*, *10*(1), 131.
7. Ryoo, J., Choi, J., Oh, C., Kim, S., Seo, M., Kim, S. Y., ... & Diaz-Griffero, F. (2014). The ribonuclease activity of SAMHD1 is required for HIV-1 restriction. *Nature medicine*, *20*(8), 936-941.

8. Guo, H., Wei, W., Wei, Z., Liu, X., Evans, S. L., Yang, W., ... & Yu, X. F. (2013). Identification of critical regions in human SAMHD1 required for nuclear localization and Vpx-mediated degradation. *PloS one*, 8(7), e66201.
9. Hrecka, K., Hao, C., Gierszewska, M., Swanson, S. K., Kesik-Brodacka, M., Srivastava, S., ... & Skowronski, J. (2011). Vpx relieves inhibition of HIV-1 infection of macrophages mediated by the SAMHD1 protein. *Nature*, 474(7353), 658.
10. Laguette, N., Sobhian, B., Casartelli, N., Ringard, M., Chable-Bessia, C., Ségéral, E., ... & Benkirane, M. (2011). SAMHD1 is the dendritic–and myeloid–cell–specific HIV–1 restriction factor counteracted by Vpx. *Nature*, 474(7353), 654.
11. Lahouassa, H., Daddacha, W., Hofmann, H., Ayinde, D., Logue, E. C., Dragin, L., ... & Pancino, G. (2012). SAMHD1 restricts the replication of human immunodeficiency virus type 1 by depleting the intracellular pool of deoxynucleoside triphosphates. *Nature immunology*, 13(3), 223-228.
12. Pauls, E., Ruiz, A., Badia, R., Permanyer, M., Gubern, A., Riveira-Muñoz, E., ... & Crespo, M. (2014). Cell cycle control and HIV-1 susceptibility are linked by CDK6-dependent CDK2 phosphorylation of SAMHD1 in myeloid and lymphoid cells. *The Journal of Immunology*, 193(4), 1988-1997.
13. Ruiz, A., Pauls, E., Badia, R., Torres-Torronteras, J., Riveira-Muñoz, E., Clotet, B., ... & Esté, J. A. (2015). Cyclin D3-dependent control of the dNTP pool and HIV-1 replication in human macrophages. *Cell cycle*, 14(11), 1657-1665.
14. Welbourn, S., Dutta, S. M., Semmes, O. J., & Strebel, K. (2013). Restriction of virus infection but not catalytic dNTPase activity is regulated by phosphorylation of SAMHD1. *Journal of virology*, 87(21), 11516-11524.

15. White, T. E., Brandariz-Nuñez, A., Valle-Casuso, J. C., Amie, S., Nguyen, L. A., Kim, B., ... & Diaz-Griffero, F. (2013). The retroviral restriction ability of SAMHD1, but not its deoxynucleotide triphosphohydrolase activity, is regulated by phosphorylation. *Cell host & microbe*, 13(4), 441-451.
16. Ballana, E., Badia, R., Terradas, G., Torres-Torronteras, J., Ruiz, A., Pauls, E., ... & Esté, J. A. (2014). SAMHD1 specifically affects the antiviral potency of thymidine analog HIV reverse transcriptase inhibitors. *Antimicrobial agents and chemotherapy*, 58(8), 4804-4813.
17. Huber, A. D., Michailidis, E., Schultz, M. L., Ong, Y. T., Bloch, N., Puray-Chavez, M. N., ... & Landau, N. R. (2014). SAMHD1 has differential impact on the efficacies of HIV nucleoside reverse transcriptase inhibitors. *Antimicrobial agents and chemotherapy*, 58(8), 4915-4919.
18. Amie, S. M., Daly, M. B., Noble, E., Schinazi, R. F., Bambara, R. A., & Kim, B. (2013). Anti-HIV host factor SAMHD1 regulates viral sensitivity to nucleoside reverse transcriptase inhibitors via modulation of cellular deoxyribonucleoside triphosphate (dNTP) levels. *Journal of Biological Chemistry*, 288(28), 20683-20691.
19. Hollenbaugh, J. A., Schader, S. M., Schinazi, R. F., & Kim, B. (2015). Differential regulatory activities of viral protein X for anti-viral efficacy of nucleoside reverse transcriptase inhibitors in monocyte-derived macrophages and activated CD4+ T cells. *Virology*, 485, 313-321.
20. Balzarini, J. (2000). Effect of antimetabolite drugs of nucleotide metabolism on the anti-human immunodeficiency virus activity of nucleoside reverse transcriptase inhibitors. *Pharmacology & therapeutics*, 87(2), 175-187.

21. Parker, W. B. (2009). Enzymology of purine and pyrimidine antimetabolites used in the treatment of cancer. *Chemical reviews*, 109(7), 2880.
22. Hurwitz, S. J., & Schinazi, R. F. (2013). Prodrug strategies for improved efficacy of nucleoside antiviral inhibitors. *Current opinion in HIV and AIDS*, 8(6), 556-564.
23. Neuberger, M. S., Di Noia, J. M., Beale, R. C., Williams, G. T., Yang, Z., Rada, C., & Yang, Z. (2005). Somatic hypermutation at AT pairs: polymerase error versus dUTP incorporation. *Nature Reviews Immunology*, 5(2).
24. Mathews, C. K. (2015). Deoxyribonucleotide metabolism, mutagenesis, and cancer.
25. Weinberg, G., Ullman, B., & Martin, D. W. (1981). Mutator phenotypes in mammalian cell mutants with distinct biochemical defects and abnormal deoxyribonucleoside triphosphate pools. *Proceedings of the National Academy of Sciences*, 78(4), 2447-2451.
26. Gao, W. Y., Cara, A., Gallo, R. C., & Lori, F. (1993). Low levels of deoxynucleotides in peripheral blood lymphocytes: a strategy to inhibit human immunodeficiency virus type 1 replication. *Proceedings of the National Academy of Sciences*, 90(19), 8925-8928.
27. Hu, W. S., & Hughes, S. H. (2012). HIV-1 reverse transcription. *Cold Spring Harbor perspectives in medicine*, 2(10), a006882.
28. Akbari, M., Peña-Diaz, J., Andersen, S., Liabakk, N. B., Otterlei, M., & Krokan, H. E. (2009). Extracts of proliferating and non-proliferating human cells display different base excision pathways and repair fidelity. *DNA repair*, 8(7), 834-843.
29. Lloyd, S. B., Kent, S. J., & Winnall, W. R. (2014). The high cost of fidelity. *AIDS Research and Human Retroviruses*, 30(1), 8-16.
30. Preston, B. D., Poiesz, B. J., & Loeb, L. A. (1988). Fidelity of HIV-1 reverse transcriptase. *Science*, 242(4882), 1168-1171.

31. Ji, X., Wu, Y., Yan, J., Mehrens, J., Yang, H., DeLucia, M., ... & Xiong, Y. (2013). Mechanism of allosteric activation of SAMHD1 by dGTP. *Nature structural & molecular biology*, 20(11), 1304-1309.
32. White, T. E., Brandariz-Nuñez, A., Valle-Casuso, J. C., Amie, S., Nguyen, L., Kim, B., ... & Diaz-Griffero, F. (2013). Contribution of SAM and HD domains to retroviral restriction mediated by human SAMHD1. *Virology*, 436(1), 81-90.
33. Hollenbaugh, J. A., Gee, P., Baker, J., Daly, M. B., Amie, S. M., Tate, J., ... & Koyanagi, Y. (2013). Host factor SAMHD1 restricts DNA viruses in non-dividing myeloid cells. *PLoS pathogens*, 9(6), e1003481.
34. Seamon, K. J., Hansen, E. C., Kadina, A. P., Kashemirov, B. A., McKenna, C. E., Bumpus, N. N., & Stivers, J. T. (2014). Small molecule inhibition of SAMHD1 dNTPase by tetramer destabilization. *Journal of the American Chemical Society*, 136(28), 9822.
35. Matsuda, A., & Sasaki, T. (2004). Antitumor activity of sugar-modified cytosine nucleosides. *Cancer science*, 95(2), 105-111.
36. Li, N. S., & Piccirilli, J. A. (2003). Synthesis of the Phosphoramidite Derivative of 2'-Deoxy-2'-C- β -methylcytidine. *The Journal of organic chemistry*, 68(17), 6799-6802.
37. Sofia, M. J., Bao, D., Chang, W., Du, J., Nagarathnam, D., Rachakonda, S., ... & Bansal, S. (2010). Discovery of a β -d-2'-deoxy-2'- α -fluoro-2'- β -C-methyluridine nucleotide prodrug (PSI-7977) for the treatment of hepatitis C virus. *Journal of medicinal chemistry*, 53(19), 7202-7218.
38. Zhou, L., Zhang, H. W., Tao, S., Bassit, L., Whitaker, T., McBrayer, T. R., ... & Amblard, F. (2015). β -D-2'-C-methyl-2, 6-diaminopurine ribonucleoside phosphoramidates are potent and selective inhibitors of hepatitis C virus (HCV) and are

- bioconverted intracellularly to bioactive 2, 6-diaminopurine and guanosine 5'-triphosphate forms. *Journal of medicinal chemistry*, 58(8), 3445-3458.
39. Hansen, E. C., Seamon, K. J., Cravens, S. L., & Stivers, J. T. (2014). GTP activator and dNTP substrates of HIV-1 restriction factor SAMHD1 generate a long-lived activated state. *Proceedings of the National Academy of Sciences*, 111(18), E1843-E1851.
40. Amie, S. M., Bambara, R. A., & Kim, B. (2013). GTP is the primary activator of the anti-HIV restriction factor SAMHD1. *Journal of Biological Chemistry*, 288(35), 25001-25006.
41. Traut, T. W. (1994). Physiological concentrations of purines and pyrimidines. *Molecular and cellular biochemistry*, 140(1), 1-22.
42. Diamond, T. L., Roshal, M., Jamburuthugoda, V. K., Reynolds, H. M., Merriam, A. R., Lee, K. Y., ... & Kim, B. (2004). Macrophage tropism of HIV-1 depends on efficient cellular dNTP utilization by reverse transcriptase. *Journal of Biological Chemistry*, 279(49), 51545-51553.
43. Arnold, L. H., Kunzelmann, S., Webb, M. R., & Taylor, I. A. (2015). A continuous enzyme-coupled assay for triphosphohydrolase activity of HIV-1 restriction factor SAMHD1. *Antimicrobial agents and chemotherapy*, 59(1), 186-192.
44. Miazzi, C., Ferraro, P., Pontarin, G., Rampazzo, C., Reichard, P., & Bianchi, V. (2014). Allosteric regulation of the human and mouse deoxyribonucleotide triphosphohydrolase sterile α -motif/histidine-aspartate domain-containing protein 1 (SAMHD1). *Journal of Biological Chemistry*, 289(26), 18339-18346.

45. Hollenbaugh, J. A., Tao, S., Lenzi, G. M., Ryu, S., Kim, D. H., Diaz-Griffero, F., ... & Kim, B. (2014). dNTP pool modulation dynamics by SAMHD1 protein in monocyte-derived macrophages. *Retrovirology*, *11*(1), 63.
46. Kim, B., Nguyen, L. A., Daddacha, W., & Hollenbaugh, J. A. (2012). Tight interplay among SAMHD1 protein level, cellular dNTP levels, and HIV-1 proviral DNA synthesis kinetics in human primary monocyte-derived macrophages. *Journal of Biological Chemistry*, *287*(26), 21570-21574.
47. Shewach, D. S., Reynolds, K. K., & Hertel, L. A. R. R. Y. (1992). Nucleotide specificity of human deoxycytidine kinase. *Molecular pharmacology*, *42*(3), 518-524.
48. Salguero, I., Guarino, E., Shepherd, M. E., Deegan, T. D., Havens, C. G., MacNeill, S. A., ... & Kearsey, S. E. (2012). Ribonucleotide reductase activity is coupled to DNA synthesis via proliferating cell nuclear antigen. *Current Biology*, *22*(8), 720-726.
49. Elledge, S. J., Zhou, Z., & Allen, J. B. (1992). Ribonucleotide reductase: regulation, regulation, regulation. *Trends in biochemical sciences*, *17*(3), 119-123.
50. Nordlund, P., & Reichard, P. (2006). Ribonucleotide reductases. *Annu. Rev. Biochem.*, *75*, 681-706.
51. Behrendt, R., Schumann, T., Gerbaulet, A., Nguyen, L. A., Schubert, N., Alexopoulou, D., ... & Wittmann, S. (2013). Mouse SAMHD1 has antiretroviral activity and suppresses a spontaneous cell-intrinsic antiviral response. *Cell reports*, *4*(4), 689-696.
52. Rampazzo, C., Miazzi, C., Franzolin, E., Pontarin, G., Ferraro, P., Frangini, M., ... & Bianchi, V. (2010). Regulation by degradation, a cellular defense against deoxyribonucleotide pool imbalances. *Mutation Research/Genetic Toxicology and Environmental Mutagenesis*, *703*(1), 2-10.

53. Sommer, A. F., Rivière, L., Qu, B., Schott, K., Riess, M., Ni, Y., ... & Welzel, K. (2016). Restrictive influence of SAMHD1 on Hepatitis B Virus life cycle. *Scientific reports*, 6, 26616.
54. Chen, Z., Zhu, M., Pan, X., Zhu, Y., Yan, H., Jiang, T., ... & Ying, S. (2014). Inhibition of Hepatitis B virus replication by SAMHD1. *Biochemical and biophysical research communications*, 450(4), 1462-1468.
55. Kim, E. T., White, T. E., Brandariz-Núñez, A., Diaz-Griffero, F., & Weitzman, M. D. (2013). SAMHD1 restricts herpes simplex virus 1 in macrophages by limiting DNA replication. *Journal of virology*, 87(23), 12949-12956.
56. Rampazzo, C., Tozzi, M. G., Dumontet, C., & Jordheim, L. P. (2016). The druggability of intracellular nucleotide-degrading enzymes. *Cancer chemotherapy and pharmacology*, 77(5), 883-893.

Chapter 3

A CRISPR/Cas9 approach reveals that the polymerase activity of DNA Polymerase β is dispensable for HIV-1 infection in dividing and nondividing cells

This research was published in *Journal of Biological Chemistry*.

Russell W. Goetze, Dong-Hyun Kim, Raymond F. Schinazi, and Baek Kim.

A CRISPR/Cas9 approach reveals that the polymerase activity of DNA Polymerase β is dispensable for HIV-1 infection in dividing and nondividing cells.

Journal of Biological Chemistry. 2017, 292(34), 14016-14025.

© The American Society for Biochemistry and Molecular Biology, Inc.

Conceptualization: DHK RFS BK.
Data curation: RWG.
Formal analysis: RWG.
Funding acquisition: RFS BK.
Investigation: BK RWG.
Methodology: BK RWG.
Project administration: RWG RFS BK.
Resources: RWG.
Software: RWG.
Supervision: RFS BK.
Validation: RWG.
Visualization: RWG.
Writing – original draft: RWG BK.
Writing – review & editing: RWG BK.

A. Abstract

Retrovirus integration into the host genome relies on several host enzymes, potentially including Pol β . However, whether human Pol β is essential for lentivirus replication in human cells is unclear. Here, we abolished Pol β expression by targeting its DNA polymerase domain with CRISPR/Cas9 in human monocytic THP-1 cells to investigate Pol β 's role in HIV-1 transduction in both dividing and nondividing macrophage stages of THP-1 cells. Pol β -knockout was confirmed by enhanced sensitivity to MMS-induced DNA damage. Of note, nuclear extracts from Pol β -knockout THP-1 cells prepared from both dividing and nondividing stages displayed significantly reduced capability to repair the gapped HIV-1 integration intermediate DNA substrate in a biochemical simulation. However, nuclear extract from both dividing and nondividing stages of the Pol β -KO cells had detectable gap repair activity, suggesting that other host DNA polymerases also repair gapped HIV-1 DNA, particularly in dividing cells. Next, when we compared transduction using HIV-1 and simian immunodeficiency virus in control and Pol β -KO cells, the loss of the Pol β expression did not affect transduction efficiency of these lentiviruses in both dividing and nondividing stages. Finally, the gap repair assay indicated that limited cellular dNTP pools, but not Pol β expression, are a primary factor for HIV-1 DNA gap repair, particularly in nondividing cells. These data support the idea that Pol β polymerase activity is dispensable for HIV-1 infection in both dividing and nondividing stages of human cells targeted by the virus.

B. Background

One of the hallmarks of retrovirus replication is integration of viral DNA into a host chromosome of infected cells. Integration of lentiviruses such as human immunodeficiency virus

Type 1 (HIV-1) and simian immunodeficiency virus (SIV) requires highly coordinated actions of both viral and host players. After the viral dsDNA is synthesized from the viral genomic RNA by RT, a number of viral and host proteins coordinate to assemble the PIC, which transports the viral dsDNA into the nucleus where it is inserted into a host chromosome (1). The integration process consists of three distinct and sequential steps: 1) two to three nucleotides are removed from both 3' ends of the viral dsDNA by the viral integrase (IN), 2) the 3' ends of the viral dsDNA are covalently linked to the host's chromosomal DNA by transesterification catalyzed by IN (2), and 3) a four to six nucleotide single stranded (ss) DNA gap between the 5' end of the viral DNA and 3' end of the host chromosomal DNA is filled and ligated after removing mismatches at the 5' ends of the viral DNA (3), resulting in a completely integrated provirus. While the viral IN catalyzes the first two steps, the third step is thought to be largely carried out by the host DNA repair machinery (4).

Among the host proteins involved in the DNA repair process, Pol β is speculated to be the enzyme responsible for filling the ssDNA gap resulting from viral integration (4). Pol β is known to act in BER, which repairs DNA damage resulting from sources such as alkylating agents and reactive oxygen species (5). Aberrations in Pol β expression and activity have been reported in various cancers (6-8). Recently, a study reported that Pol β knockdown by RNAi in HeLa cells reduces HIV-1 transduction in a targeted screen of DNA repair enzymes (9). Additionally, reduction in HIV-1 and FIV infectivity were reported in mouse embryonic fibroblasts from *POLB*^{-/-} animals (10). Results from these studies support the role of Pol β and other BER enzymes in lentivirus integration. Our laboratory has also reported that immunodepletion of Pol β from primary CD4⁺ T cell and macrophage nuclear extract reduces

HIV-1 ssDNA gap repair activity biochemically (11). However, genetic evidence clarifying the role of human Pol β in lentivirus replication in human cells remains to be reported.

Another unique feature of lentiviruses relative to other members of the *Retroviridae* family is the ability to replicate in both dividing and nondividing cells (12). In the case of HIV-1 and SIV, activated CD4⁺ T cells and macrophages, respectively, represent important targets of infection within this classification. Since nondividing cells lack chromosomal DNA synthesis, it is plausible that the DNA repair mechanisms used by lentiviruses during integration may be regulated differently between these two cell types. In fact, to address questions relating to dividing and nondividing target cells, the THP-1 cell model, a monocytic leukemia cell line, has been extensively used because dividing THP-1 cells can be differentiated to a nondividing macrophage-like phenotype by treatment with phorbol 12-myristate 13-acetate (PMA) (13,14).

In the present study, we generated novel *POLB* KO THP-1 cell lines using a CRISPR/Cas9 system (15). These KO cell lines were validated and shown to both display enhanced sensitivity to alkylating agents and to lack efficient ssDNA gap repair activity *in vitro*. Unlike the previously reports, which showed more pronounced reductions in viral transduction efficiency in the Pol β knockdown human cells and mouse knockout cells (9,10), we observed only minor, yet statistically significant, effects of the loss of Pol β on HIV-1 and SIV transduction efficiency in both dividing and nondividing *POLB* KO THP-1 cells. Furthermore, we show that the rate of ssDNA gap repair is limited at physiological dNTP concentrations, which are further restricted in nondividing cells. Our results suggest that Pol β is not essential to the ssDNA gap repair during lentiviral transduction in both dividing and nondividing cells. Additionally, this repair process is kinetically limited by cellular dNTP concentrations particularly in nondividing cells.

C. Results

POLB KO in THP-1 cells using CRISPR/Cas9-based gene editing

Previously reported (10) cellular *POLB* KO models used to study HIV-1 replication are derived from mice, which may not faithfully recapitulate the normal host environment of primate lentiviruses. Also, only RNAi-based tests have been used to study the role of human Pol β in HIV integration (9). In order to generate a novel and relevant human cellular model, we employed LentiCRISPRv2 (15), a lentiviral vector-based CRISPR/Cas9 delivery system expressing target sgRNA, Cas9 nuclease, and a puromycin selection marker to induce *POLB* deletion. We selected single guide RNA (sgRNA) sequences (Fig. 1A) from the Genome-scale CRISPR KO (GeCKO) database (16) targeting two different regions near the polymerase active site of the Pol β palm subdomain (Fig. 1B). More specifically, sgRNA1 targets exon 10 of the *POLB* gene, a region within the highly structured palm domain, which encodes the metal binding triad, dNTP binding site, primer binding site, and active site. sgRNA2 targets exon 9 and corresponds to a structured region in the palm domain proximal to the active site, but does not directly encode any catalytic residues.

Next, we chose the human monocytic THP-1 cell line for *POLB* KO because this cell line is both able to be efficiently infected by HIV-1 and can be differentiated to a nondividing macrophage stage by treatment with PMA. THP-1 cells were transduced with each of the constructed lentiviral vectors including the empty vector as a control. Following transduction, puromycin selection, and single-cell sorting, clonal cells were expanded and assessed for successful *POLB* KO by Western blot in both dividing (-PMA) and nondividing, differentiated stages (+PMA) (Fig. 1C). We isolated genomic DNAs from Western blot hit clones, sequenced exons 9 (Fig. 1D) and 10 (Fig. 1E) of *POLB*, and then chose one clone corresponding to each

sgRNA for further characterization. We found that the clone edited with sgRNA1 (KO1) had several point mutations near the target site, which induce amino acid changes and a 7-base pair frameshifting deletion that introduces a premature stop codon downstream approximately 50 base pairs of the deletion. The clone edited with sgRNA2 (KO2) also had several point mutations near the target sequence and a 20-base pair frameshifting deletion that introduces a premature stop codon approximately 100 base pairs downstream. Additionally, clonal THP-1 cells transduced with the LentiCRISPRv2 transfer vector lacking a sgRNA insert (empty vector) were selected for use as a control that expresses Pol β in both dividing and nondividing stages – consistent with what we observed in the parental THP-1 cells (Fig. 1C). These data provide sufficient molecular and genetic evidence that the selected clones were *POLB* null to proceed with further functional analysis.

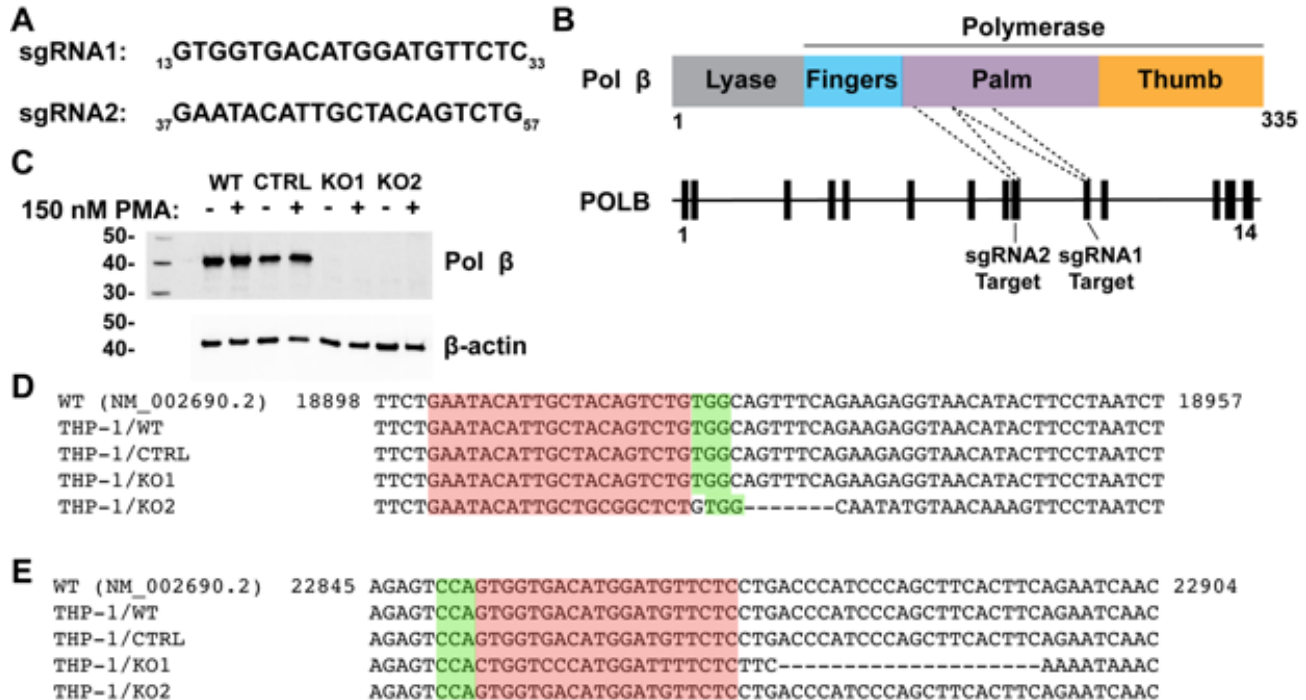


Figure 1: Generation of *POLB* KO THP-1 cell lines by CRISPR/Cas9. (A) Single guide RNA (sgRNA) sequences used in this study. The nucleotide numbers within exon 10 (sgRNA1) or exon 9 (sgRNA2) of the *POLB* gene are indicated as a subscript. (B) Map of the Pol β protein and *POLB* gene. sgRNA1 and sgRNA2 target regions within exon 10 and 9, respectively. Both targets are within a coding region that corresponds to the palm subdomain of the DNA polymerase domain. Amino acid numbering and subdomains of the Pol β protein are indicated. Exon numbers are indicated for the *POLB* gene. (C) Nuclear extracts were isolated from the dividing (-PMA) or nondividing macrophage (+PMA) stages of THP-1 cells. Nuclear extracts (10 μg/lane) from wild-type (WT) THP-1, empty vector control (CTRL), and *POLB* KO THP-1 cells (KO1 and KO2) were probed with a monoclonal anti-Pol β antibody targeting the C-

terminal region. Blots were stripped and re-probed for β -actin as a loading control. Positions of molecular weight markers are indicated on the left side of the blot. Results are representative of two independent experiments. Genomic DNAs from WT THP-1, CTRL, KO1 and KO2 cells were isolated and PCR amplicons flanking the CRISPR/Cas9-targeted regions were sequenced. Sequence alignments of bases 18898-18957 (exon 9) (**D**) and 22845-22904 (exon 10) (**E**) of the *POLB* gene are shown. Numbering is based on the entire *POLB* gene sequence using the reference gene RefSeq NM_002690.2.

POLB KO THP-1 cells are sensitive to MMS-induced DNA damage

POLB KO has been validated in previous cellular systems using sensitivity to MMS (5,17), which induces DNA damage repaired by the BER pathway. We treated our THP-1 clones as well as the polyclonal parental THP-1 cells with a range of MMS concentrations and evaluated cell sensitivity to MMS using an XTT-based cell proliferation assay. *POLB* KO cell lines, but not empty vector control cells, showed an enhanced susceptibility to MMS (Fig. 2A) that was consistent with previously published values using growth inhibition assays (5,17).

Additionally, we stimulated THP-1 cells with PMA to induce a macrophage-like phenotype as previously described (13). In this state, THP-1 cells have decreased dNTP concentrations (18) and are nondividing with little cellular DNA synthesis (Fig. S1). Next, we tested whether nondividing THP-1 cells were also sensitive to DNA damage by MMS. Nondividing KO1 and KO2 cells showed sensitivity to MMS-induced DNA damage compared to parental THP-1 and CTRL cells (Fig. 2B) similar to the results observed in dividing THP-1 cells. Based on these functional results, we concluded that the cellular phenotype presented by our *POLB* KO cells was consistent with previously reported findings and supports the validity of our molecular analysis.

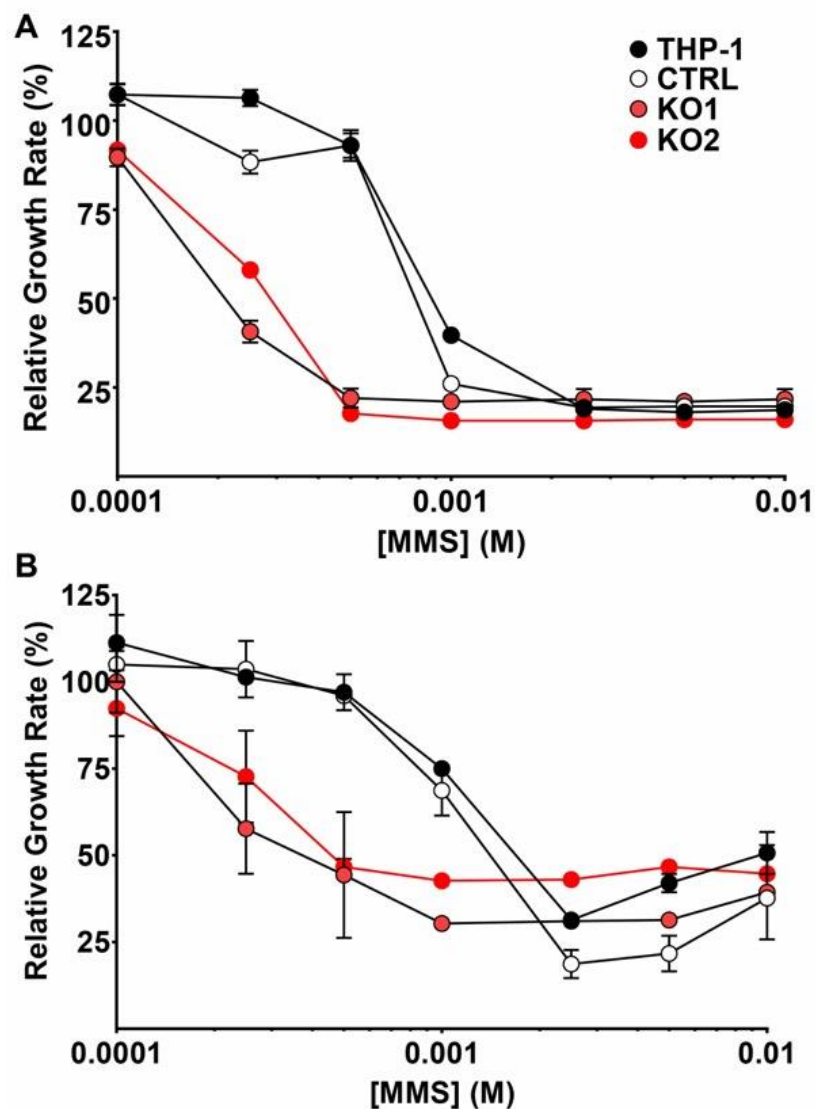


Figure 2: *POLB* KO THP-1 cells are sensitive to MMS-induced DNA damage. 2.5×10^4 THP-1 cells per well were seeded in 96-well plates in the dividing (A) or nondividing (B) stage. WT THP-1, CTRL, KO1, and KO2 cells were treated with varying concentrations of the DNA alkylating agent MMS for 2 h. Cells were washed three times with 1X PBS and cultured for 72 h. Cell viability was measured using the XTT assay and values were normalized to untreated control for each group. Results from two independent experiments performed in triplicate are shown as mean \pm S.D.

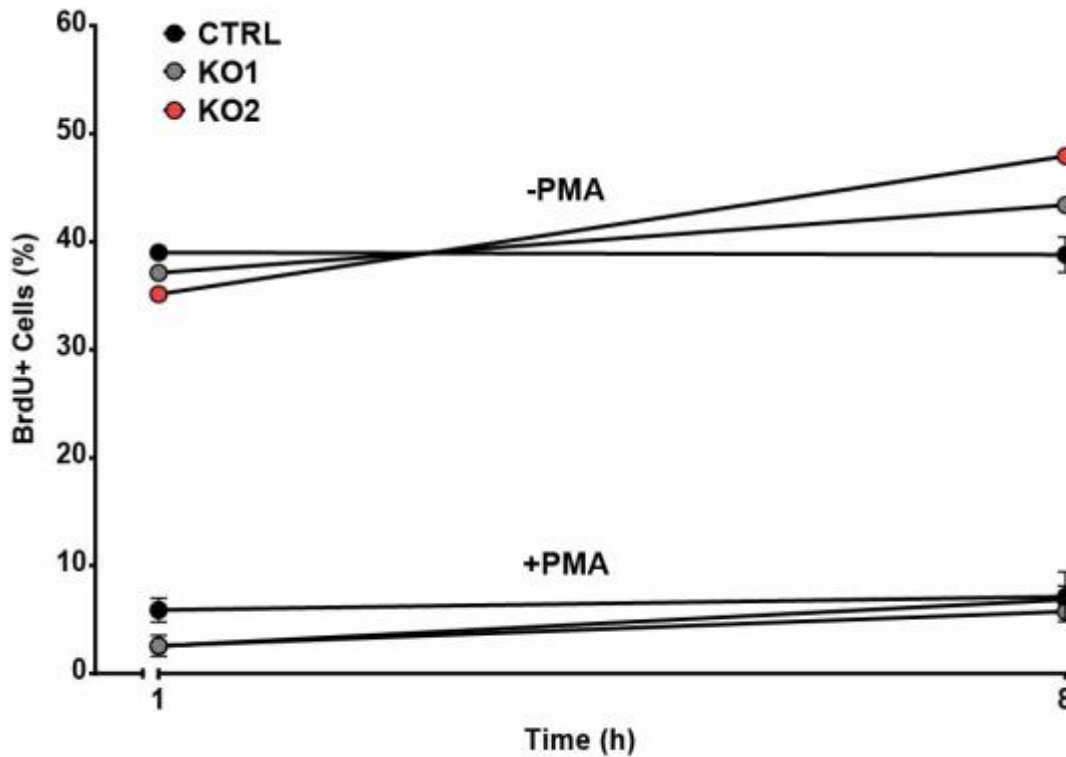


Figure S1: PMA-treated THP-1 cells have minimal levels of DNA synthesis. DNA synthesis was measured in the dividing and non-dividing stages of THP-1 CTRL, KO1, and KO2 cells using BrdU incorporation. Cells were cultured in complete media containing 10 μ M BrdU for 1 or 8 h. Approximately 40% of dividing stage cells were positive for BrdU incorporation after 8 h treatment for all three cell lines. In contrast, PMA-treated cells in the non-dividing/macrophage stage showed only up to 8% of cells as positive after 8 h treatment, indicating only a low level of background DNA synthesis in these cells. Data are shown as mean \pm S.D. of two independent experiments performed in triplicate.

POLB KO THP-1 nuclear extracts have impaired HIV-1 ssDNA gap repair activity in vitro

We previously reported an *in vitro* assay that simulates the single-strand DNA gap repair mechanism that occurs during the integration step of HIV-1 by using nuclear extracts (11). This system requires three enzymatic steps to occur in order to generate a 50mer gap repair product as illustrated in Fig. 3A: (1) DNA synthesis from the ³²P-labeled 5'-end of a DNA primer across a four-nucleotide gap generated from the annealed 3' DNA primer, (2) displacement and excision of a mismatched single-nucleotide flap, and (3) ligation of the extended 5' and 3' primers, generating the 50-mer repaired product.

To test whether gap repair was restricted in *POLB* KO cells, we prepared nuclear extracts from parental THP-1, empty vector control, KO1, and KO2 cells in both dividing (-PMA) and nondividing (+PMA) stages as previously described (11). Nuclear extracts were normalized to 1 mg/mL total protein by the Bradford assay and incubated with the radiolabeled gap repair substrate described in Fig. 3A with saturating dNTPs (250 μM) for 30 min at 37 °C. As shown in Figure 3B, *POLB* KO1 and KO2 nuclear extracts generated significantly decreased 50-mer repaired product, compared to both parental and control THP-1 cells expressing Pol β. Surprisingly, however, the *POLB* KO nuclear extracts still displayed some levels of the partially extended 5' primer (see “”) in Fig. 3B), supporting that other DNA polymerases can recognize the HIV-1 gap substrate while Pol β appears to be the primary polymerase that recognizes the substrate. Also, when the repaired product in each reaction was quantitated (Fig. 3C), no significant difference in the DNA gap repair activity between dividing (-PMA) and nondividing (+PMA) stages of all cell types, suggesting that Pol β is also the major polymerase for the ssDNA gap repair in the nondividing stage. Furthermore, this observation is supported by the increased sensitivity to MMS we observed in the PMA-treated *POLB* KO cells (Figure 2B).

Taken together, these data suggest that the genetic loss of Pol β expression significantly reduces, but not completely abolish the HIV-1 ssDNA gap repair activity in the THP-1 model.

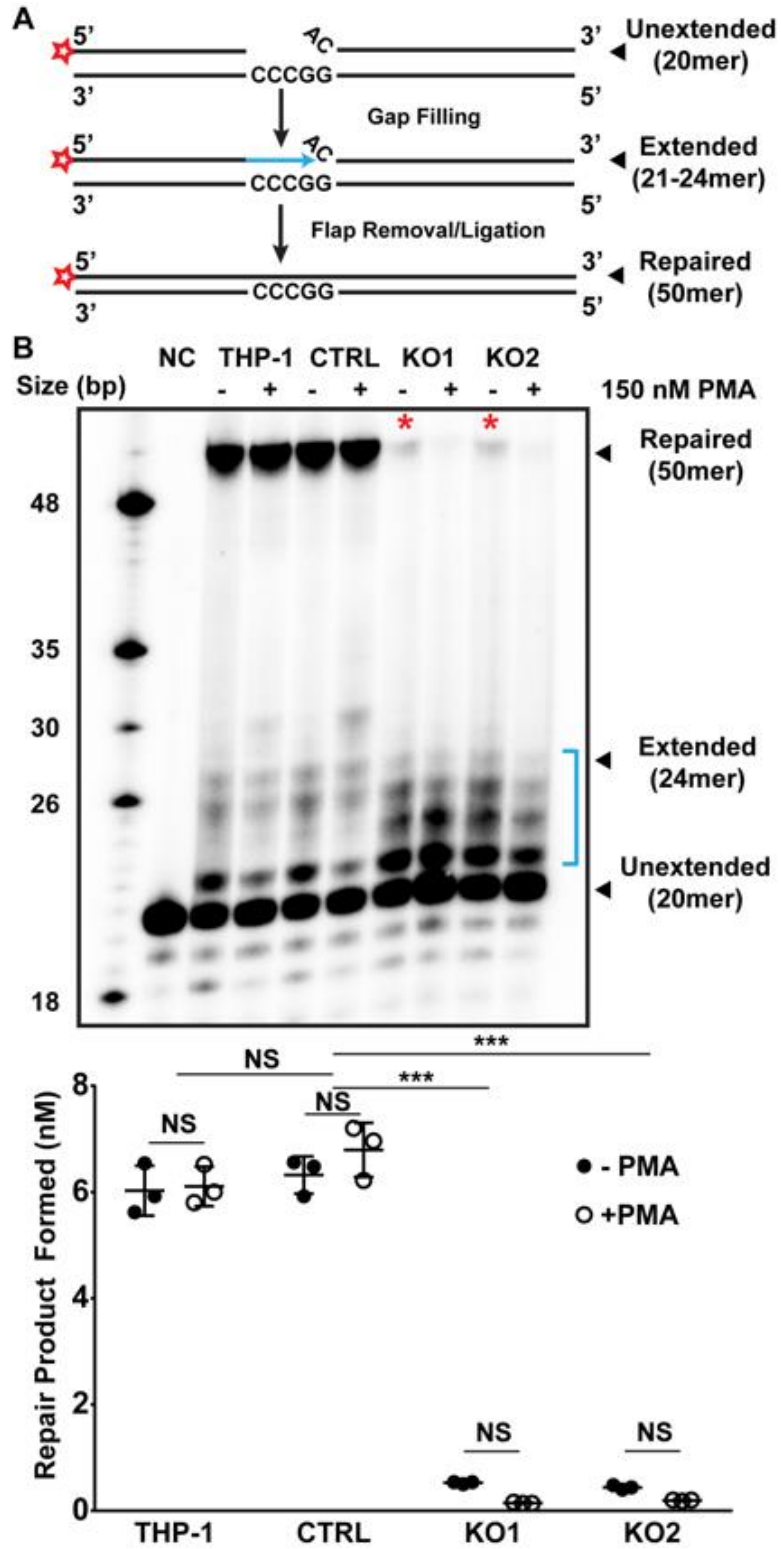


Figure 3: Effect of *POLB* KO on biochemical ssDNA gap repair activity with HIV-1 gap DNA substrate. Lentiviral gap filling was modeled *in vitro* using a previously reported assay (13). **(A)** Schematic showing the steps required for complete repair of a model substrate based on the HIV-1 LTR. A 5' end ³²P-labeled 20mer oligonucleotide primer (red stars) and an unlabeled 27mer oligonucleotide primer with a single 5'-end mismatch are annealed to a 50mer oligonucleotide template. Extension of the labeled primer by DNA polymerases yields 21-24mer products (indicated by blue arrow), which require mismatch removal and ligation to the unlabeled 27mer to form the labeled 50mer gap repair product. **(B)** 20 nM gap repair substrate was incubated with 4 μg nuclear extract from WT THP-1, CTRL, KO1, and KO2 cells in the presence of 250 μM dNTPs and 2 mM ATP. Reactions were incubated at 37 °C for 30 min then quenched with 40 mM EDTA and inactivated at 95 °C for 1 min. The substrate was also incubated with the WT THP-1 nuclear extract in the absence of dNTPs (NC) at 37 °C for 30 min (NC). Products were resolved by urea-PAGE on a 20% acrylamide gel and visualized by phosphorimaging. 20-mer unextended substrate, 24mer intermediate (including partially extended products indicated by blue “)”), and 50mer fully repaired product are indicated. The results were quantitated by densitometry in ImageLab 5.2 (BioRad). The amount of repair product was calculated as ratio of 50mer band density to total density per lane and related to the concentration of substrate in each reaction. Results from three independent experiments are shown as mean ± S.D. 2-way ANOVA was performed and Dunnett's multiple comparison test was used to determine differences between cell lines and the effect of PMA treatment. ***, P < 0.001. NS, not significant.

POLB KO has limited effects on lentivirus transduction in both dividing and nondividing THP-1 cells

A previous report showed that embryonic fibroblasts derived from *POLB*^{-/-} mice exhibited reduced lentivirus transduction compared to wild-type cells (10). However, this model is not completely relevant because mice do not carry lentiviruses. Therefore, we employed our human *POLB* KO THP-1 cells to test whether human Pol β is involved in HIV-1 transduction. For this test, THP-1 empty vector, KO1, and KO2 cells were infected in dividing and nondividing stages with VSV-G pseudotyped GFP-reporter HIV-1 (DHIV3-GFP) pseudovirus that encodes all of the NL4-3 genes except *env* and *nef*, which are replaced with GFP (19). As shown in Fig. 4A, only minor differences in HIV-1 vector transduction efficiency relative to empty vector control cells was observed in both dividing and nondividing stages of THP-1 cells. We found that transduction efficiency was reduced by approximately 20% in both dividing KO2 cells and nondividing KO1 cells. We also observed that *POLB* KO did not uniformly reduce the transduction efficiency of another lentivirus, SIV (Fig. 4B). The absence of a uniform effect in these data suggest that human Pol β is not absolutely required for HIV-1 transduction. This result is further supported by the biochemical data presented in Fig. 3 that other DNA polymerases may also recognize the HIV-1 ssDNA gap although their capability to repair the HIV-1 gap is less efficient than Pol β .

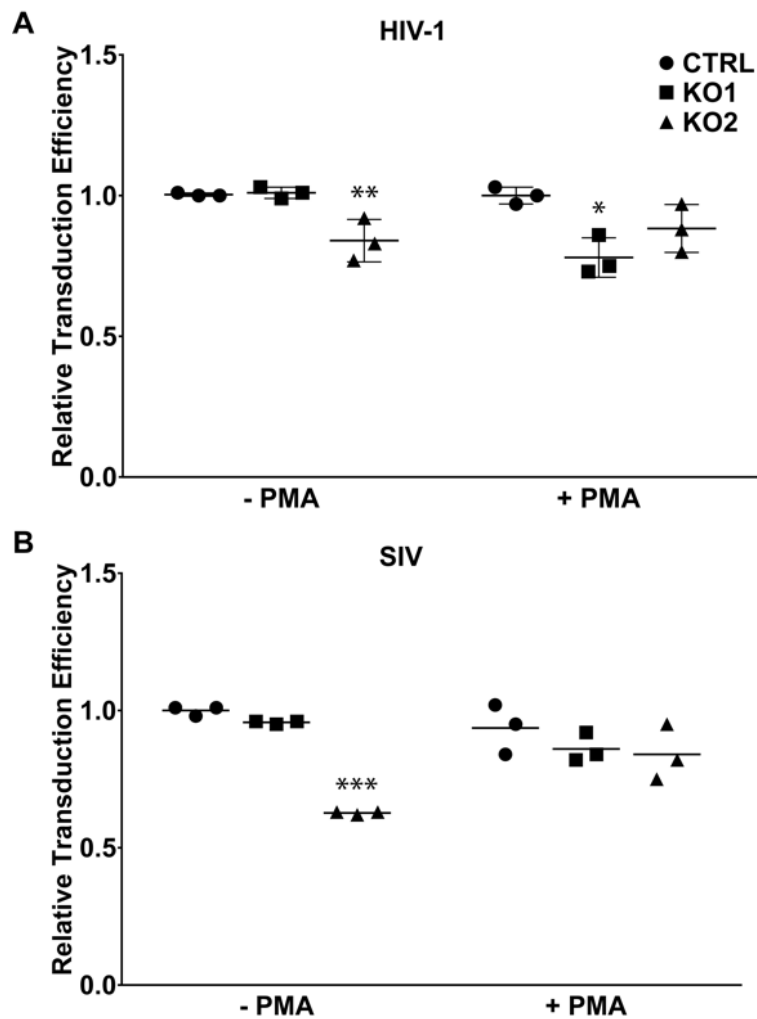


Figure 4: Effect of *POLB* KO on HIV-1 transduction in dividing and nondividing THP-1 cells. CTRL, KO1, and KO2 cells were grown in suspension culture for the dividing stage (-PMA) or treated with 150 nM PMA (+PMA) for 7 days to differentiate into the nondividing macrophage stage. Cells were transduced with VSV-G pseudotyped HIV-1 (A) or SIV_{mac239} (B) vector expressing GFP at an MOI of 0.4 and assayed by flow cytometry to measure the GFP expressing population at 24 h (dividing) or 120 h (nondividing) post-transduction. Data are reported as mean \pm S.D. of three independent experiments performed in triplicate. Data were

analyzed by 1-way ANOVA and differences between KO and CTRL cells were determined using Dunnett's multiple comparison test. *, $P < 0.05$. **, $P < 0.01$. ***, $P < 0.001$.

In vitro HIV-1 ssDNA gap repair is dependent on dNTP concentration

We previously reported that cellular dNTP level in nondividing cells such as human monocyte derived macrophages is extremely low (20-40 nM), compared to dividing cells such as activated CD4⁺ T cells (1-4 μ M) (20). The extremely limited dNTP pool in macrophages kinetically suppresses HIV-1 reverse transcription, which consumes cellular dNTP substrates for viral dsDNA synthesis (21). However, it is also clear that the HIV-1 DNA gap repair during viral integration requires cellular dNTPs. Indeed, our previous *in vitro* HIV-1 DNA gap repair assay demonstrated that cellular dNTP concentration affects the HIV-1 DNA gap repair (11). Here we tested the effect of the dNTP concentration on the HIV-1 DNA gap repair activity of the nuclear extract prepared from our THP-1 cell line model. For this test, we performed the *in vitro* HIV DNA gap repair assay using nuclear extracts from dividing (-PMA) and nondividing (+PMA) stages of parental THP-1 at dNTP concentrations found in dividing/activated CD4⁺ T cells (2.5 μ M), nondividing macrophages (40 nM), as well as a saturating concentration (250 μ M) (Fig. 5). We measured the two product populations: 1) fully repaired product (50mer product in Fig. 5A and red portions in Fig. B and C) and 2) partially extended product ("") in Fig. 5A and blue in Fig. 5B and C). First, the levels of the fully repaired 50mer product were significantly reduced at both intracellular dNTP concentrations (2.5 μ M and 40 nM), compared to saturating dNTPs (250 μ M), though repair product was still detectable at later time points at the dividing cell dNTP concentration (2.5 μ M). However, no fully repaired product was detected at the nondividing cell dNTP concentration (40nM) even at the later time points. Second, this dNTP concentration dependent gap repair activity was observed in both PMA treated and

untreated THP-1 cells (Fig. 5A). Third, when we quantitated the total primer extension level including both partially extended products and fully repaired 50mer products, the dividing cell dNTP concentration (2.5 μ M) gave higher levels (~48%) of the total extended product than the macrophage dNTP concentration (~14%) in the reactions with the PMA untreated cell extract (Fig. 5B), and similar difference in the total extended products was also observed in the reactions with the PMA treated cells (Fig. 5C). This simulation data supports that the availability of intracellular dNTPs significantly affects HIV-1 DNA gap repair and that the limited dNTP pools, not Pol β expression, is a primary limiting factor to control the HIV-1 gap repair in nondividing cells, which at least partially explains the absence of an effect of *POLB* KO on HIV-1 infectivity in the nondividing stage of THP-1 cells (Fig. 4).

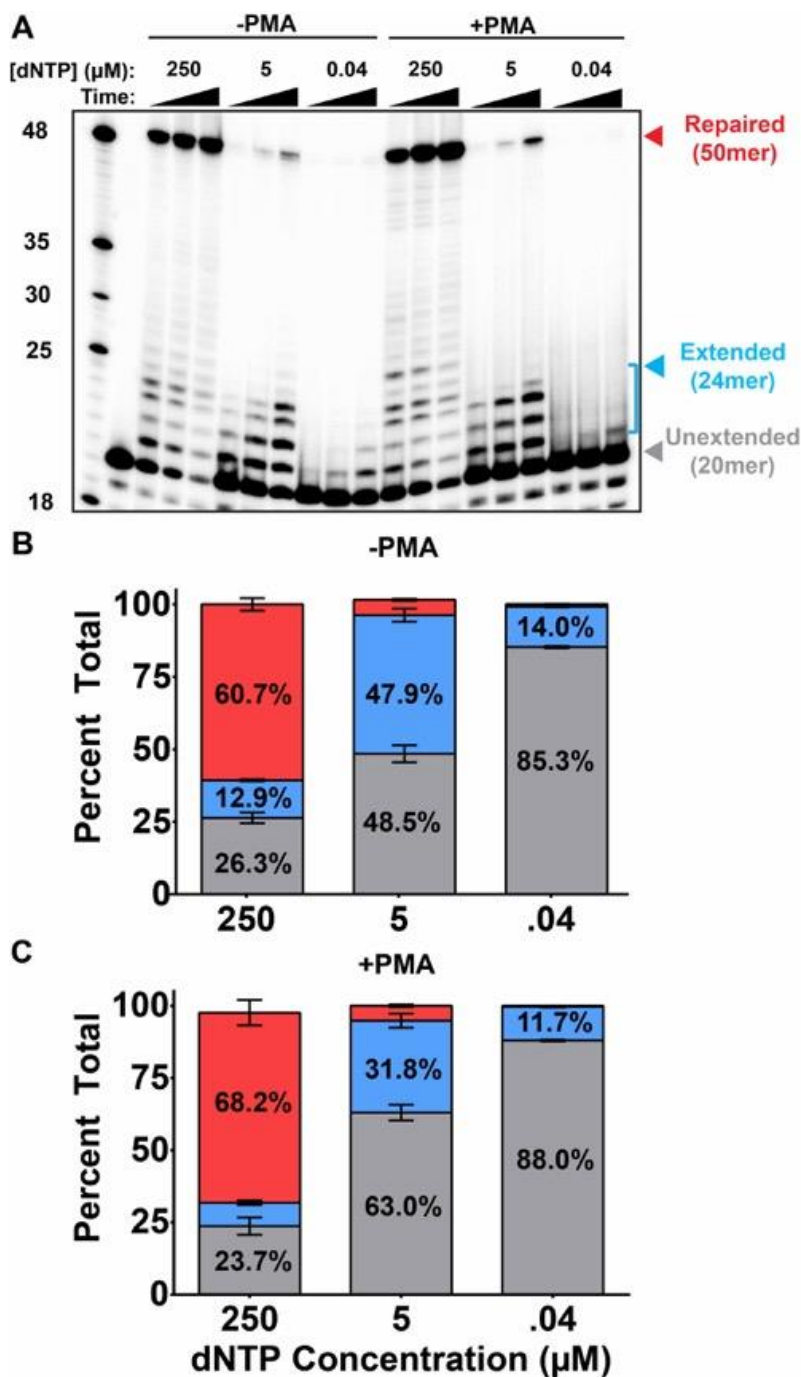


Figure 5: Effect of dNTP concentration on *in vitro* HIV-1 ssDNA gap repair activity.

Nuclear extracts from dividing (-PMA) and nondividing (+PMA) stages of THP-1 CTRL cells expressing Pol β were isolated. (A) 20 nM gap repair substrate was incubated with 4 μg nuclear extract from CTRL cells in the presence of saturating (250 μM), dividing cell (5 μM), or

nondividing cell (40 nM) concentrations of dNTPs and 2 mM ATP (required for ligation). Reactions were incubated for 30, 60 or 120 min. Data from three independent experiments were analyzed by densitometry to quantitate the amounts of fully repaired, partially extended (blue “”), and unextended radiolabeled primers, which are reported as mean \pm S.D for dividing (**B**) and nondividing (**C**) stages of THP-1 empty vector control cells. The percentage comprised by each product (repaired, partially extended, and unextended) are represented by red, blue, and gray bars, respectively. The mean percentage calculated for each product is indicated by the number inside the corresponding bar.

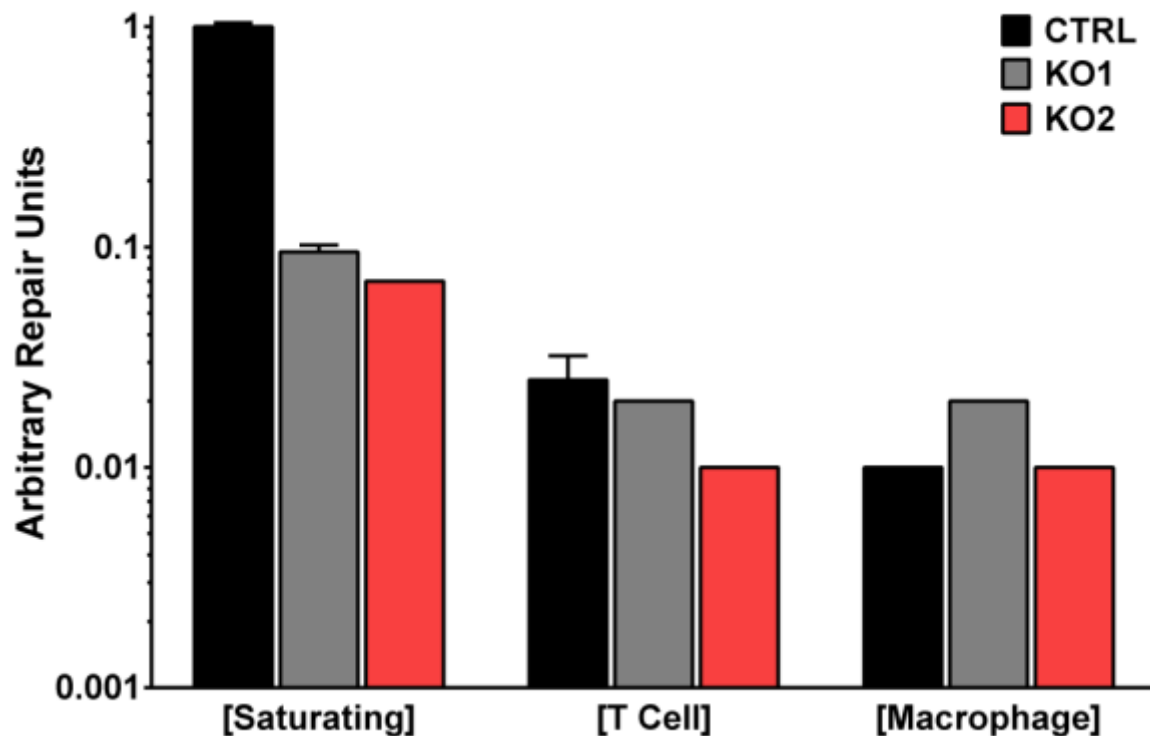


Figure S2: Effect of dNTP concentration on *in vitro* HIV-1 ssDNA gap repair activity in *POLB* KO THP-1 cells. Nuclear extracts from dividing (-PMA) and nondividing (+PMA) stages of THP-1 CTRL, KO1, and KO2 cells were isolated. 20 nM gap repair substrate was incubated with 4 μ g nuclear extract in the presence of saturating (250 μ M), dividing cell (5 μ M), or nondividing cell (40 nM) concentrations of dNTPs and 2 mM ATP (required for ligation). Reactions were incubated for 120 min. Data from two independent experiments were quantitated by densitometry to quantitate the amounts of fully repaired substrate which are reported as mean \pm S.D for dividing stages of THP-1 cells.

D. Discussion

Integration of genetic information by lentiviruses such as HIV-1 presents a significant barrier to eradicating the virus *in vivo*. While all retroviruses encode a viral IN (1), none encode enzymes that process the 5' ends of the partially integrated viral dsDNA – a substrate that requires the relatively complex removal of mismatched base pairs and repair of the ssDNA gap. This involves multiple enzymatic functions including removal of mismatched bases by flap endonuclease, DNA polymerization, and ligation of the newly synthesized DNA to a host chromosome (3). The provirus is thought to be stably integrated only after these steps have been completed. Since the host DNA repair polymerase Pol β is known to fill short ssDNA gaps during routine cellular DNA repair, it has been speculated that Pol β is involved in lentiviral 5'-end DNA gap repair. This was supported by the findings of a targeted siRNA screen that showed a modest reduction of HIV-1 transduction in HeLa cells when some BER enzymes, including Pol β , were knocked down (9). This work was further supported by findings demonstrating modest reductions in HIV-1 infectivity in embryonic fibroblasts derived from *POLB*^{-/-} mice (10). However, these results have not been confirmed by genetic evidence in human cell models. Importantly, to the best of our knowledge, the present study is the first to report human *POLB* KO cells and therefore provides the most complete system for modeling HIV-1 gap repair in human cells to date.

Lentiviruses such as HIV-1 and SIV infect terminally differentiated, nondividing myeloid cells such as macrophages (22,23). These cells lack chromosomal DNA replication, cell division, and feature additional mechanisms that present barriers to lentiviral replication. Two such mechanisms involve tight control of dNTP biosynthesis by inhibition of ribonucleotide reductase (RNR) (24) and activation of dNTP hydrolysis by sterile alpha motif and HD domain-containing

protein 1 (SAMHD1) (25,26). We have previously shown that by limiting dNTP concentration, nondividing cells restrict lentivirus replication at both the reverse transcription and integration steps (11). Since most research examining DNA repair has focused on dividing cells, the implication of these unique regulations is not well understood. In fact, it remains unclear whether such terminally differentiated, nondividing cells carry fully functional DNA repair capacity in the absence of chromosomal DNA replication and to what extent this is controlled by cell type. Transcription-coupled DNA repair appears to function in nondividing cells, but has been not been fully characterized (27). Interestingly, because of the tight dNTP regulation that occurs in nondividing cells, the cellular DNA polymerases that act in DNA repair pathways may not operate efficiently. We previously reported that macrophages harbor dNTP concentrations in the 20-50 nM range (20), which is much lower than reported K_m values of any known cellular DNA polymerase (1-100 μ M) (28-30). Therefore, it is unclear that the DNA repair machinery in nondividing lentivirus target cells are able to efficiently perform 5' end gap repair under such restrictive conditions. The evidence that we present here is the first to compare gap repair in both dividing and nondividing cells that completely lack Pol β expression. Our previous findings demonstrated that the rate of gap repair was controlled by dNTP concentration, but these experiments were performed in cells that expressed Pol β (11). These new data validate the significance of cellular dNTP regulation in determining the rate of lentiviral DNA gap repair.

In the present study, we demonstrate that HIV-1 and SIV replicate with little impairment in *POLB* KO cells under both dividing and nondividing conditions. This finding surprised us, considering that others had observed a reduction in transduction efficiency in other systems using mouse *POLB* KO or human *POLB* KD. This led us to consider two possible scenarios: 1) other DNA polymerases besides Pol β perform 5' end gap repair of partially integrated viral

dsDNA, particularly in dividing cells, or 2) lentiviruses may not require completion of 5' end gap repair to begin transcription of proviral DNA.

For the first scenario, we considered other non-replicative DNA polymerases. Pol β , Pol λ , and Pol μ are all members of DNA polymerase family X and are involved in DNA repair (31). While Pol μ appears to function primarily in B-cell maturation in lymphoid tissue, Pol λ is known to act as a back-up in BER reactions using cell extracts (32). However, the extent to which Pol λ can fill this role in nondividing cells is unknown. In contrast, Pol β is constitutively expressed with increases in mRNA expression before and during chromosomal DNA replication (33,34) and following DNA damage (35). This evidence supports the role of Pol β as the primary repair polymerase in nondividing cells, but does not exclude the possibility that other DNA polymerases can perform the same function in its absence. Indeed, our biochemical simulation assay (Fig. 3A) showed that the nuclear extracts of the *POLB* KO cells particularly prepared from the dividing stage displayed detectable HIV-1 DNA gap repair activity, supporting the possibility that other DNA polymerases were able to recognize and repair the HIV-1 gap DNA. Notably, under conditions with saturating dNTPs, the rate of gap repair was reduced by more than 90% in *POLB* KO cells (Fig. 3). This indicates that although other DNA polymerases are able to fill the gap in the absence of Pol β , the repair process is much less efficient. However, when this experiment was repeated using *POLB* KO cells and varying dNTP concentrations, the effect size on repair rate between WT and *POLB* KO cells decreased from 10-fold with saturating dNTPs to less than 2-fold under physiological dNTP concentrations (Fig. S2). These data help to explain why we observed only small differences in transduction efficiency between WT and *POLB* KO cells (Fig. 4), while *in vitro* gap repair assays showed such a strong effect (Fig. 3). Since the HIV-1 DNA gap repair is absolutely dependent on the dNTP concentration

(Figs. 5, S2), the extremely limited dNTP pools observed in nondividing cells, not Pol β expression, could be a primary factor to control the HIV-1 DNA gap repair during viral integration in nondividing cells. Notably, dNTP concentration is modestly elevated in nondividing cells in response to DNA damage by p53-dependent induction of the *p53R2* gene, which encodes an alternative small R2 subunit of RNR (24,36). However, induction of *p53R2* requires prolonged exposure to DNA damage and is not triggered by HIV-1 infection (18,36).

In addition to cellular DNA polymerases, RT is capable of filling the gapped DNA intermediate through its strand displacement activity (4,37,38). Gap filling by RT directly would also explain the absence of a strong effect on transduction efficiency in *POLB* KO cells, particularly in nondividing cells where RT's higher efficiency at low dNTP concentrations could potentially play an important role. Furthermore, there is evidence that RT and IN directly interact (39), which could support localization of RT to the site of integration thereby bypassing a need for a cellular DNA polymerase. However, it is unclear whether RT activity is maintained after the PIC enters the nucleus since reverse transcription occurs primarily in the cytoplasm (1). Additionally, gap filling by RT would not circumvent the need for cellular endonuclease and ligase activity, which may then act as the rate-limiting step in repair if gap filling by RT is indeed efficient.

For the second scenario, we speculated that immediate repair of the 5' end LTR gap may not be necessary for HIV replication, particularly in nondividing cells. DNA damage detected during chromosomal replication leads to activation of DNA damage response mechanisms, which induce cell cycle arrest initially and eventually apoptosis, if necessary (40). However, activated CD4⁺ T cells infected by HIV-1 undergo cell cycle arrest induced by viral protein R (41) and eventually cell death without resuming cell division. In some infected CD4⁺ T cells that

become quiescent, the immediate need for DNA repair may also be bypassed since these cells are no longer cycling. The same logic follows for macrophages, which are also nondividing. Finally, it is not known whether and how the unrepaired 5' end gap at the LTR affects HIV-1 transcription. Furthermore, transcriptional machinery assembles at structures located within the LTR (1), which would avoid potentially stalled processivity across the 5' end gap. While this scenario is purely speculative, it can be tested using methods to detect the unrepaired 5' end gap of HIV-1 DNA. However, there is currently no reliable quantitative assay for measuring the partially integrated HIV-1 DNA and we were unable to adapt an existing assay used to detect the gap for Molony Murine Leukemia Virus (42).

In addition to DNA polymerase activity, both Pol β and Pol λ have distinct 5'-2-deoxyribose-5-phosphate (dRP) lyase activity (43-45). Recently, it was reported that Pol β 5'-dRP lyase activity, but not polymerase activity, is required for efficient HIV transduction in mouse embryonic fibroblasts (46). In our study, we considered that because CRISPR-induced deletions were downstream of the Pol β lyase domain that it was possible that a fragment retaining this activity may still be expressed in our *POLB* KO cells. We probed nuclear extracts from WT and *POLB* KO THP-1 cells using a polyclonal antibody raised against whole Pol β protein and were unable to detect any specific band that might represent a truncated form of Pol β (data not shown). While this is a caveat that could explain our failure to reproduce a reduction in infectivity, it is important to note that these previously reported results relied on expression of a full-length Pol β construct with point mutations in the polymerase or lyase active sites. Since our *POLB* KO cells lack nearly all of palm domain and all of thumb domain, it is unlikely that such a truncated protein would even retain the ability to interact with DNA even if a functional lyase subdomain was expressed. Future experiments can target the lyase domain of Pol β in order

to generate a complete deletion to conclusively determine whether the Pol β lyase is also dispensable for lentivirus replication.

In conclusion, our genetic biochemical investigations revealed that Pol β 's polymerase activity appears to be dispensable for HIV-1 transduction in both dividing and nondividing THP-1 cells. This study raises new possibilities for consideration in HIV-1 5' end gap repair: 5' end gap repair of lentiviral DNA may promiscuously utilize cellular DNA polymerases and/or viral RT during integration or that immediate repair of the 5' end gap may not be necessary for viral replication.

E. Materials and Methods

Cell Culture and Lentiviral Vectors

THP-1 cells (ATCC TIB-202) were cultured in RPMI 1640 medium (Corning) supplemented with 10% FBS and 1% penicillin/streptomycin according to the supplier's recommended sub-culturing method. THP-1 cells were differentiated by continuous stimulation with 150 nM PMA (Sigma) for 7 days with media replaced every 2 days. All cells were grown at 37 °C, 5% CO₂. 293FT cells (Invitrogen) were cultured in DMEM (Gibco) supplemented with 10% FBS and 1% penicillin/streptomycin according to the supplier's recommended sub-culturing method. 293FT cells were transfected to produce lentiviral vector as previously described (21). Briefly, cells were grown to 70% confluency and transfected using polyethylenimine (Sigma) complexed plasmid DNA. Transfection medium was removed after 8 h and supernatant was collected at 24 and 48 h post-transfection. Supernatant was filtered through a 0.45 μ m filter and concentrated using a Beckman Coulter Optima XE90 ultracentrifuge. Concentrated virus pellets were resuspended in 1X HBSS (Gibco), aliquotted,

and stored at -80 °C. Pseudoviruses were produced in 293FT cells co-transfected with GFP-expressing lentivirus plasmid and pCMV-VSV-G (vesicular stomatitis virus G protein under control of the cytomegalovirus immediate-early enhancer and promoter) (47). HIV-1 pseudovirus was produced using pDHIV3-GFP (NL4-3-based Δenv , Δnef) (19). SIV pseudovirus was produced using pSIV-GFP and pSIV Δvpx -GFP (SIV_{mac239}-based Δenv) (48). Core antigen was measured using p24 and p27 ELISA (Advanced BioScience Laboratories Inc.) and RT activity was measured as previously described (49).

Lentiviral Vector Transduction

The pseudovirus vector input was normalized by RT activity then THP-1 cells were infected in the presence 30 µg/mL DEAE dextran (Sigma) for 2 h, washed 3 times with 1X PBS (Gibco), and analyzed for GFP expression 24 or 120 h post-transduction for dividing and nondividing cells, respectively. GFP measurement was performed using a MACSQuantVYB flow cytometer (Miltenyi Biotec) and data were analyzed using MACSQuantify software (Miltenyi Biotec).

Human POLB KO by LentiCRISPRv2

LentiCRISPRv2 plasmids targeting *POLB* were constructed using methods previously described (15,16). Briefly, complimentary oligonucleotides containing the specific sgRNA sequence and overhangs complementary to overhangs generated by BsmBI digestion of LentiCRISPRv2 were annealed to the BsmBI digested LentiCRISPRv2 plasmid to generate the functional transfer vector. Undigested LentiCRISPRv2 plasmid lacking a sgRNA sequence was used for pseudovirus production as a control. LentiCRISPRv2 vector was generated as described

for HIV-1 and SIV pseudoviruses, except that the psPAX2 packaging plasmid (Addgene) was co-transfected with the LentiCRISPRv2 (15) and pCMV-VSV-G plasmids. THP-1 cells were infected with concentrated LentiCRISPRv2 pseudovirus. 48 h after transduction, media was replaced with complete RPMI containing 1 $\mu\text{g}/\text{mL}$ puromycin (Gibco) and maintained in selection media for 14 days. Selected cells were single-cell sorted into 96-well plates using a BD FACS Aria II Cell Sorter (BD Biosciences). Single cells were expanded and assayed for Pol β expression by Western blot. Cells negative for Pol β by Western blot were further analyzed by PCR amplification of genomic DNA flanking the CRISPR-targeted region. The forward primers 5'-CTTGCCTTGTCAGTAGACAGCA-3' and 5'-CTCTGTGTTGACTGGGTTGGTC-3' and the reverse primers 5'-AACTTGGGCAGTTGGGCACAGT-3' and 5'-CCCGGCCATCTCTATGTTTTCT-3' were used to amplify exons 9 and 10, respectively. Exon 9 was sequenced using the forward primer 5'-GCTGTTGTCATCTCAGTGAATTC-3' and the reverse primer 5'-CCACAACCTTCACTATCATCCAG-3'. Exon 10 was sequenced using the forward primer 5'-CCAATTACTGTTGTCATCACAG-3' and the reverse primer 5'-TAGACTGTCCTCCCAGCAACTC-3'. Multiple sequence alignments were performed using Clustal Omega (50).

BrdU Incorporation Assay

DNA synthesis was assessed in THP-1 cells using previously described methods. Briefly, THP-1 cells were stimulated with PMA for 7 days or grown in suspension culture. Media was replaced with complete RPMI containing 10 μM 5-bromo-2'-deoxyuridine (Sigma). Cells were grown in the presence of BrdU for 1 or 8 hours, harvested, and fixed by addition of 70% ice-cold ethanol. Cells were permeabilized by addition of 0.5% Triton X-100 and DNA was denatured

with 2N HCl, neutralized, washed, and stained with an anti-BrdU antibody (Cell Signaling Technology; Bu20a) diluted 1:50 in a solution of 1X PBS, 1% BSA, and 0.1% tween-20. Cells were washed then stained with AlexaFluor 488 goat-anti-mouse antibody (Invitrogen) diluted 1:50. Cells were washed and analyzed using a MACSQuantVYB flow cytometer (Miltenyi Biotec) and data were analyzed using MACSQuantify software (Miltenyi Biotec).

Western Blotting

Anti- β -actin (Abcam; ab6276) and anti-Pol β (Abcam; ab175197) antibodies were used for Western blotting. Anti-Pol β antibodies were first validated for Western blotting using nuclear and whole cell extracts from THP-1, Jurkat, HeLa and 293FT cells. Lysates were resolved by SDS-PAGE on a 4-15% gel (BioRad) and proteins were transferred to a nitrocellulose membrane (BioRad). Primary antibodies were diluted 1:5000 in TBS-T with 5% dry milk. Anti-species secondary antibodies were diluted 1:10000 in TBS-T with 5% dry milk. Blots were imaged by chemiluminescence (SuperSignal West Femto maximum sensitivity substrate, Thermo Scientific) using a ChemiDoc Touch imaging system (BioRad) and analyzed in ImageLab 5.2 software (BioRad). A specific band at approximately 38 kD corresponding to the predicted molecular weight for Pol β was detected in all samples tested with slightly varying levels of expression depending on cell type.

MMS Sensitivity Assay

Sensitivity to the DNA damaging agent MMS (17) was determined by measuring growth inhibition using the tetrazolium salt-based XTT assay (ATCC) (51). Assay linearity was predetermined by varying cell seeding density, incubating cells at 37 °C, 5% CO₂ for 72 h, and

measuring specific absorbance (475 nm – 660 nm) using an Epoch microplate spectrophotometer (BioTek) after a 4 h incubation with XTT reagent. For evaluation of MMS cytotoxicity, cells were incubated with varying concentrations of MMS (Sigma) for 2 h, washed 3 times with 1X PBS, and incubated at 37 °C, 5% CO₂ for 72 h before being assayed as described above.

Preparation of Nuclear Extracts

Nuclear extracts were prepared as previously described (52). Briefly, cells were washed in 1X PBS, resuspended in hypotonic buffer, and Dounce homogenized. Lysed cells were centrifuged at $3300 \times g$ for 15'. The nuclear pellet was resuspended in low salt extraction buffer and mixed dropwise with high salt buffer (1.6 M KCl). Extracted nuclei were centrifuged at $22065 \times g$ for 30'. Supernatant was collected and centrifuged for an additional 15' at $22065 \times g$. Extracts were dialyzed against storage buffer for 2 h, aliquotted, and stored at -80 °C. Total protein concentration was determined by the Bradford assay (BioRad).

In Vitro Gap Repair Assay

In vitro gap repair assays were performed as previously described (11) using previously published oligonucleotides (4). The primers KEY35 (5'-ATTCGAGCTATCCTTGCGCG-3') and KEY31 (5'-ACTGCTAGAGATTTTCCACACTGACTA-3') and the template KEY36 (5'-TAGTCAGTGTGGAAAATCTCTAGCAGGCCCGCGCAAGGATAGCTCGAAT-3') were obtained from Integrated DNA Technologies. KEY35 was 5'-end labeled with γ -³²P using T4 polynucleotide kinase (New England Biolabs). Gap repair substrate was made by annealing 800 nM KEY35, 2.4 μ M KEY31, and 1.6 μ M KEY36.

Gap repair reactions were performed in 20 μL volumes containing 20 nM substrate, 2 mM ATP, dNTPs (60 nM, 2.5 μM , or 250 μM) and reaction buffer. Reactions were started by adding 4 μL 1 mg/mL nuclear extract, incubated at 37 $^{\circ}\text{C}$ for 30', 60', or 120', then stopped by addition of 10 μL 40 mM EDTA/99% formamide and heated for 1' at 95 $^{\circ}\text{C}$. A 4 μL aliquot from each reaction was resolved by 20% urea-PAGE (American Bio). Gels were visualized by phosphorimaging on a PharoFX Molecular Imager (BioRad) and quantitated using ImageLab 5.2 software (BioRad).

F. References

1. Coffin, J.M., Hughes, S.H., and Varmus, H.E. (1997) *Retroviruses*, Cold Spring Harbor Laboratory Press, Cold Spring Harbor, NY.
2. Bushman, F.D., and Craigie, R. (1991) Activities of human immunodeficiency virus (HIV) integration protein *in vitro*: specific cleavage and integration of HIV DNA. *Proc. Natl. Acad. Sci. U.S.A.* **99**, 1339-1343.
3. Fujiwara, T., and Mizuuchi, K. (1988) retroviral DNA integration: structure of an integration intermediate. *Cell* **54**, 497-504.
4. Yoder, K.E., and Bushman, F.D. (2000) Repair of gaps in retroviral DNA integration intermediates. *J. Virol.* **74**, 11191-11200.
5. Sobol, R.W., Horton, J.K., Kuhn, R., and Gu, H. (1996) Requirement of mammalian DNA polymerase-beta in base-excision repair. *Nature* **379**, 183-186.
6. Wang, L., Patel, V., Ghosh, L., and Banerjee, S. (1992) DNA polymerase beta mutations in human colorectal cancer. *Cancer Research* **52**, 4824-4827.
7. Sweasy, J.B., Lang, T., Starcevic, D., Sun, K.-W., Lai, C.-C., DiMaio, D., and Dalal, S. (2005) Expression of DNA Polymerase Beta cancer-associated variants in mouse cells results in cellular transformation. *Proc. Natl. Acad. Sci. United States Am.* **102**, 14350-14355.
8. Yamtich, J., Nemecek, A.A., Keh, A., and Sweasy, J.B. (2012) A germline polymorphism of DNA Polymerase Beta induces genomic instability and cellular transformation. *PLoS Genet.* **8**, e1003052.

9. Espeseth, A.S., Fishel, R., Hazuda, D., Huang, Q., Xu, M., Yoder, K., and Zhou, H. (2011) siRNA screening of a targeted library of DNA repair factors in HIV infection reveals a role for base excision repair in HIV integration. *PLoS ONE* **6**, e17612.
10. Yoder, K.E., Espeseth, A., Wang, X.H., Fang, Q., Russo, M.T., Lloyd, R.S., Hazuda, D., Sobol, R.W., and Fishel, R. (2011) The base excision repair pathway is required for efficient lentivirus integration. *PLoS ONE* **6**, e17862.
11. Van Cor-Hosmer, S.K., Kim, D.H., Daly, M.B., Daddacha, W., and Kim, B. (2013) Restricted 5'-end gap repair of HIV-1 integration due to limited cellular dNTP concentrations in human primary macrophages. *J. Biol. Chem.* **288**, 33253-33262.
12. Lewis, P.F., and Emerman, M. (1994) Passage through mitosis is required for oncoretroviruses but not for the human immunodeficiency virus. *J. Virol.* **68**, 510-516.
13. Auwerx, J. (1991) The human leukemia cell line, THP-1: a multifaceted model for the study of monocyte-macrophage differentiation. *Experientia* **47**, 22-31.
14. Bonifati, S., Daly, M.B., St. Gelais, C., Kim, S.H., Hollenbaugh, J.A., Shepard, C., Kennedy, E.M., Kim, D.H., Schinazi, R.F., and Kim, B. (2016) SAMHD1 controls cell cycle status, apoptosis and HIV-1 infection in monocytic THP-1 cells. *Virology* **495**, 92-100.
15. Sanjana, N.E., Shalem, O., and Zhang, F. (2014) Improved vectors and genome-wide libraries for CRISPR screening. *Nat. Methods* **11**, 783-784.
16. Shalem, O., Sanjana, N.E., Hartenian, E., Shi, X., Scott, D.A., Mikkelsen, T.S., Heckl, D., Ebert, B.L., Root, D.E., Doench, J.G., and Zhang, F. (2014) Genome-scale CRISPR-Cas9 KO screening in human cells. *Science* **343**, 84-87.

17. Ochs, K., Sobol, R.W., Wilson, S.H., and Kaina, B. (1999) Cells deficient in DNA polymerase beta are hypersensitive to alkylating agent-induced apoptosis and chromosomal breakage. *Cancer Research* **59**, 1544-1551.
18. Lahouassa, H., Daddacha, W., Hofmann, H., Ayinde, D., Logue, E.C., Dragin, L., Bloch, N., Maudet, C., Bertrand, M., Gramberg, T., Pancino, G., Priet, S., Canard, B., Laguette, N., Benkirane, M., Transy, C., Landau, N.R., Kim, B., and Margottin-Goguet, F. (2013) SAMHD1 restricts HIV-1 by reducing the intracellular pool of deoxynucleotide triphosphates. *Nat. Imm.* **13**, 223-228.
19. Andersen, J.L., DeHart, J.L., Zimmerman, E.S., Ardon, O., Kim, B., Guillaume, J., Benichou, S., and Planelles, V. (2006) HIV-1 Vpr-induced apoptosis is cell cycle dependent and requires Bax but not ANT. *PLoS Pathogens* **2**, e127.
20. Diamond, T.L., Roshal, M., Jamburuthugoda, V.K., Reynolds, H.M., Merriam, A.R., Lee, K.Y., Balakrishnan, M., Bambara, R.A., Planelles, V., Dewhurst, S., and Kim, B. (2004) Macrophage tropism of HIV-1 depends on efficient cellular dNTP utilization by reverse transcriptase. *J. Biol. Chem.* **279**, 51545-51553.
21. Kim, B., Nguyen, L.A., Daddacha, W., and Hollenbaugh, J.A. (2012) Tight interplay among SAMHD1 protein level, cellular dNTP levels, and HIV-1 proviral DNA synthesis kinetics in human primary monocyte-derived macrophages. *J. Biol. Chem.* **287**, 21570-21574.
22. Skasko, M., Weiss, K.K., Reynolds, H.M., Jamburuthugoda, V., Lee, K., and Kim, B. (2005) Mechanistic differences in RNA-dependent DNA polymerization and fidelity between murine leukemia virus and HIV-1 reverse transcriptases. *J. Biol. Chem.* **280**, 12190-12200.

23. Operario, D.J., Reynolds, H.M., and Kim, B. (2005) Comparison of DNA polymerase activities between recombinant feline immunodeficiency and leukemia virus reverse transcriptases. *Virology* **335**, 106-121.
24. Håkansson, P., Hofer, A., and Thelander, L. (2006) Regulation of mammalian ribonucleotide reduction and dNTP pools after DNA damage and in resting cells. *J. Biol. Chem.* **281**, 7834-7841.
25. Laguette, N., Sobhian, B., Casartelli, N., Ringeard, M., Chable-Bessia, C., Ségéral, E., Yatim, A., Emiliani, S., Schwartz, O., and Benkirane, M. (2011) SAMHD1 is the dendritic- and myeloid-cell-specific HIV-1 restriction factor counteracted by Vpx. *Nature* **474**, 654-657.
26. Goldstone, D.C., Ennis-Adeniran, V., Hedden, J.J., Groom, H.C.T., Rice, G.I., Christodoulou, E., Walker, P.A., Kelly, G., Haire, L.F., Yap, M.W., de Carvalho, L.P.S., Stoye, J.P., Crow, Y.J., Taylor, I.A., and Webb, M. (2011) HIV-1 restriction factor SAMHD1 is a deoxynucleoside triphosphate triphosphohydrolase. *Nature* **480**, 379-382.
27. Hanawalt, P.C., and Spivak, G. (2008) Transcription-coupled DNA repair: two decades of progress and surprises. *Nat. Rev. Mol. Cell Biol.* **9**, 958-970.
28. Choi, J.Y., and Guengerich, P. (2006) Kinetic evidence for inefficient and error-prone bypass across bulky N²-guanine DNA adducts by human DNA polymerase ϵ . *J Biol. Chem.* **281**, 12315-12324.
29. Nishida, M., Hada, T., Kuramochi, K., Hideki, Y., Yonezawa, Y., Kuriyama, I., Sugawara, F., Yoshida, H., and Mizushima, Y. (2008) Diallyl sulfides: selective inhibitors of family X DNA polymerases from garlic (*Allium sativum* L.). *Food Chemistry* **108**, 551-560.

30. Schmitt, M.W., Venkatesan, R.N., Pillaire, M.J., Hoffman, J.S., Sidorova, J.M., and Loeb, L.A. (2010) Active site mutations in mammalian DNA polymerase δ alter accuracy and replication fork progression. *J. Biol. Chem.* **285**, 32264-32272.
31. Yamtich, J., and Sweasy, J.B. (2009) DNA polymerase family X: function, structure, and cellular roles. *Biochimica et Biophysica Acta* **1804**, 1136-1150.
32. Braithwaite, E.K., Prasad, R., Shock, D.D., Hou, E.W., Beard, W.A., and Wilson, S.H. (2005) DNA polymerase λ mediates a back-up base excision repair activity in extracts of mouse embryonic fibroblasts. *J. Biol. Chem.* **280**, 18469-18475.
33. Suzuki, H., Menegazzi, M., de Prati, A.C., Ogura, T., Esumi, H., Matsukage, A., and Libonati, M. (1991) Induction of DNA polymerase beta during proliferation of mitogen-stimulated human lymphocytes. *Biochem. Biophys. Res. Comm.* **181**, 623-628.
34. Menegazzi, M., de Prati, A.C., Ogura, T., Columbano, A., Ledda-Columbano, G.M., Libonati, M., Esumi, H., and Suzuki, H. (1992) Involvement of DNA polymerase beta in proliferation of rat liver induced by lead nitrate or partial hepatectomy. *FEBS Lett.* **310**, 135-138.
35. Fornace, A.J., Zmudzka, B., Hollander, M.C., and Wilson, S.H. (1989) Induction of beta-polymerase mRNA by DNA-damaging agents in Chinese hamster ovary cells. *Mol. Cell. Biol.* **9**, 851-853.
36. Tanaka, H., Arakawa, H., Yamaguchi, T., Shiraishi, K., Fukuda, S., Matsui, K., Takei, Y., and Nakamura, Y. (2000) A ribonucleotide reductase gene involved in a p53-dependent cell-cycle checkpoint for DNA damage. *Nature* **404**, 42-49.

37. Hottiger, M., Podust, V.N., Thimmig, R.L., McHenry, C., and Hübscher, U. (1994) Strand displacement activity of the human immunodeficiency virus type I reverse transcriptase heterodimer and its individual subunits. *J. Biol. Chem.* **269**, 986-991.
38. Brin, E., Yi, J., Skalka, A.M., and Leis, J. (2000) Modeling the late steps in HIV-1 retroviral integrase-catalyzed DNA integration. *J. Biol. Chem.* **275**, 39287-29295.
39. Wilkinson, T.A., Januszyk, K., Phillips, M.L., Tekeste, S.S., Zhang, M., Miller, J.T., Le Grice, S.F., Clubb, R.T., and Chow, S.A. (2009) Identifying and characterizing a functional HIV-1 reverse transcriptase-binding site on integrase. *J. Biol. Chem.* **284**, 7931-7939.
40. Roos, W.P. and Kaina, B. (2006) DNA damage-induced cell death by apoptosis. *Trends in Molecular Medicine.* **12**, 440-450.
41. He, J., Choe, S., Walker, R., Di Marzio, P., Morgan, D.O., and Landau, N.R. (1995) Human immunodeficiency virus type 1 viral protein R (Vpr) arrests cells in the G2 phase of the cell cycle by inhibiting p34cdc2 activity. *J. Virol.* **69**, 6705-6711.
42. Roe, T., Chow, S.A., and Brown, P.O. (1997) 3'-end processing and kinetics of 5'-end joining during retroviral integration in vivo. *J. Virol.* **71**, 1334-1340.
43. Allinson, S.L., Dianova, I.I., and Dianov, G.L. (2001) DNA polymerase β is the major dRP lyase involved in repair of oxidative base lesions in DNA by mammalian cell extracts. *EMBO J.* **20**, 6919-6926.
44. Garcia-Diaz, M., Bebenek, K., Kunkel, T.A., and Blanco, L. (2001) Identification of an intrinsic 5'-deoxyribose-5-phosphate lyase activity in human DNA polymerase lambda: A possible role in base excision repair. *J. Biol. Chem.* **276**, 34659-34663.

45. Dalal, S., Chikova, A., Jaeger, J., and Sweasy, J.B. (2008) The leu22pro tumor-associated variant of DNA Polymerase Beta is dRP lyase deficient. *Nucleic Acids Res.* **36**, 411-422.
46. Bennett, G.R., Peters, R., Wang, X.H., Hanne, J., Sobol, R.W., Bundschuh, R., Fishel, R., and Yoder, K.E. (2014) Repair of oxidative DNA base damage in the host genome influences the HIV integration site sequence preference. *PLoS One* **9**, e103164.
47. Stewart, S.A., Dykxhoorn, D.M., Pilliser, D., Mizuno, H., Yu, E.Y., An, D.S., Sabatini, D.M., Chen, I.S., Hahn, W.C., Sharp, P.A., et al. (2003) Lentivirus-delivered stable gene silencing by RNAi in primary cells. *RNA* **9**, 493-501.
48. Cowan, S., Hatzioannou, T., Cunningham, T., Muesing, M.A., Gottlinger, H.G., and Bieniasz, P.D. (2002) Cellular inhibitors with Fv1-like activity restrict human and simian immunodeficiency virus tropism. *Proc. Nat. Acad. Sci.* **99**, 11914-11919.
49. Schinazi, R.F., Eriksson, B.F., and Hughes, S.H. (1989) Comparison of inhibitory activities of various antiretroviral agents against particle-derived and recombinant human immunodeficiency virus type 1 reverse transcriptases. *Antimicrob. Agents Chemother.* **33**, 115-117.
50. McWilliam, H., Li, W., Uludag, M., Squizzato, S., Park, Y.M., Buso, N., Cowley, A.P., and Lopez, R. (2013) Analysis tool web services from the EMBL-EBI. *Nucleic Acids Res.* **41**, W597-600.
51. Scudiero, D.A., Shoemaker, R.H., Paull, K.D., Monks, A., Tierney, S., Nofziger, T.H., Currens, M.J., Seniff, D., and Boyd, M.R. (1988) Evaluation of a soluble tetrazolium/formazan assay for cell growth and drug sensitivity in culture using human and other tumor cell lines. *Cancer Research* **48**, 4827-4833.

52. Abmayr, S.M., Yao, T., Parmely, T., and Workman, J.L. (2006) *Curr. Protoc. Mol. Biol.*

Chater 12, unit 12.1

Chapter 4

General Discussion

A. Discussion of Collective Results

The cellular mechanisms that regulate the availability of dNTPs are critical to ensure that DNA synthesis and repair occur efficiently yet within well-coordinated constraints. In fact, limiting the availability of dNTPs in the absence of DNA synthesis restricts the resources required by DNA viruses and serves as a protective mechanism against these particular invaders. Furthermore, because many nucleoside analogue pharmaceuticals are used to treat viral disease and cancers, careful consideration of the cellular metabolic pathways that act on these molecules is necessary and is likely to affect decisions regarding personalized medicine. In Chapter 2, we present data demonstrating that SAMHD1 metabolizes not only nucleoside analogues built from a ribose sugar, but also from arabinose analogues. Collectively, these data allow us to predict what types of modifications will define whether or not a nucleoside analogue will be a substrate for SAMHD1. Drugs that are substrates for SAMHD1 may face this additional barrier to achieve therapeutically relevant concentrations in target cells and these findings may help to explain potential suboptimal pharmacokinetic exposure when using certain antimetabolites for cancer treatment (1,2).

Coincidentally, lentiviruses that have adopted the Vpx-coding approach to overcoming SAMHD1 restriction in nondividing cells may have also strengthened their ability to resist treatment with NRTIs, many of which are not predicted to be substrates for SAMHD1 because of modifications to the 3' position of the sugar ring. Recent work by our laboratory and others has shown that Vpx-treatment using VLPs suppresses the efficacy of NRTIs because of the corresponding increase in canonical dNTPs, which then compete with NRTIs (3-5). However, because the metabolic pathways that generate the active forms of NNRTIs vary by base identity and modifications to the base and/or sugar moieties, it is not necessarily straightforward to

predict whether a particular NRTI's efficacy will be significantly impacted by cellular exposure to Vpx (4). Regardless, development of a more complex model of cellular metabolism of NRTIs and potential effects on efficacy will certainly rely, in part, upon accurately predicting whether a particular molecule will be a substrate for SAMHD1. Furthermore, the collective results of these studies urges that care should be taken when selecting the cellular systems and viruses (Vpx coding or noncoding) used to evaluate NRTI potency and efficacy (5).

While this work has provided additional information about the structural features of nucleoside analogues that determine fit for the SAMHD1 active site, we were unable to test hypotheses about the key structural determinants of SAMHD1 itself that control this specificity. We generated two SAMHD1 mutants, L150A and Y374A, to test whether these residues act as a steric gate that impedes binding and degradation of rNTPs – an exclusionary mechanism common to DNA polymerases and that has been proposed for SAMHD1 (6). Unfortunately, mutating these residues results in a loss of catalytic activity either due to disruption of the catalytic pocket or due to enzyme misfolding. Since we were unable to determine whether these residues are important for controlling SAMHD1 substrate specificity, additional work will be needed to understand the mechanistic constraints used to exclude ribonucleotides, whether these residues are mutable, and whether this occurs naturally in any disease states. Furthermore, additional studies to understand the role of SAMHD1 in cancer development and progression will be important to resolve potential concerns about antimetabolite therapy.

With respect to developing SAMHD1 inhibitors for use in a clinical setting, it is unclear whether such a therapeutic modality would provide more benefit than risk. Recently, work by our laboratory showed that SAMHD1 KO cells were shown to display augmented proliferation associated with a corresponding increase in cellular dNTPs (7). Since SAMHD1 expression has

been linked to cell cycle control, inhibition may alter control over cell division in normal cells. Furthermore, because of its role in the inherited autoimmune disease, Aicardi-Goutieres Syndrome, SAMHD1 has been hypothesized to suppress endogenous retroelements, such as the LINE1 retrotransposon (8,9). Inhibiting SAMHD1 may therefore lead to unintended deleterious effects should an increase in LINE1 activity occur.

DNA repair during retrovirus integration is an area of research where speculation abounds. Much of the knowledge that the field has about which and how efficiently enzymes function in repairing the gapped DNA intermediate relies on reductionist approaches that use *in vitro* repair assays (10). While these data are helpful for establishing a minimal requirement for completing integration biochemistry, they fail to consider the context of the cellular environment in which the process is naturally occurring. We know that DNA damage and repair processes are highly dependent on context, timing, and other factors that are determined by complex factors that are difficult to address using a simple biochemical system. In Chapter 3, we examined the role of Pol β in HIV-1 gap repair in both dividing and nondividing cells. In our current study, we consider this difference by using the THP-1 cellular model, which can flexibly explore these contexts separately in a human cell type that is relevant to natural HIV infection (11).

POLB deletion is embryonic lethal in mice, which restricted experiments to the use of immortalized embryonic fibroblasts for studies examining the role Pol β in lentivirus replication. This is problematic for several reasons: 1) fibroblasts are not target cells for lentivirus infection, 2) mice do not carry any known lentiviruses, and 3) mouse embryonic fibroblasts are dividing cells with relatively high dNTP concentration. As we show in the current work using cellular extracts in an *in vitro* repair assay, dNTP concentration has a very strong effect on the rate of repair. As seen in Chapter 3 (Fig. S2), increasing dNTP concentration correlates with higher

repair rates in Pol β expressing cells. This is not surprising since previous studies have shown that Pol β is the primary repair polymerase in BER, which is possibly the primary mechanism that repairs the lentiviral gapped DNA. However, our data indicate that in dividing THP-1 cells, which have fairly high dNTP concentrations, there is relatively little difference in the repair rate. Therefore, it is important to consider that Pol β expression may be important in cells that have higher than typical dNTP availability, but that this is likely not a rate-limiting step in integration or in viral replication in general. Again, this is unsurprising because cellular DNA polymerases have adapted in the presence of the high dNTP concentrations that are sustained during DNA replication ($k_m \sim 1-100 \mu\text{M}$) (12-14). Since this type of damage is not too dissimilar from what might normally occur during other types of SSBs, it seems likely that even if repair is not immediate, that we would expect it to be repaired efficiently, if not more slowly in cells that host lower dNTP concentrations.

Our current model is not without limitations. Since monocytes are not targets of HIV infection *in vivo*, generating a CD4 T cell model (using Jurkat cells, for example) would be a better way to assess whether Pol β expression impacts replication kinetics when dNTP concentrations are high. Current gene editing technology makes it possible to ask this question using primary cells, but even though this would use a system that most closely resembles actual *in vivo* target cells, it fails to recapitulate the stromal environment of a living being. Therefore, given the complexity of further testing the importance of Pol β in a living system and based on our findings presented here, it seems likely that the redundancy of Pols in DNA damage repair is sufficient overcome the barrier of a single lost repair Pol.

Though we do not present the data in this dissertation, we generated a number of other KO THP-1 cell lines using the Lenti-CRISPR system that may be of great interest to the field in

the future, though these cell lines have yet to be validated. Due in part to the discovery of SAMHD1 as an HIV restriction factor, there has been a recent surge in interest surrounding the role of innate immunity, including nucleic acid pattern recognition that drives the interferon response (15-17). Interferon has largely been ignored in the context of HIV research because infection triggers IFN activation, but does not suppress viral replication. Instead, chronic activation of interferon may negatively impact the health of infected individuals due to chronic immune dysregulation (18). Recent evidence in support of this claim shows that blocking interferon signaling may help restore normal immune function (19). Further work into determining the mechanisms that are most critical for detection of HIV patterns and subsequent activation of the interferon response may lead to promising immunotherapy strategies that reduce the risk for negative effects on the immune system that put patients at risk for developing secondary infections due to treatment with broadly immunosuppressive agents. We think that developing relevant, easily tractable cellular model systems will be critical for bettering our understanding of innate immunity in the context of HIV infection.

B. References

1. Herold, N., Rudd, S. G., Sanjiv, K., Kutzner, J., Bladh, J., Paulin, C. B., ... & Schaller, T. (2017). SAMHD1 protects cancer cells from various nucleoside-based antimetabolites. *Cell Cycle*, *23*(2), 1-10.
2. Rudd, S. G., Schaller, T., & Herold, N. (2017). SAMHD1 is a barrier to antimetabolite-based cancer therapies. *Molecular & Cellular Oncology*, *4*(2), e1287554.
3. Amie, S. M., Daly, M. B., Noble, E., Schinazi, R. F., Bambara, R. A., & Kim, B. (2013). Anti-HIV host factor SAMHD1 regulates viral sensitivity to nucleoside reverse transcriptase inhibitors via modulation of cellular deoxyribonucleoside triphosphate (dNTP) levels. *Journal of Biological Chemistry*, *288*(28), 20683-20691.
4. Huber, A. D., Michailidis, E., Schultz, M. L., Ong, Y. T., Bloch, N., Puray-Chavez, M. N., ... & Landau, N. R. (2014). SAMHD1 has differential impact on the efficacies of HIV nucleoside reverse transcriptase inhibitors. *Antimicrobial agents and chemotherapy*, *58*(8), 4915-4919.
5. Hollenbaugh, J. A., Schader, S. M., Schinazi, R. F., & Kim, B. (2015). Differential regulatory activities of viral protein X for anti-viral efficacy of nucleoside reverse transcriptase inhibitors in monocyte-derived macrophages and activated CD4+ T cells. *Virology*, *485*, 313-321.
6. Ji, X., Wu, Y., Yan, J., Mehrens, J., Yang, H., DeLucia, M., ... & Xiong, Y. (2013). Mechanism of allosteric activation of SAMHD1 by dGTP. *Nature structural & molecular biology*, *20*(11), 1304-1309.

7. Bonifati, S., Daly, M. B., Gelais, C. S., Kim, S. H., Hollenbaugh, J. A., Shepard, C., ... & Wu, L. (2016). SAMHD1 controls cell cycle status, apoptosis and HIV-1 infection in monocytic THP-1 cells. *Virology*, *495*, 92-100.
8. Zhao, K., Du, J., Han, X., Goodier, J. L., Li, P., Zhou, X., ... & Cheung, L. E. (2013). Modulation of LINE-1 and Alu/SVA retrotransposition by Aicardi-Goutieres syndrome-related SAMHD1. *Cell reports*, *4*(6), 1108-1115.
9. Hu, S., Li, J., Xu, F., Mei, S., Le Duff, Y., Yin, L., ... & Guo, F. (2015). SAMHD1 inhibits LINE-1 retrotransposition by promoting stress granule formation. *PLoS genetics*, *11*(7), e1005367.
10. Yoder, K. E., & Bushman, F. D. (2000). Repair of gaps in retroviral DNA integration intermediates. *Journal of Virology*, *74*(23), 11191-11200.
11. Auwerx, J. (1991). The human leukemia cell line, THP-1: a multifaceted model for the study of monocyte-macrophage differentiation. *Experientia*, *47*(1), 22-31.
12. Choi, J.Y., and Guengerich, P. (2006) Kinetic evidence for inefficient and error-prone bypass across bulky N2-guanine DNA adducts by human DNA polymerase ϵ . *J Biol. Chem.* **281**, 12315-12324.
13. Nishida, M., Hada, T., Kuramochi, K., Hideki, Y., Yonezawa, Y., Kuriyama, I., Sugawara, F., Yoshida, H., and Mizushima, Y. (2008) Diallyl sulfides: selective inhibitors of family X DNA polymerases from garlic (*Allium sativum* L.). *Food Chemistry* **108**, 551-560.
14. Schmitt, M.W., Venkatesan, R.N., Pillaire, M.J., Hoffman, J.S., Sidorova, J.M., and Loeb, L.A. (2010) Active site mutations in mammalian DNA polymerase δ alter accuracy and replication fork progression. *J. Biol. Chem.* **285**, 32264-32272.

15. Solis, M., Nakhaei, P., Jalalirad, M., Lacoste, J., Douville, R., Arguello, M., ... & Hiscott, J. (2011). RIG-I-mediated antiviral signaling is inhibited in HIV-1 infection by a protease-mediated sequestration of RIG-I. *Journal of virology*, 85(3), 1224-1236.
16. Gao, D., Wu, J., Wu, Y. T., Du, F., Aroh, C., Yan, N., ... & Chen, Z. J. (2013). Cyclic GMP-AMP synthase is an innate immune sensor of HIV and other retroviruses. *Science*, 341(6148), 903-906.
17. Biswas, N., Wang, T., Ding, M., Tumne, A., Chen, Y., Wang, Q., & Gupta, P. (2012). ADAR1 is a novel multi targeted anti-HIV-1 cellular protein. *Virology*, 422(2), 265-277.
18. Deeks, S. G., Odorizzi, P. M., & Sekaly, R. P. (2017). The interferon paradox: can inhibiting an antiviral mechanism advance an HIV cure?. *The Journal of clinical investigation*, 127(1), 103-105.
19. Cheng, L., Ma, J., Li, J., Li, D., Li, G., Li, F., ... & Tsao, L. C. (2017). Blocking type I interferon signaling enhances T cell recovery and reduces HIV-1 reservoirs. *The Journal of clinical investigation*, 127(1), 269.